Simplified operation of flavin-dependent halogenases using H_2-driven flavin recycling



Jiayu Peng

St Peter's College

Hilary Term 2025

A Thesis submitted to the Board of the Faculty of Physical Sciences, for the degree of Doctor of Philosophy, University of Oxford

Simplified operation of flavin-dependent halogenases using H_2-driven flavin recycling

Jiayu Peng, St Peter's College, University of Oxford

A Thesis submitted for the degree of Doctor of Philosophy, Hilary Term 2025

Over the years, biocatalysis has emerged as a powerful tool in synthetic chemistry. It offers high selectivity under mild reaction conditions and promises a greener alternative to traditional chemical synthesis. Despite its advantages, the industrial application of biocatalysis is often limited by the reliance on expensive cofactors and their recycling systems. Cofactors are non-protein molecules which are essential for enzymatic activity. Flavins, including riboflavin, FAD and FMN, are particularly valuable redox cofactors but remain underutilised in industrial applications due to the lack of efficient and cost-effective recycling methods. Conventional flavin recycling methods rely on auxiliary enzymes and sacrificial reductants, which increase costs, operational complexity, and waste production, making them unsuitable for large-scale applications. Previous research in the Vincent group had investigated a method of flavin recycling using O_2-tolerant NiFe hydrogenase 1 from *E. coli*. This study demonstrated that Hyd-1 can directly reduce flavins to their hydroquinone forms by using H_2 as the sole reductant.

Halogenated compounds are essential in pharmaceuticals, agrochemicals, and materials science due to the significant ability of halogen substituents to alter the characteristics of small molecules. However, traditional chemical halogenation relies on toxic reagents, harsh conditions, and often lacks selectivity, leading to significant environmental impact. Halogenases, particularly flavin-dependent halogenases, offer a greener alternative and provide high regio- and stereoselectivity under mild conditions using simple halide salts. Despite these advantages, their low catalytic efficiency and the reliance on complex and expensive flavin recycling systems has limited their applications.

This research introduces a simplified operation system for flavin-dependent halogenases which utilises *E. coli* hydrogenase 1 as the flavin recycling system. The robustness of hydrogenase 1, including its O_2 tolerance and stability under varying temperatures and solvent conditions, allows for operation in safe H_2 / O_2 mixtures. This eliminates the need for separate reductase enzymes and auxiliary cofactor recycling components, simplifying the reaction setup. The coupling of hydrogenase 1 with halogenases was optimised for selective chlorination and bromination reactions. By fine-tuning conditions such as O_2 concentration and flavin concentration, the system demonstrated high conversion rates and reproducibility.

The system was successfully coupled to flavin-dependent halogenases for selective chlorination and bromination reactions. Under optimised conditions, the H_2-driven system achieved full conversion for 5.5 mM L-tryptophan chlorination catalysed by PyrH, with a total turnover number 275. For non-native substrates such as 0.5 mM antranilamide and anthranilic acid, full conversions also were achieved. The system was also extended to the halogenase PrnA, achieving selective halogenation with comparable conversions. To explore alternative reductant strategies, a DuBois-type nickel bis-diphosphine complex, was also investigated for its ability to reduce flavins. This complex demonstrated activity under aerobic conditions, indicating its potential for use in non-enzymatic flavin reduction pathways. Furthermore, the H_2-driven system was extended to flavin-dependent monooxygenases, specifically styrene monooxygenase. Using 0.5 mM *trans*-β-methylstyrene as a model substrate, the Hyd-1/FAD system enabled efficient epoxidation to (*S*)-styrene oxide, achieving up to 40% conversion with under optimised gas flow conditions and flavin concentrations. Substrate evaporation was identified and mitigated by adding DMSO as a co-solvent.

The findings of this study are promising for a scalable and sustainable flavin-dependent biocatalysis in industrial applications. Moreover, this work has the possibility for the broader adoption of flavin-dependent enzymes in the

production of pharmaceuticals, agrochemicals, and fine chemicals, offering a cleaner and more cost-effective alternative to current practices.

Acknowledgements

First and foremost, I am grateful to my supervisor, Professor Kylie Vincent, for her continuous support and patient guidance. She encouraged me and helped find solutions when I faced academic challenges, and provided deep meaning and comfort when I experienced setbacks in significant competitions. Without her, I would not have achieved my current academic progress.

I would like to thank Dr. Miguel Ramirez for the overexpression protocols of halogenase and his guidance at the start of the project, as well as his patience in answering my ongoing questions. I am also thankful to Dr. Stephen Carr and Plastida Synteng Umwi for their help with the production of Hyd-1. Additionally, I am grateful to Dr. Shiny Srinivasan for her guidance and support over several months, and her continued care and assistance even after leaving our group.

I owe a huge debt of gratitude to my family, including my beloved mother, father, and twin brother. My parents funded my DPhil studies, without which I would not have been able to conduct my research here. They have also been a constant source of encouragement during my lows. My twin brother has been by my side, offering mutual encouragement and support, making my time abroad less lonely.

I must also thank the few but true friends I have made here. Although I am quite introverted and not very social, I have been fortunate to find genuine friends who have been incredibly supportive. I am equally thankful to my partner, who patiently listens to and comforts me through my emotional ups and downs, constantly motivating me. Lastly, I am grateful to the University of Oxford for the opportunity and platform to excel and make an impact.

My life in Oxford has been enriching and memorable because of all of you. Thank you for being part of my journey.

Abbreviations

NADH 1,4-dihydronicotinamide adenine dinucleotide

NAD^+ nicotinamide adenine dinucleotide

NADPH nicotinamide adenine dinucleotide phosphate

e^- electron

ATP adenosine triphosphate

BNAH 1-benzyl-1,4-dihydronicotinamide

FMN flavin mononucleotide

FAD flavin adenine dinucleotide

KREDs ketoreductases

FDH formate dehydrogenase

MV methyl viologen

CO_2 carbon dioxide

GDH glucose dehydrogenase

FeS iron-sulfur

TOF turnover frequency

H4MPT tetrahydromethanopterin

E. coli *Escherichia coli*

Hyd-1 *E. coli* NiFe hydrogenase 1

DMSO dimethylsulfoxide

MeCN acetonitrile

Hyd-2 *E. coli* NiFe hydrogenase 2

OYE old yellow enzyme

SAM S-adenosyl-L-methionine

FD-halogenase flavin-dependent halogenase

α-KG α-ketoglutarate

FMOs flavin-dependent monooxygenases

mCPBA meta-chloroperoxybenzoic acid

UV-vis ultraviolet-visible spectroscopy

HPLC high-performance liquid chromatography

MS mass spectroscopy

LLPC liquid-liquid partition chromatography

IEC ion exchange chromatography

EDTA ethylenediaminetetraacetic acid

ROS reactive oxygen species

LEL lower explosive limit

UEL upper explosive limit

H_2O_2 hydrogen peroxide

O_2^- superoxide

SOD superoxide dismutase

MFC mass flow controller

CLEAs cross-linked enzyme aggregates

Table of Contents

Chapter 1. Introduction 1

1.1. Biocatalysis for chemical synthesis 2

1.2. Cofactors and cofactor recycling 3

1.2.1. Nicotinamide adenine dinucleotide (phosphate) 5

1.2.2. Artificial cofactors 7

1.2.3. Flavins 9

1.2.4. Cofactor recycling 10

1.3. Hydrogenases in cofactor recycling 14

1.3.1. Introduction to hydrogenases 14

1.3.1.1. NiFe hydrogenases 15

1.3.1.2. FeFe hydrogenases 16

1.3.1.3. Fe-only hydrogenases 19

1.3.2. *E.coli* NiFe hydrogenase 1 and 2 20

1.3.2.1. Hydrogenase in NADH recycling 24

1.3.2.2. Flavin recycling 26

1.4. Enzymes studied in this thesis 28

1.4.1. Halogenases 28

1.4.1.1. Flavin-dependent halogenases 30

1.4.1.2. Other halogenases 37

1.4.2. Flavin-dependent monooxygenases 40

1.5. Aims of this project 42

Chapter 2. Experiment and characterisation methods 44

2.1. Enzymes and chemicals 45

2.1.1. Overexpression and isolation of Hyd-1 40

2.1.2. Overexpression and isolation of FD-halogenase PyrH and flavin reductase Fre 47

2.2. Equipment, chemicals and experimental protocol 49

2.2.1. Procedure A (conventional PyrH operation with GDH/glucose) 50

2.2.2. Procedure B (H_2-driven chlorination by PyrH with Hyd-1/H_2 with pulsed delivery of O_2) 51

2.2.3. Procedure C (H_2-driven bromination by PyrH with Hyd-1/H_2 with pulsed delivery of O_2) 52
2.2.4. Procedure D (H_2-driven chlorination by PyrH with Hyd-1 and a safe mixture of H_2/O_2) 53

Chapter 3. Coulping hydrogenase 1 with halogenases to achieve H_2-driven halogenation with safe H_2/O_2 mixtures 56
3.1. Introduction 57
3.2. Results 61
3.2.1. H_2-driven reduction of FAD and riboflavin by UV measurement 61
3.2.2. Calibration curve for HPLC 62
3.2.3. Testing of halogenase with conventional GDH system 63
3.2.3.1. Testing of halogenase with different flavins 68
3.2.4. Coupling Hyd-1 and FD-halogenase 70
3.2.4.1. Primary test 70
3.2.4.2. Optimisation of reaction conditions 74
3.2.4.2.1. FAD concentration optimisation 85
3.2.4.2.2. O_2 concentration optimisation 90
3.2.5. Extending to biobromination 94
3.2.6. Increasing substrate concentrations 96
3.2.7. Extending to other non-native Substrate 97

Chapter 4. Optimisation and extending to other halogenases 100
4.1. Optimisation of operations 101
4.2. Hyd-2 for flavin recycling system… 109
4.3. Exploring constant gas environment for the halogenation system…. 113
4.4. Extending to FD-halogenase PrnA… 116
4.5. Ni-complex for flavin recycling system…. 121

Chapter 5. Coulping Hyd-1 with FMO 126
5.1. Introduction 127

5.2. Results 129
5.2.1. BNAH-driven bioepoxidation 129
5.2.2. Substrate evaporation test 130
5.2.3. Reaction conditions optimisation 133
5.2.4. Addressing the evaporation problem 136
5.3. Discussion and future direction 138

Chapter 6. Future plans, opportunities and challenges 142
6.1. Conclusion 143
6.2. Discussion 145
6.2.1. Future scope for the scale-up 147
6.2.2. Application of H_2-driven flavin recycling system 151

References 154

Appendix 175

1

Chapter 1

1.1 Biocatalysis for chemical synthesis

Chemical synthesis is fundamental to the industrial production of complex compounds, including pharmaceuticals, dyes, and agrochemicals. Its versatility enables the creation of novel drugs with specific therapeutic effects, exemplified by the synthesis of aspirin from salicylic acid.[1,2,3] Another major advantage is that chemical synthesis could be scaled up relatively simply. Typically, processes designed at the lab scale could be operated at the industrial production level.[4] This enables mass production of vital chemicals and pharmaceuticals, thus is important for meeting global demand. However, traditional chemical synthesis often involves hazardous reagents and it will typically generate unwanted by-products that can cause pollution and pose risks to human health and the environment. In addition, many chemical synthetic processes are energy-intensive and hazardous, which further exacerbate the environmental concerns and increase the cost of production.[5,6]

In contrast, biocatalysis offers an effective and green alternative to chemical synthesis. Biocatalysis involves natural catalysts such as enzymes, or the whole cell for conducting chemical reactions. Enzymes are highly specific to certain substrates and are efficient. They can typically operate under mild reaction conditions and are often more sustainable and environmentally friendly than traditional chemical synthesis.[7] One of the most significant advantages is the environmental friendliness of biocatalysis. This is particularly attractive in the pharmaceutical industry, where the ability to perform selective transformations with high selectivity is critical during the manufacture of complex medicines.[8,9] For instance, synthesis

of the cholesterol-lowering drug statin includes a biocatalytic step for higher conversion and decreased waste.[10] Despite its advantages, biocatalysis faces several challenges. For example, enzyme stability is a significant limitation of the exploitation of enzymes, and they are sensitive to changes in temperature, pH, and the presence of organic solvents.[11] Moreover, the production and purification of enzymes on a large scale incurs initial costs which can render biocatalysis less cost-effective.[12,13] Additionally, the optimisation of biocatalytic processes can also be cumbersome and requires an in-depth understanding of enzymes and the chemical reactions they catalyse (Figure 1).

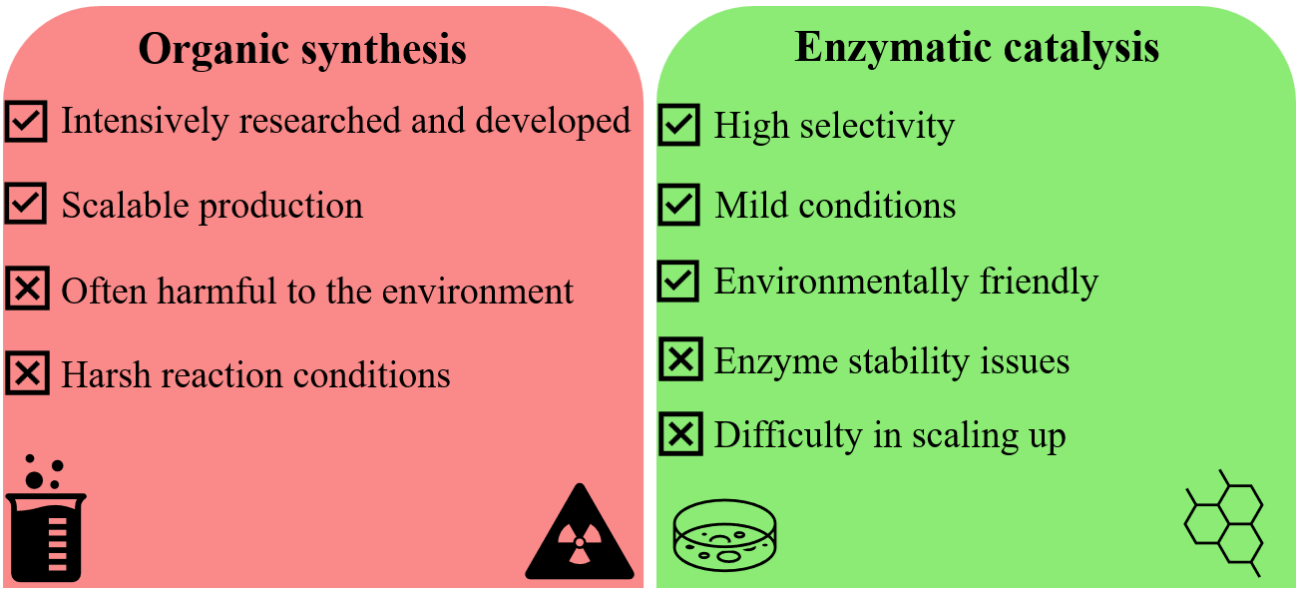


Figure 1. Advantages and disadvantages of chemical synthesis and enzyme catalysis.

1.2 Cofactors and cofactor recycling

Cofactors are non-protein chemical compounds or metallic ions which are essential for the catalytic activity of enzymes. They function as either tightly bound prosthetic groups or

temporarily bound coenzymes.[14] These cofactors play diverse roles, including stabilising enzyme structures and participating directly in the catalytic process by accepting or donating electrons or functional groups.[15] Cofactors can be divided into two categories: inorganic cofactors and organic cofactors (coenzymes). Inorganic cofactors are typically metal ions, including copper, zinc, and iron, etc. These metals stabilise the enzyme structure or maintain function as electron acceptors or donors during the reactions.[16] They also play a crucial role in the catalytic activities at the active sites of enzymes (Figure 2). For instance, zinc ions assist in accelerating the conversion of ethanol to acetaldehyde in the catalytic process of alcohol dehydrogenase.[17] Another category of cofactors are organic cofactors, also called coenzymes. This category includes molecules that are derived from vitamins. For example, nicotinamide adenine dinucleotide (NAD^+) is derived from nicotinic acid, and flavin adenine dinucleotide (FAD) is derived from riboflavin. These cofactors are important in redox reactions and biocatalytic reactions.[18] Other coenzymes, such as biotin, play significant roles in carboxylation reactions such as the synthesis of fatty acids.[19]

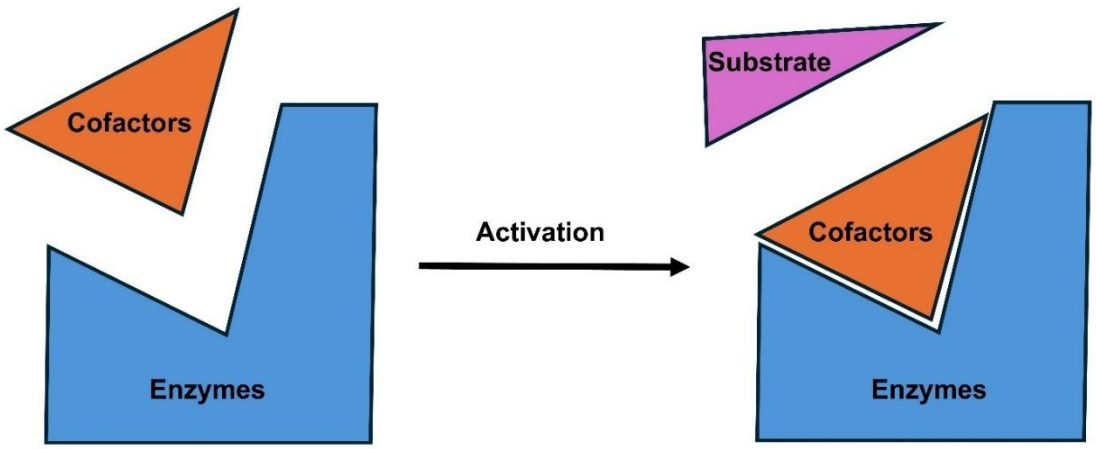


Figure 2. Activation of apoenzymes by cofactors. The enzyme (apoenzyme) becomes catalytically active only upon binding with its required cofactor, forming a holoenzyme.

1.2.1. Nicotinamide adenine dinucleotide (phosphate)

Nicotinamide adenine dinucleotide (NADH/NAD^+) and nicotinamide adenine dinucleotide phosphate (NADPH/$NADP^+$) are important cofactors derived from nicotinic acid (vitamin B3) in living organisms. They are structurally similar molecules, but the key difference lies in the presence of an additional phosphate group in NADPH (Figure 3). Both molecules share a core structure consisting of a nicotinamide moiety (responsible for redox activity), two ribose sugars, an adenine base, and a phosphate group bridging the two ribose sugars. However, NADPH has an extra phosphate group attached to the 2'-position of the ribose sugar linked to the adenine base. NADH is mainly involved in catabolic processes, such as the transfer of electrons in the mitochondrial electron transport chain to help generate adenosine triphosphate (ATP) which is an energy-storing molecule. NADPH, on the other hand, plays a role in anabolism by providing the reducing power for biosynthesis of fatty acids and cholesterol, for example, and in the cytoplasm by participating in the antioxidant system to help neutralise free radicals and reactive oxygen species (ROS).[20,21]

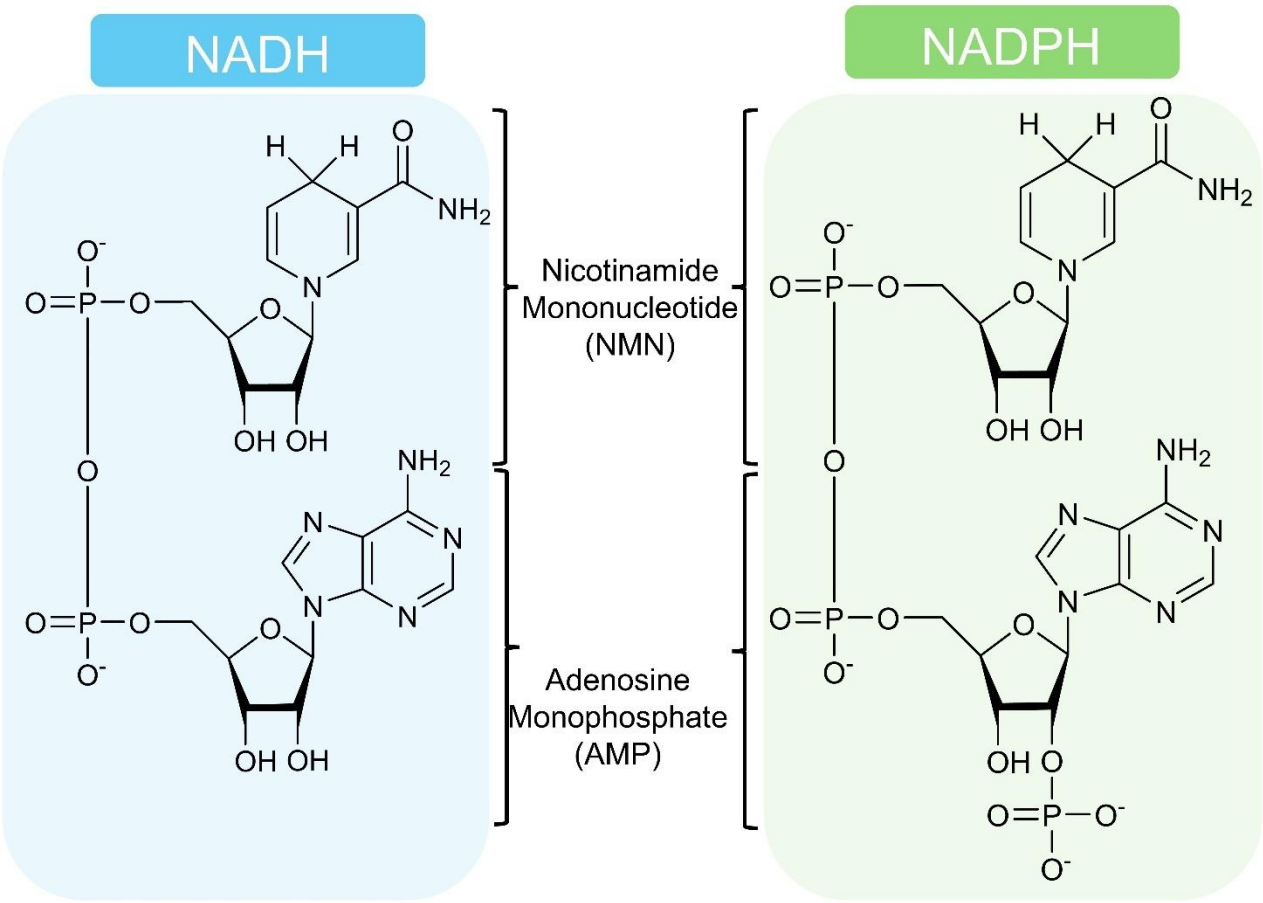


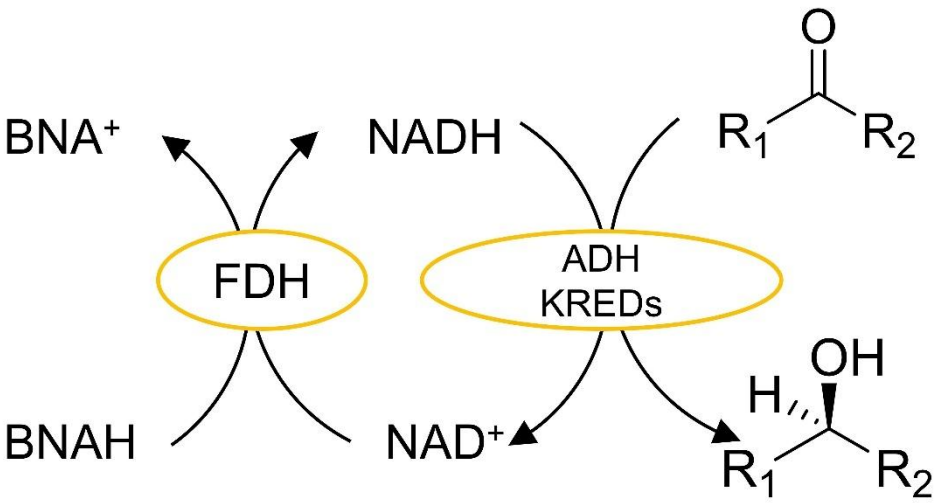
Figure 3. Structures of NADH and NADPH.

Additionally, NADH and NADPH are essential cofactors in biocatalysis, and they play a role in transferring electrons in redox reactions catalysed by a variety of enzymes. For example, NADH is involved in lactate dehydrogenase and alcohol dehydrogenase, where it is used to reduce the substrate and to help generate energy through oxidative phosphorylation.[22] NADPH, on the other hand, is mainly used in anabolic pathways (e.g. to provide reducing equivalents in fatty acid and cholesterol synthesis),[23,24] and also to provide electrons to cytochrome P450 reductase, which is essential for drug metabolism and steroid biosynthesis.[25] Given the cost of NADH and NADPH and their stoichiometric requirements

in industrial biocatalytic processes, the development of methods for their regeneration has become critical.[26]

1.2.2. Artificial cofactors

Artificial cofactors are synthetic molecules designed to mimic the role of natural cofactors in biological processes. A commonly studied cofactor analogue of NADH, 1-benzyl-1,4-dihydronicotinamide (BNAH), serves as a hydride source capable of directly reducing important cofactors such as NADH and flavins to their reduced forms. This reduction process can be coupled with NADH- or flavin-dependent enzymes to facilitate biocatalysis. For example, studies have demonstrated that BNAH can act as a hydride donor in enzymatic systems, providing an alternative to natural nicotinamide cofactors. In one study, BNAH was employed in conjunction with alcohol dehydrogenases (ADHs) and ketoreductases (KREDs) as a hydride source for asymmetric catalysis (Scheme 1). While BNAH showed limited activity with purified enzymes, it effectively facilitated the recycling of NADH through intermolecular hydride transfer, as evidenced by its use with formate dehydrogenase (FDH) in a coupled reaction system.[27]



Scheme 1. Biocatalytic system for asymmetric ketone reduction using alcohol dehydrogenases or ketoreductases, coupled with NADH recycling via formate dehydrogenase. In this system, NADH is regenerated from NAD^+ using BNAH as an artificial hydride donor.

Another widely studied artificial cofactor, methyl viologen (MV), shows great promise in bioelectrochemical systems due to its role as an efficient redox mediator. Methyl viologen is a bipyridine-based molecule that can undergo redox cycling and mainly acts as an electron donor in enzymatic processes. Unlike NADH, which provides both electrons and protons simultaneously, $MV^{\bullet+}$ only transfers electrons, making it highly efficient and stable under electrochemical conditions. In biocatalysis, MV has been effectively applied to facilitate the reduction of carbon dioxide (CO_2) to formic acid using formate dehydrogenase. For example, the bipyridinium-based salts of methyl viologen (MV^{2+}) has been electrochemically regenerated to achieved a 97% conversion of formic acid with high selectivity. This avoided the challenges of NADH regeneration, such as inefficiency and dimerization.[28] The thermodynamic properties of MV provide a stronger driving force for reduction, and its stability allows for clean and efficient electrochemical recycling without sacrificial reagents. However,

challenges such as its possible toxicity and the scalability of industrial applications still remain. Future directions for development include expanding the use of MV with other enzyme systems (such as flavin-dependent monooxygenases), integrating MV recycling with renewable energy sources, and designing derivatives to enhance enzyme compatibility with the target enzyme and selectivity.[29]

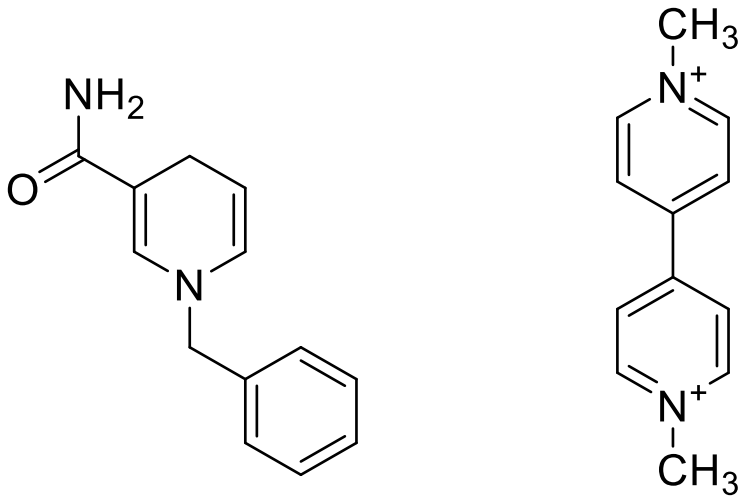


Figure 4. The structure of BNAH (left) and MV (right).

1.2.3. Flavins

Flavins, encompassing riboflavin (vitamin B2), flavin mononucleotide (FMN), and flavin adenine dinucleotide (FAD), are essential cofactors characterised by the isoalloxazine ring. Riboflavin acts as a precursor to FMN and FAD and both of them are essential cofactors in numerous flavoproteins.[30] These molecules are vital to various biological processes, primarily due to their ability to undergo reversible redox reactions as well as hydride transfer. They play a critical role in the electron transport chain, the Krebs cycle, and fatty acid

oxidation, where they facilitate the transfer of electrons (Figure 5).[31] In the field of biocatalysis, flavins are highly versatile and are utilised to catalyse a diverse range of oxidative reactions. These include the hydroxylation, dehydrogenation, and epoxidation of organic substrates, etc. Their ability to mediate selective oxidations and reductions makes flavins valuable in industrial and pharmaceutical applications, and the bioremediation of environmental pollutants.[32] In aqueous solution, oxidised flavin is yellow, blue in its semiquinone (partially reduced) form and colourless when fully reduced.[33]

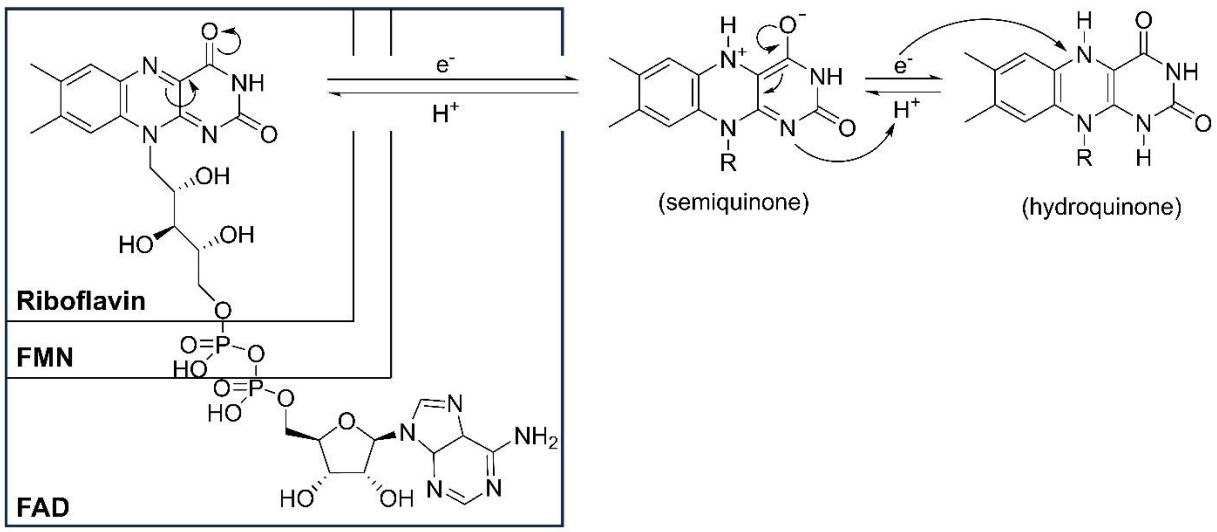


Figure 5. Scheme of flavin adenine dinucleotide (FAD), flavin mononucleotide (FMN), riboflavin and their hydroquinone forms.

1.2.4. Cofactor recycling

Cofactor recycling is the biochemical process of regenerating these molecules after they have been consumed in enzymatic reactions. This could allow them to be re-utilised in subsequent biocatalytic cycles.[34,35] Typically, cofactors are relatively expensive (FAD and FMN

approximately £633 and £220 per gram respectively, NADH approximately £21 per gram), so an available cofactor recycling system is critical to improving the efficiency of biochemical and industrial processes by reducing costs and increasing sustainability. Through cofactor recycling, the need for continuous replenishment can be minimised, thus reducing overall costs. This process also maintains optimal cofactor concentrations, ensuring that enzymes function efficiently and high reaction rates are maintained.[36]

Cofactor recycling methods are diverse and can be broadly categorised into industrially significant methods and approaches emerging from academic research (Scheme 2). Enzymatic recycling is the most widely used method in industrial applications. In contrast, chemical and electrochemical methods, although promising, are predominantly explored in research settings because they can generate non-native or inactive cofactor forms. For example, side reactions can occur that lead to the formation of 1,2- or 1,6-dihydro-NAD(P)H isomers instead of the biologically active 1,4-dihydro form. These isomers cannot participate effectively in enzymatic redox reactions because they do not interact properly with NAD(P)H-dependent enzymes.[37] This lack of regio- and stereoselectivity in chemical reduction compromises the utility of these methods in biocatalysis. The enzymatic recycling typically utilises specific enzymes such as formate dehydrogenase to reduce NAD^+ to NADH by oxidation of formate, and this method is widely used for reactions requiring large amounts of NADH due to its high efficiency and biocompatibility. Glucose dehydrogenase (GDH), on the other hand, oxidises glucose to gluconolactone and simultaneously reduces $NAD(P)^+$ to

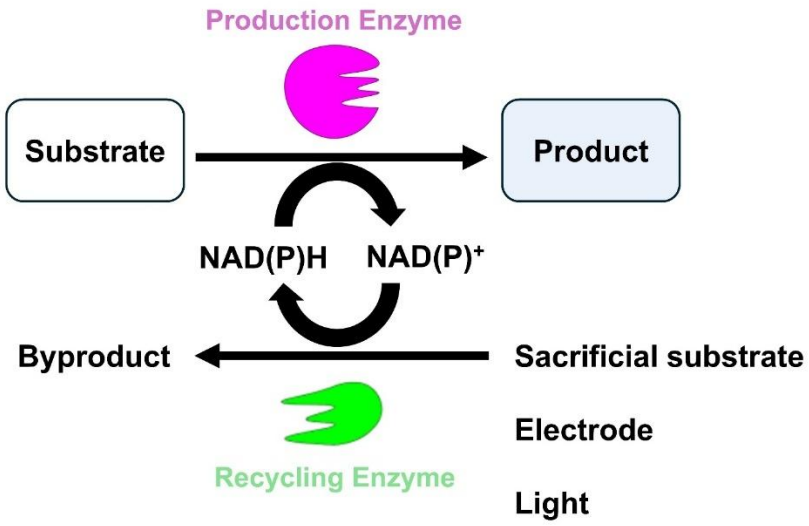
NAD(P)H, making it suitable for those synthetic pathways that require NAD(P)H.[38] Enzymatic recycling is highly applicable and scalable for industrial use due to its high specificity, mild reaction conditions, and proven biocompatibility. In addition to this, chemical methods directly reduce $NAD(P)^+$ by adding an external reducing agent. For example, borohydride (such as sodium cyanoborohydride) is used as a reducing agent to reduce $NAD(P)^+$. Chemical recycling is easy to implement in laboratory settings but has limited industrial scalability due to poor regioselectivity, harsh conditions, and high reagent costs.[39] In addition, the reaction conditions of chemical methods are sometimes harsh and may affect the stability of the substrate or product.

Electrochemical methods regenerate NAD(P)H by directly reducing $NAD(P)^+$ on the electrode. The process of electrochemical regeneration can accurately control the generation rate of NAD(P)H by adjusting the electrode potential and current density. Different types of electrode materials can be used to optimise the reduction process.[40] For example, carbon-based electrodes (such as glassy carbon or multi-walled carbon nanotubes) are often used for electrochemical reduction because they have good conductivity and large specific surface area, which can effectively promote electron transfer.[41,42,43,44] Metal electrodes (such as copper or gold electrodes) can also be used.[45,46] These electrode materials facilitate direct reduction reactions, rather than acting as catalysts. Electrochemical recycling offers controllable and potentially scalable regeneration of NAD(P)H, but requires further optimisation of electrode materials and system design for large-scale implementation.

Another recycling method is to use enzyme-modified materials, which combines the advantages of enzymatic catalysis and robust materials' characteristics. For example, enzymes such as glycerol dehydrogenase or ADH can be immobilised on the magnetically separable and spherical mesocellular silica foam to prepare nanoscale enzyme reactors, and NADH can be recycled quickly and efficiently through the catalytic action of the enzyme and the reduction action of the electrode. The magnetic properties of the material are due to the embedded magnetite (Fe_3O_4) nanoparticles.[47] Moreover, studies have demonstrated that co-immobilising and co-localising multi-enzyme systems, such as ADH and glutamate dehydrogenase, on porous materials can significantly enhance NADH recycling efficiency. This spatial arrangement optimises the mass transport of substrate between the enzymes, leading to improved catalytic performance.[48] However, the complexity of synthesising and uniformly dispersing magnetite nanoparticles, potential enzyme deactivation over time, and the difficulty of maintaining mass transfer efficiency in scaled-up systems limit their widespread industrial application. Enzyme-modified materials combine biocatalytic efficiency with reusability, offering medium scalability, though integration into continuous flow or large-scale systems remains challenging.

Other methods, such as photolysis use light energy to reduce $NAD(P)^+$ to NAD(P)H through photosensitizers or photocatalysts, which is an environmentally friendly and energy-saving coenzyme regeneration technology. It can generate excited state electrons from a sacrificial donor by absorbing photons or combine the light-driven catalysis of reducing agents and

enzymes to complete the reduction reaction. This method reduces the use of chemical reducing agents, waste generation, and effectively utilises renewable energy, which is particularly suitable for sustainable biochemical synthesis.[49,50] Photolysis methods are promising for sustainable synthesis. However, the low efficiency of these methods, and their dependence on specific light sources make them challenging to apply on an industrial scale. These are the challenges faced by the industrial application of redox enzymes and coenzyme circulation systems. Therefore, their development and optimisation are urgently needed.



Scheme 2. Different methods for the cofactor recycling.

1.3 Hydrogenases in cofactor recycling

1.3.1. Introduction to hydrogenases

Hydrogenases are the natural metalloenzymes which catalyse the reversible oxidation of H_2 ($H_2 \rightleftharpoons 2\ H^+ + 2\ e^-$). These enzymes play an important role in microbial metabolism. They enable organisms to use H_2 as an electron donor or H^+ as acceptor, depending on different

environmental needs. In addition, hydrogenases are also promising for the use in H_2 production and valuable chemicals through biotechnology applications. There are three types of hydrogenases, distinguished by the metal content in their active sites: Fe-only hydrogenases, FeFe hydrogenases and NiFe hydrogenases.[51,52]

1.3.1.1. NiFe hydrogenases

NiFe hydrogenases are most intensively studied among the three types of hydrogenases. They can catalyse both H_2 uptake and evolution, but tend to be more active in the H_2 uptake. The active site of NiFe hydrogenases consists of an iron and nickel atom which are coordinated by four cysteines. Two of the cysteines act as the bridging ligands between the two metal atoms in the NiFe active site. In addition, the iron atom of the active centre is coordinated with one carbonyl (CO) and two cyano (CN) ligands, which provide the unique chemical environment of the active centre (Figure 6). The strong donor property of the CN ligands contributes to the modulation of the redox potential of iron and helps to minimise build-up of charge during catalysis.[53,54]

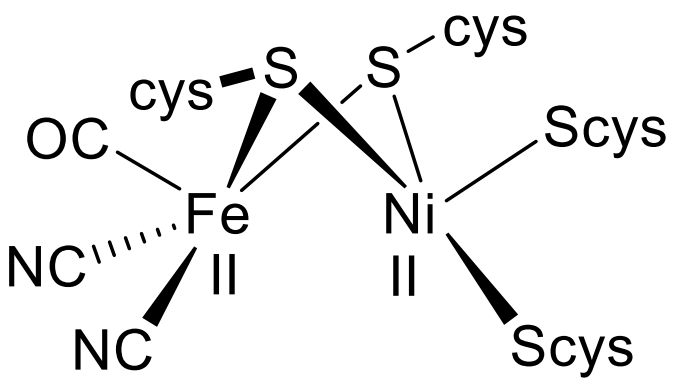


Figure 6. The structure of the NiFe active site of hydrogenase.

NiFe hydrogenases consist of small subunits which contain iron-sulfur clusters (FeS clusters) and large subunits which contain the NiFe active site (Figure 7). During H_2 oxidation, a proton is released via heterolytic splitting of H_2, leaving a hydride at the NiFe active site. Subsequently, the second proton is released via sequential electron transfer from H_2 oxidation. these electrons are transferred by FeS clusters to terminal acceptors.[55]

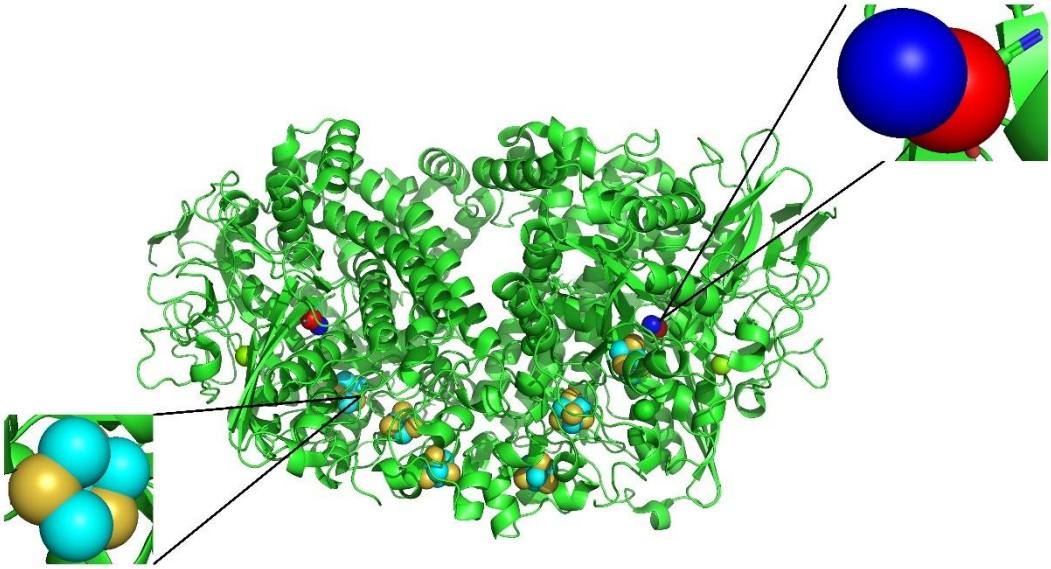


Figure 7. The structure of the O_2-tolerant NiFe hydrogenase 1 from *E. coli* (PDB: 6FPW, cyan and yellow spheres: small subunits containing FeS clusters. Blue and red balls and sticks: large subunits containing NiFe active site). Terminal electron acceptors: ubiquinone.[56]

1.3.1.2. FeFe hydrogenases

Unlike NiFe hydrogenase, FeFe hydrogenases contain an Fe-Fe active site with a bridging aza-dithiolate ligand. The unique active site of FeFe hydrogenases is called the H-cluster, which consists of the [2Fe] site connected to a [4Fe4S] cluster by a cysteine sulfur bridge.

Specifically, the two iron atoms of the [2Fe] subsite are each coordinated to a carbonyl group and a cyanide group (Figure 8, 9).[57,58] This structure makes the [2Fe] subcluster very efficient in the redox reaction of H_2. An iron-sulfur cluster relay in the FeFe hydrogenases is similar to NiFe hydrogenase, enabling long range electron transfer to and from the active centre to external electron acceptors.[59,60]

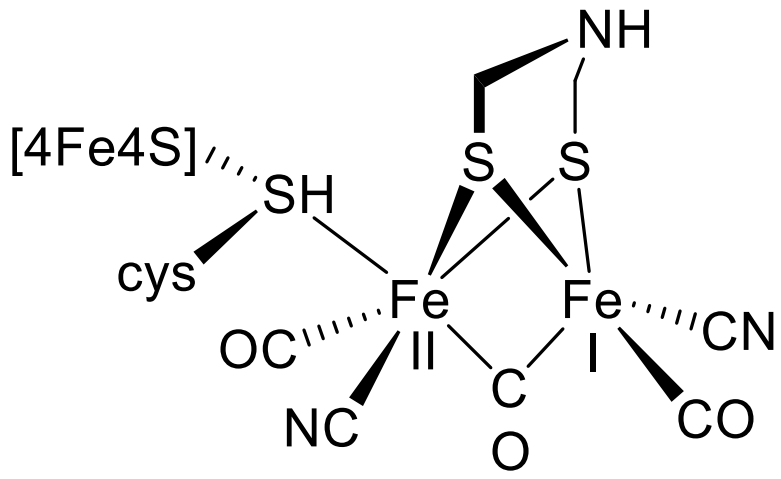


Figure 8. The structure of the FeFe active site of hydrogenases.

[FeFe]-hydrogenase activates H_2 via a Frustrated Lewis Pair (FLP)-like mechanism centred at its H-cluster, a unique organometallic cofactor composed of a [4Fe4S] cluster covalently linked to a diiron subsite bridged by an azadithiolate (ADT) ligand. In this architecture, the distal iron provides an open coordination site that functions as a Lewis acid, while the pendant amine on the ADT acts as an internal Lewis base. Their proximity creates a built-in FLP that polarizes incoming H_2. Upon substrate binding, the H–H bond is heterolytically cleaved: the distal iron accepts a hydride, and the ADT amine accepts a proton, forming a transient [Fe–H···H–N] intermediate. This is followed by rapid electron transfer to the [4Fe4S] cluster and

proton transfer through a dedicated hydrogen-bonded proton relay to the protein surface.[61,62,63]

[FeFe] hydrogenases contain multiple accessory FeS clusters in addition to the H-cluster active site. In the bifurcating *T. maritima* HydABC, a linear chain of four FeS clusters bridges the H-cluster to the FMN cofactor, with inter-cluster distances <15 Å, supporting ultrafast single-electron transfer. Inter-protomer [4Fe4S] clusters are separated by ~9.0 Å, facilitating redox balancing between protomers.[64] In *C. acetobutylicum*, [FeFe] hydrogenases include F-clusters such as a [2Fe2S] and a [4Fe4S]-His-coordinated cluster. Square wave voltammetry showed midpoint potentials of -420 mV and -565 mV for the [2Fe2S] and [4Fe4S] clusters, respectively (pH 8.8), which further shifts to -630 mV upon substitution of His with Cys in the [4Fe4S] ligand sphere. These highly reducing clusters operate between $[4Fe4S]^{+2/+1}$ and $[2Fe2S]^{+2/+1}$ redox couples, ensuring unidirectional electron flow toward H_2 oxidation or proton reduction in anaerobic systems.[65]

In contrast to NiFe hydrogenases, FeFe hydrogenases tend to be more active in H_2 evolution with a turnover frequency (TOF) of 10,000 s^{-1} reported for the [FeFe] hydrogenase from *Clostridium pasteurianum*.[66] Due to their efficient H_2 evolution catalytic activity, FeFe hydrogenases have been considered for biological production of H_2.[67] However, since FeFe hydrogenases are mostly found in anaerobic microorganisms, most FeFe hydrogenases are extremely sensitive to O_2 and are rapidly inactivated in aerobic environments.[68] Even though

some slightly O_2-tolerant FeFe hydrogenases have been discovered, ensuring that they are not completely inactivated in O_2 and can be recovered in H_2 environments, they still have to be carefully operated under O_2. This is one of the main challenges in biocatalytic applications of these enzymes.[69,70]

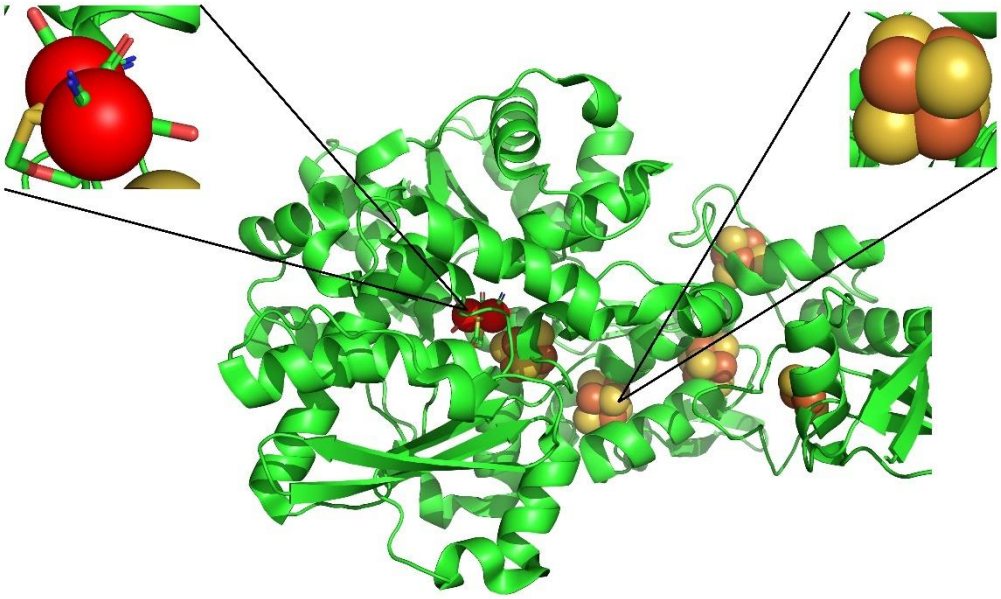


Figure 9. The structure of the FeFe hydrogenase from *Clostridium pasteurianum* (PDB: 3C8Y, orange and yellow spheres: FeS clusters. Red balls and sticks: [2Fe] active site). Terminal electron acceptors: ferredoxin.[71]

1.3.1.3. Fe-only hydrogenases

Unlike NiFe and FeFe hydrogenases, Fe-only hydrogenases do not contain a second atom in the active site and are FeS cluster-free.[72] Fe-only hydrogenases do not have long-distance relay chains of FeS clusters but act via direct hydride transfer at the active site (Figure 10). It is worth noting that Fe-only hydrogenases are also called H_2-forming

methylenetetrahydromethanopterin (methylene-H4MPT) dehydrogenase, so its function is not H_2 uptake or evolution like NiFe and FeFe hydrogenases, but the reversible reduction of hydride transfer to methenyl-H4MPT$^+$ to generate methylene-H4MPT.[73,74]

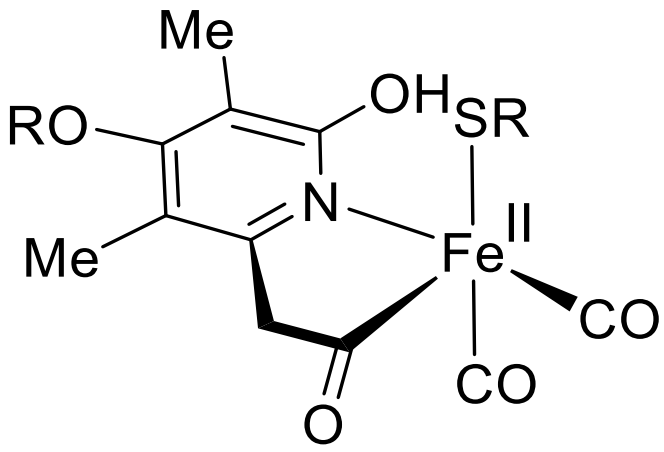


Figure 10. The structure of the Fe-only hydrogenase active site.

1.3.2. *E. coli* NiFe hydrogenase 1 and 2

Most of the hydrogenases are O_2-sensitive, but some of the hydrogenases are O_2-tolerant, making them particularly attractive towards biotechnological applications in industry. NiFe hydrogenase 1 from *E. coli* (Hyd-1, Figure 7) is a robust NiFe hydrogenase, stable under a wide range of pH and temperature. Importantly, Hyd-1 is O_2-tolerant, and is able to oxidise H_2 in the presence of O_2, although activity drops somewhat in the presence of O_2.[75] It is also tolerant to some organic co-solvents such dimethylsulfoxide (DMSO) and acetonitrile (MeCN). Like other NiFe hydrogenases, Hyd-1 consists of FeS clusters and [NiFe] active site, it transfers electrons from the oxidation of H_2 at the [NiFe] active site to physiological acceptors, such as cytochromes, via the FeS clusters.[76] To be specific, an O_2-tolerant NiFe

hydrogenases can catalyse the four-electron reactions of 2 H_2 + O_2 ⇌ H_2O, which is equivalent to H_2 combustion. During O_2 reduction, most of the O_2 is removed via a four-electron pathway, whereas a small part of the reaction is the inevitable one or two-electron pathway that produces hydrogen peroxide (H_2O_2) and superoxide. Overall, the unique electron relay chains and reaction pathways make the O_2-tolerant NiFe hydrogenases ensure the conversion of O_2 to harmless water and the survival of their catalytic NiFe active sites.[49,77]

Different from standard O_2-sensitive NiFe hydrogenases, the O_2-tolerance of NiFe hydrogenases such as Hyd-1, is significantly enhanced through unique structural adaptations and sophisticated electron relay mechanisms. Central to this tolerance is the unusual coordination of the proximal FeS cluster nearest the active site. Unlike the typical four-cysteine coordination found in O_2-sensitive hydrogenases from anaerobic organisms, the proximal cluster of Hyd-1 is surrounded by six cysteines. This additional cysteine coordination stabilises the enzyme against oxidative stress because the cluster can donate an additional electron for reduction of O_2 which is then lost as water.

NiFe hydrogenase 1 used in this study is shown to have three FeS clusters and the distal cluster is a [4Fe4S] cluster, which consist of four iron atoms and four sulfur atoms. The Fe is usually in a tetrahedral coordination environment. In addition, the iron atom is coordinated with the thiolate of cysteine side chains of the protein. The medial cluster is the [3Fe4S] cluster, which is a cluster consisting of three iron atoms and four sulfur atoms, usually

presenting a trigonal pyramidal structure. The special proximal [4Fe3S] cluster can exist in different redox states, making them efficient electron transfer agents.[78,79,80] The edge-to-edge distances between these clusters are approximately 7.7 Å (proximal to medial), 10.6 Å (medial to distal), and ~11.1 Å between distal clusters of adjacent protomers in the dimer, allowing efficient electron tunnelling (<14 Å).[80] The proximal [4Fe3S] cluster exhibits three oxidation states: PC1 (+3), PC2 (+4), and PC3 (+5). Upon oxidation to PC3, the 4Fe site changes from a four- to five-coordinate geometry via ligation from a glutamate and a backbone amide nitrogen. These clusters mediate electron transfer from the NiFe site to the membrane via a stepwise single-electron transfer relay. Midpoint redox potentials (vs SHE) are approximately +211 mV (PC3/PC2), +212 mV ([3Fe–4S] $^{+1/0}$), +4 mV (PC2/PC1), and -176 mV ([4Fe–4S] $^{+2/+1}$). The dimer interface enables distal-to-distal cluster electron sharing, promoting redox balance and O_2 tolerance.[81]

NiFe hydrogenase-2 (Hyd-2) from *E. coli* is an integral part of the ability of bacterium to utilise H_2 under anaerobic conditions (Figure 11). It is characterised as a membrane-bound, O_2-sensitive enzyme that plays a crucial role in anaerobic respiration by functioning as a proton pump. This enzyme is particularly interesting because it converts the energy derived from H_2 oxidation into a proton gradient across the membrane which is an essential process for the energy metabolism of the bacterium. Hyd-2 is encoded by the hybOABCDEFG operon and is expressed under anaerobic respiratory conditions. The structural setup of Hyd-2 includes a core catalytic module comprising large (HybC) and small (HybO) subunits, alongside an

FeS protein (HybA) and an integral membrane protein (HybB). The catalytic activity of Hyd-2, which involves both the oxidation and evolution of H_2, is facilitated through this complex arrangement of subunits that allows for efficient electron transfer and enzyme reactivity. Recent advances in overexpression and purification of Hyd-2 have significantly contributed to a deeper understanding of the structure and function of Hyd-2.[82] The enzyme operates through a finely tuned interaction of its subunits, where the HybOC heterodimer forms the fundamental operational unit. This heterodimer is associated with the periplasmic side of the inner membrane, facilitating direct interaction with the electron transport chain through the quinone pool.

Hyd-2 also contains a small subunit with three FeS clusters: proximal [4Fe4S], medial [3Fe4S], and distal [4Fe4S]. The maximum intramolecular cluster spacing is ~10.7 Å, with inter-dimer distal-to-distal cluster distances of ~12.3 Å, supporting efficient electron flow. The FeS relay links the NiFe active site to the membrane-associated HybB subunit, facilitating proton reduction through the quinone pool. All three clusters participate in reversible one-electron transfers, with redox cycling between [4Fe4S] $^{+2/+1}$ and [3Fe4S] $^{+1/0}$ states. Although precise redox potentials are not well-characterised, Hyd-2 functions optimally at potentials below -100 to -150 mV, suggesting its clusters operate more negatively than those in Hyd-1. Hyd-2 is less O_2-tolerant and is primarily active under anaerobic or highly reducing conditions. Therefore, the sensitivity of Hyd-2 to O_2 has been assumed to limit its biocatalytic applications under aerobic conditions. However, although it is classified as O_2-sensitive, it is also able to

retain some H_2 oxidation activity under O_2 and recover when put back under H_2.[82] Therefore, further work is still needed to properly understand the O_2 tolerance of hydrogenase to best exploit them.[83,84]

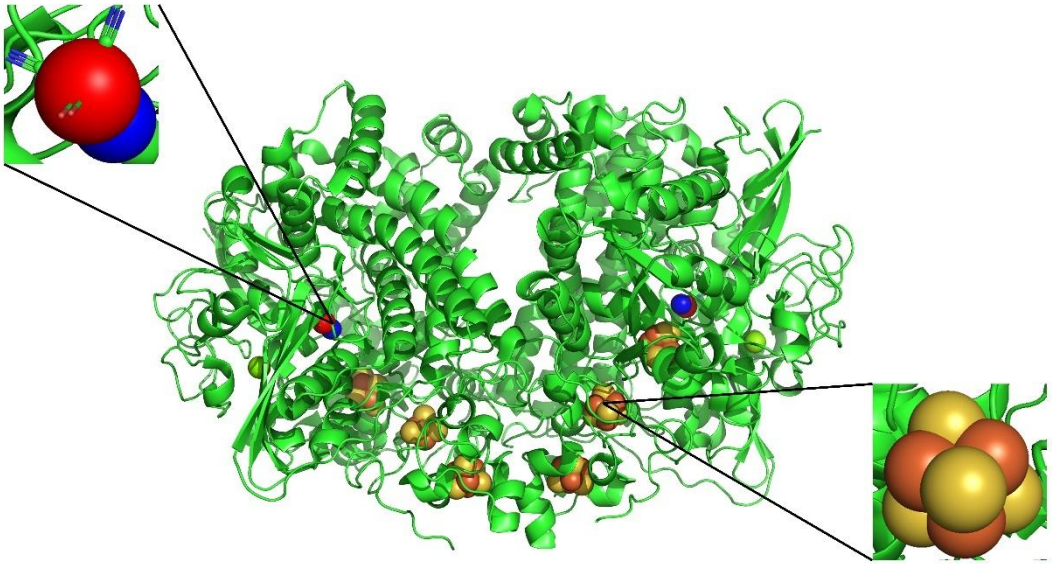


Figure 11. The structure of the NiFe hydrogenase 2 from *E. coli* (PDB: 6EHQ, orange and yellow spheres: small subunits containing FeS clusters. Blue and red balls and sticks: large subunits containing NiFe active site). Terminal electron acceptors: ubiquinone.[83]

1.3.2.1. Hydrogenase in NADH recycling

Due to the high efficiency of H_2 uptake by NiFe hydrogenase, a H_2-driven NADH recycling system was developed using Hyd-1 or Hyd-2. This method achieves selective biocatalytic hydrogenation via enzyme-modified carbon particles. The system co-immobilises hydrogenase and NAD^+ reductase on conductive carbon particles (e.g. graphite), where the hydrogenase uses H_2 to generate electrons, which are passed within the carbon particles to

the NAD^+ reductase to reduce NAD^+ to NADH. This approach is different from the conventional method which relies on, for example, a GDH system and a sacrificial reductant for NADH regeneration (Figure 12). This H_2-driven NADH recycling system eliminates the need for additional reductant and avoids the generation of by-products and achieves 100% atom economy. The system has been shown to operate well in the pH 6-8 range and at low H_2 pressures (below 1 bar), to regenerate NADH efficiently and to maintain high conversion (over 98%). Moreover, remarkable enzyme stability over multiple cycles is retained, with a total turnover number of more than 130,000. In addition, this enzyme-modified system is simple to operate and can be recovered by centrifugation and reuse, which greatly improves the economy and operability for practical applications. In addition, the system can be operated in buffer-free water and adapted for different reaction conditions. This system significantly demonstrated great flexibility and possibility of slotting in different hydrogenases for a wide range of applications, especially for NADH-dependent biocatalytic reactions requiring high selectivity and low by-product generation, such as the production of pharmaceuticals and fine chemicals.[85]

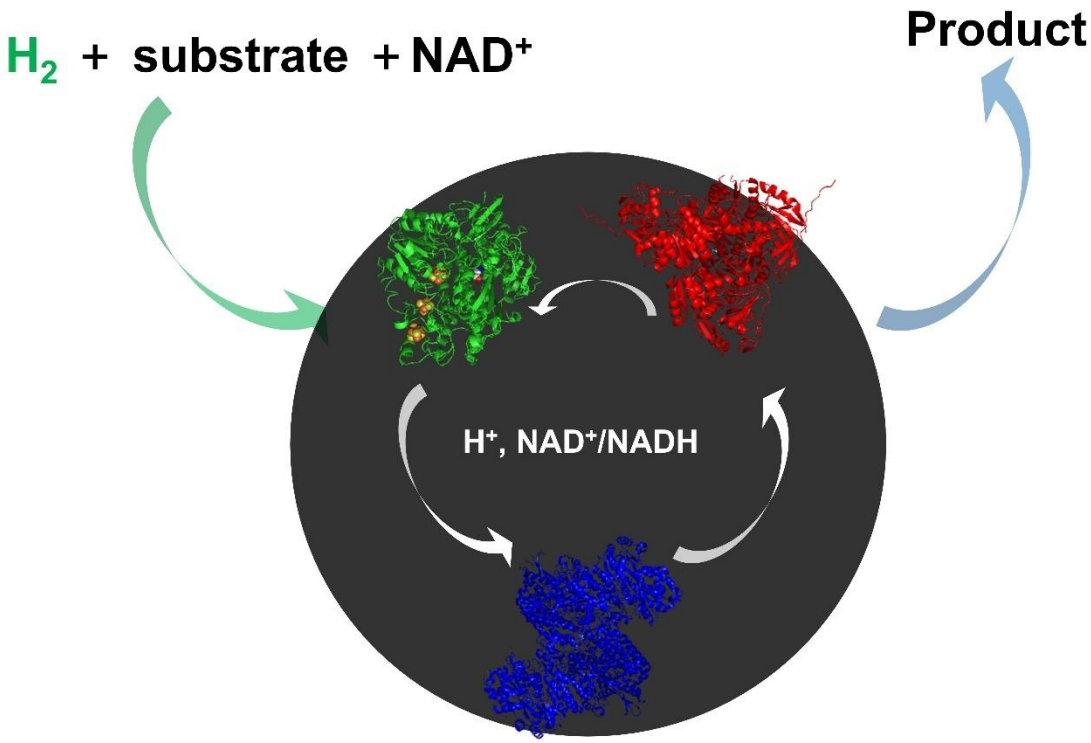
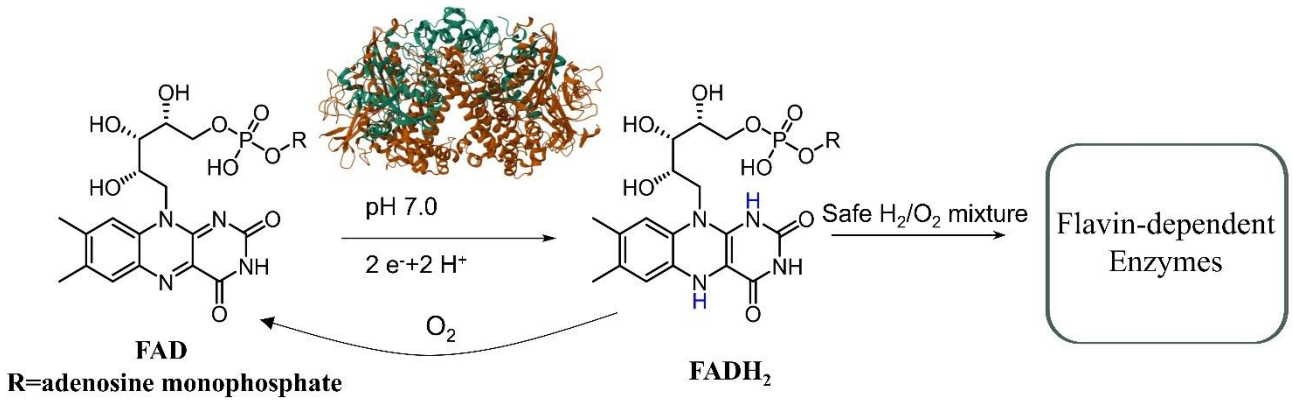


Figure 12. The enzyme-modified particles for H_2-driven NADH recycling system. Hyd-2 (green, PDB: 6EHQ), NAD^+ reductase (blue, PDB: 5XFA), alcohol dehydrogenase (red, PDB: 4Z6K).

1.3.2.2. Flavin recycling

Joseph Srinivasan *et al*. reported that Hyd-1 is able to efficiently reduce the important cofactors riboflavin, FMN and FAD using H_2 as a simple and fully atomically economical reducing agent.[56] The resulting reduced flavins ($FMNH_2$ and $FADH_2$) can be directly supplied to old yellow enzyme (OYE)-like alkene reductases for efficient asymmetric reduction of olefins. This process exhibits excellent catalytic performance with Hyd-1 over a wide temperature range (25-70 ℃) while remaining stable over long reaction times, demonstrating the adaptability of Hyd-1 in diverse complex environments.

A significant advantage of the Hyd-1 system is that it is simpler and more environmentally friendly than traditional cofactor recovery methods relying on NAD(P)H. This dramatically minimises costs and reduces chemical waste, making it particularly suitable for biotechnology applications where sustainability is important. In addition, the ability of Hyd-1 to operate stably in the presence of O_2 and its wide pH range make it more flexible and practical for industrial processes. For example, Hyd-1 has been successfully applied in NADH-independent biocatalytic systems, where it facilitates the reduction of FMN to its hydroquinone form $FMNH_2$, which then serves as a reductant for nitroreductases. This application is particularly significant for the clean and efficient hydrogenation of nitro groups to amines as this is a process that has been widely used in the pharmaceutical and fine chemical industries.[86] In the future, this system is expected to find application in a wider range of flavin-dependent enzymes including, but not limited to, halogenases (for chlorination, bromination, and iodination) and flavoprotein monooxygenases (for epoxidation, hydroxylation, and Baeyer-Villiger oxidation), which are under-utilised in industrial biotechnology due to the lack of simplified flavin recovery systems (Scheme 3). The performance of Hyd-1 in industrial catalysis could be enhanced by further optimising its structure and function, e.g. by mutating it to increase its unnatural flavin-reducing activity. The promise of Hyd-1 for clean and efficient flavin recycling offers great promise for the development of more sustainable and economical biocatalytic solutions, which are expected to play a key role in pharmaceuticals, fine chemicals production, and broader biomanufacturing.[87,88]



Scheme 3. H_2-driven flavin recycling system by Hyd-1.

1.4. Enzymes studied in this thesis

1.4.1. Halogenases

Halogen compounds occupy an irreplaceable position in the life sciences and chemical manufacturing industries, and their importance is reflected in many fields such as pharmaceuticals, agrochemicals, and organic synthesis. About 20% of small molecule drugs and 30% of agricultural chemicals contain halogen atoms.[89] Adding halogens can not only significantly change the physical and chemical properties of the molecules, but may also significantly affect their biological activity and metabolic processes.[90] Specifically, for drug molecules, the introduction of a halogen can often improve the selectivity and binding of the targeting molecule, increase its ability to pass through the cell membrane, or adjust the half-life of a drug in the body.[91,92,93] In addition to small molecule drugs, halogens also play an important role in the modification of peptides, proteins and nucleic acids, helping to develop new biopharmaceuticals and diagnostic tools.[94,95] Moreover, halogen compounds also play a crucial role in metal-catalysed cross-coupling reactions, such as Suzuki, Heck, and

Buchwald-Hartwig coupling reactions. These reactions are widely used in the synthesis of complex molecules, especially in drug and materials science to build key backbones and functionalised moieties.[96,97,98]

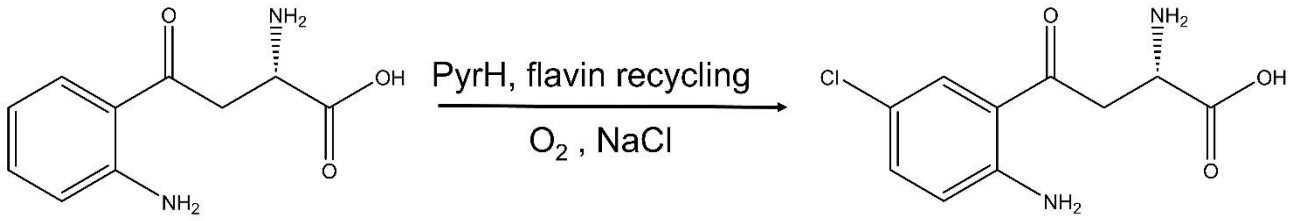
Traditionally, halogenated compounds are mainly obtained through chemical synthesis, and these synthesis methods usually involve high energy consumption, the use of toxic reagents, and the generation of large amounts of by-products and waste, resulting in serious environmental pollution and resource waste.[99,100] For example, halogenating agents commonly used in chemical halogenation processes, such as chlorine gas, bromine water, and hydrogen iodide, are highly corrosive and toxic, pose high operational risks, and have poor reaction selectivity. These could easily generate a series of halogenated waste that are difficult to separate.[101] In addition, traditional chemical methods tend to have low stereoselectivity and regioselectivity and cannot precisely control the introduction position of halogens in the molecule, which is particularly critical in drug development because the three-dimensional structure of the molecule is crucial to its biological activity.[102,103]

The rise of biocatalytic technologies, especially the application of halogenases, provides innovative solutions to these challenges. Halogenases can efficiently catalyse specific halogenation reactions under mild conditions and have excellent stereo and regioselectivity. These enzymes originate from microorganisms, plants, and marine organisms in nature, and they have evolved through natural selection to be highly selective for specific substrates,

which is particularly beneficial for the fine modification of complex molecules. In addition, with the development of protein engineering and directed evolution technologies, natural halogenases have been able to be modfied to enhance their catalytic activity, substrate adaptability, and operational stability. This greatly expands the application range of halogenases in the synthesis of complex organic molecules.[104,105,106,107]

1.4.1.1. Flavin-dependent halogenases

To date, there are four main types of halogenases: haloperoxidase, nonheme Fe(II) α-ketoglutarate-dependent halogenase, S-adenosyl-L-methionine (SAM) dependent halogenase and flavin-dependent halogenase (FD-halogenase).[108] Among these major halogenases, flavin-dependent halogenase usually acts on aromatic compounds and has a strict substrate specificity and stereoselectivity, making it a practical tool for biosynthesis and catalytic halogenation.[109]



Scheme 4. Representative halogenation reaction catalysed by a flavin-dependent halogenase PyrH. PyrH catalyses the regioselective chlorination of L-kynurenine to yield 5-chloro-L-kynurenine using a flavin recycling system under aerobic conditions in the presence of NaCl.

They typically consist of two domains – an N-terminal FAD-binding domain (with a conserved Rossmann fold and motifs for binding the flavin) and a C-terminal substrate-binding domain

– forming a bifunctional active site separated by an ~10 Å tunnel.[108] The cofactor flavin adenine dinucleotide (FAD) is bound in the enzyme and is first reduced to $FADH_2$ by a partner flavin reductase using NADH or NADPH. This reduced flavin then reacts with molecular oxygen to form a C4a-hydroperoxyflavin (FAD-OOH) intermediate. A halide ion (usually chloride, though bromide can often be utilized) bound near the flavin cofactor attacks this peroxide, resulting in formation of a hypohalous acid (e.g. HOCl) as the reactive halogenating species. Because the flavin cofactor site and the substrate pocket are distinct, the nascent HOX intermediate diffuses through the internal tunnel to the substrate-binding site. For example, in a tryptophan 7-halogenase PrnA, a conserved active-site lysine K79 helps position and polarise the HOX to direct the electrophilic halogen to the substrate either via hydrogen bonding or a transient Lys–Cl adduct. The π-electron density of the indole ring nucleophilically attacks the electrophilic chlorine, forming a C–Cl bond and resulting in a non-aromatic σ-complex (Wheland intermediate) in which the positive charge is delocalised across the conjugated indole system, particularly stabilised by the lone pair of the nitrogen and adjacent π orbitals. This intermediate is subsequently rearomatised by base-assisted deprotonation, most likely facilitated by glutamate acid E346, which abstracts the C7 proton and allows reformation of the aromatic π-system. The reaction thus combines electrophile generation, regioselective attack, and proton elimination within a confined and pre-organised active site, allowing PrnA to achieve site-specific halogenation of tryptophan under mild physiological conditions with a precision difficult to replicate in traditional chemical halogenation. (Figure 13).[110,111]

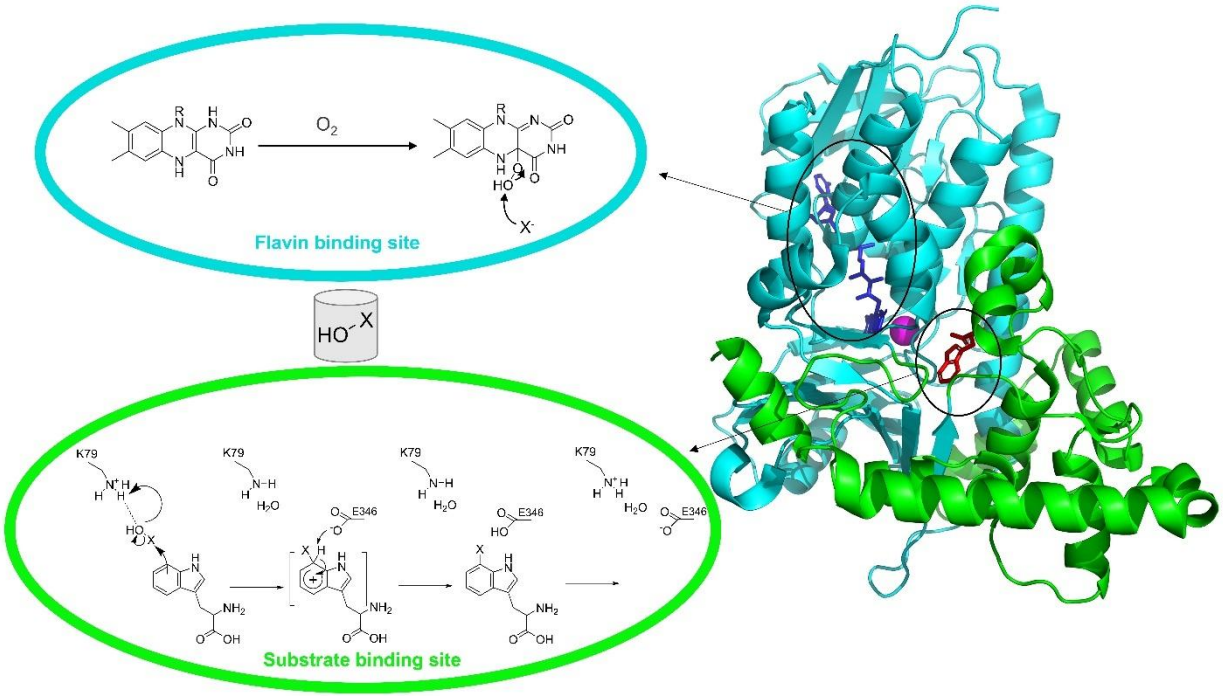


Figure 13. Catalytic mechanism of FD-halogenase PrnA (PDB: 2AQJ, the flavin binding site is coloured cyan, the substrate binding site is coloured green, blue sticks: FAD, red sticks: tryptophan, pink sphere: Cl^- ion).

To date, no flavin-dependent halogenase has been reported to catalyse fluorination reactions, likely due to the high electronegativity of fluorine and the instability of hypofluorous acid (HOF) as a potential fluorine donor. Currently, these enzymes are limited to catalysing chlorination, bromination, and iodination reactions.[112,113,114] Also, their application is currently limited by relatively low activity, poor stability, and substrate-product inhibition, as these enzymes evolved for secondary metabolic pathways rather than essential functions.[115,116] To address these limitations, significant efforts are underway to engineer flavin-dependent halogenases with improved catalytic efficiency, broader substrate scope, and enhanced stability through techniques such as rational mutagenesis, directed evolution, and the discovery of thermostable variants from extremophiles. These advances aim to adapt flavin-dependent

halogenases for industrial-scale applications, providing more efficient and sustainable processes for the production of halogenated compounds in various chemical industries.[117]

With the development of genome mining and gene sequencing, more and more halogenases are being discovered. The major substrates are L-tryptophan, pyrrole-like compounds, phenolic compounds and indole.[118] To broaden the substrate scope, research into protein engineering of flavin-dependent halogenases has been conducted. Payne et al., for example, carried out preliminary directed evolution to improve the stability of the wild-type FDH RebH. Since the substrate scope was limited to tryptophan-like compounds, they further evolved the stabilized RebH variant to enhance the substrate scope, and two notable variants were identified. Variant 3-SS is able to achieve high conversion of tricyclic tryptoline derivatives, while variant 4-V could accept a wide range of large indoles and carbazoles that are typically not accepted by wild-type RebH. Their directed evolution efforts revealed key regions of the enzyme that govern substrate specificity. Mutations such as N467T, N470S, and G112S in variant 3-SS, located in the active site, contributed to improved substrate binding and regioselectivity. Additionally, the A442V mutation in variant 4-V, despite being distant from the active site, played a crucial role in broadening the substrate scope, demonstrating that allosteric effects can significantly influence enzyme function.[119] Furthermore, Lang et al. explored altering the regioselectivity of the flavin-dependent tryptophan 7-halogenase PrnA through site-directed mutagenesis. By analysing the enzyme's structure and comparing it with the tryptophan 5-halogenase PyrH, key residues (F103A) was identified for mutation.

The F103A variant led to a mixture of 7- and 5-halogenated tryptophan products, indicating a shift in substrate orientation within the active site.[120]

One study on tryptophan 6-halogenase Thal has revealed several factors that lead to its low catalytic efficiency.[121] This research found significant leakage of hypohalous acid (HOX) from the active site, which greatly decreases the product coupling ratios. This leakage results in inefficient use of the HOX intermediate (Figure 14), because instead of taking part in the tryptophan halogenation, HOX escapes.

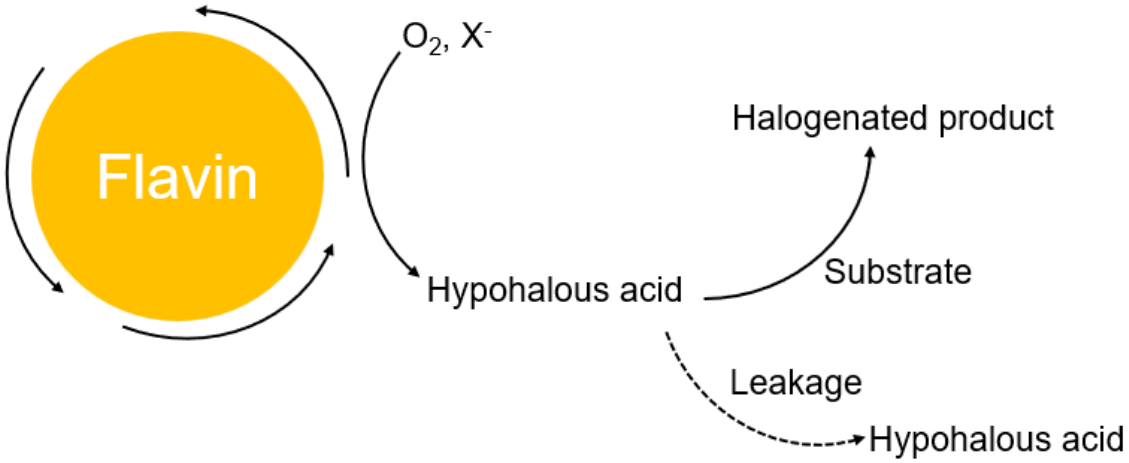


Figure 14. Leakage of hypohalous acid during the catalysis by flavin-dependent halogeanses.

In addition, the study emphasises the crucial role of the conserved amino acid Lys79, which is essential for the enzyme's function. Mutations at this site will make the enzyme inactive. It suggests that Lys79 may act as a proton donor in the catalysis process rather than forming a chloramine or bromamine intermediate. The study also provides an understanding of the

enzyme's interaction with different halides including iodide, bromide and chloride. In the reaction, iodide, bromide and chloride show different reaction rates because of their different physical and chemical properties. Iodide ions have a larger ionic radius and a more diffuse electron cloud, which makes their combination with C4aOOH - FAD (peroxyflavin intermediate) more effective. Calculations suggest that the transition state formed is more stable, leading to lower activation energy and a faster reaction rate. In contrast, chloride ions have a smaller ionic radius and a more concentrated electron cloud. Their combination with C4aOOH - FAD is weaker and a slower reaction rate. The properties of bromide ions are between those of iodide and chloride ions, and its reaction rate is also in the middle. Moreover, structural analyses through crystallography further explain these phenomena. In particular, they show that the structural limitations in the substrate binding sites prevent Thal from effectively iodinating tryptophan, although it has the ability to form hypoiodous acid. Based on this, Prakinee et al. have shown that the tunnel engineering and site-saturation mutagenesis within the enzyme can effectively contain hypohalous acid and minimise its leakage. For example, the study of the Thal: V82I (mutant of Thal) provided insights into how specific amino acid alterations can improve enzymatic function. This mutation resulted in a wider substrate scope, higher melting point of the protein, and greater pH tolerance. Molecular dynamics simulations supported these findings by showing that the V82I mutation facilitated the alteration of the hydrophobic interactions within the enzyme’s tunnel. This modification led to a 50% reduction in HOBr leakage and enhanced the overall reaction rate. [122]

To overcome the inherent instability of flavin-dependent halogenases, Minges et al. have turned to disulfide bond engineering.[123] Taking tryptophan 6-halogenase Thal and tryptophan 5-halogenase PyrH as research objects, cysteine residues were introduced at the dimer interface. This design led to the emergence of variants such as 'Thal CC'. Compared with the wild type, its thermal stability was significantly enhanced (T_{50} = 15.7 K, where T_{50} represents the temperature at which 50% of the enzyme activity is lost after a defined incubation time), and the time stability at high temperatures was also greatly improved. More importantly, this stabilization strategy was successfully extended to other halogenases, and through the optimisation of cysteine mutations at alternative sites on the dimer interface, the thermal stability of PyrH was further improved. Directed evolution has also been employed to improve the performance of flavin-dependent tryptophan 6-halogenase. Error-prone PCR and semi-rational mutagenesis techniques were combined to overcome the difficulties in improving thermal stability and catalytic efficiency and to systematically study the impact of active site mutations on enzyme performance. After arduous exploration, the triple variant 'Thal – GLV' was successfully obtained. Compared with the wild-type enzyme, the thermal stability of this variant was greatly improved (melting temperature = 23.5 K), and it exhibited higher activity at room temperature (25 °C).[124]

Flavin-dependent halogenases require a continuous supply of reduced FAD to function, which normally requires the incorporation of glucose, glucose dehydrogenase, flavin and flavin reductase (Fre). This method enables the recycling of the expensive coenzymes FAD

and NADH (Figure 15). However, these additional components can complicate the entire catalytic process and produce unwanted waste gluconolactone and the biocatalysis becomes harder to scale up. Other current cofactor recycling methods such as light-driven cofactor recycling, use of NADH mimics, etc. suffer from a loss in activity or lower turnover frequency compared to enzymatic methods.[125]

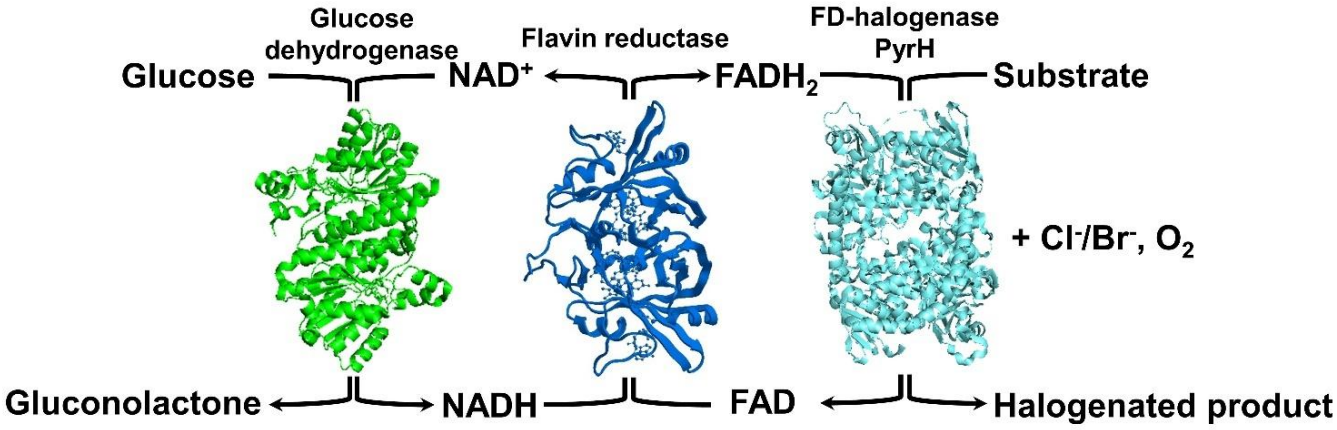


Figure 15. Conventional operation in which NADH and FADH2 are recycled via catalysis of two enzymes, glucose dehydrogenase (PDB: 1GCO) and reductase Fre (PDB: 2ED4), to support catalysis by the FD-halogenase PyrH (PDB: 2WEU) which requires $FADH_2$, O_2 and halide source.

1.4.1.2. Other halogenases

Besides FD-halogenases, haloperoxidases are also a class of halogenases. They are enzymes that use hydrogen peroxide as an oxidant to catalyse halogenation reactions. In addition, they are divided into two main types according to the different metal auxiliary groups they rely on: iron-containing porphyrin ring haloperoxidases (haem iron haloperoxidases) and vanadium-dependent haloperoxidases.[126,127] Among them, vanadium-dependent haloperoxidases catalyse halogenation reactions by generating vanadium-bound peroxide

intermediates, which can also oxidise halide ions and generate corresponding hypohalous acids. These hypohalous acids then react non-enzymatically with electron-rich aromatic substrates. For instance, V-HPOs from *Curvularia inaequalis* can catalyse the bromination of 1,3,5-trimethoxybenzene to form 2-bromo-1,3,5-trimethoxybenzene, a typical aromatic halogenation reaction.[128,129] The catalytic mechanism of haem iron haloperoxidases is to use the iron centre to react with hydrogen peroxide to generate highly active iron oxo intermediates, which further oxidise halide ions (such as Cl^- or Br^-) to form hypohalous acids. These intermediates then halogenate substrates outside the active site. A typical reaction is the chlorination of anisole (methoxybenzene) to form 4-chloroanisole. However, the activity of haloperoxidases depends on hydrogen peroxide, which limits their application in systems without an external hydrogen peroxide source. In addition, the hypohalous acid generated in the catalysis may lack selectivity for specific substrates, which may lead to non-specific halogenation and affect the purity and conversion of the product.[130]

Another type of halogenases is the non-heme iron-dependent halogenases, which use non-heme iron and α-ketoglutarate(αKG)-dependent catalytic mechanism to perform halogenation reactions.[131] Their catalytic mechanism involves the interaction of the iron (II) centre with α-KG and O_2 to form complex reaction intermediates. First, iron (II) reacts with α-KG and O_2 to form an energetic intermediate containing iron (IV) oxo group. This intermediate generates a carbon-basded radical through the abstraction of a hydrogen atom of the substrate, which then reacts with halide ions in the solution to form the corresponding

halogenated derivative.[132,133] A representative example is SyrB2, which catalyses the chlorination of L-threonine tethered to a carrier protein (SyrB1) at the γ-position to form 4-chloro-L-threonine. This type of enzyme usually performs highly selective halogenation on non-activated carbon centres, but this also means that it has strict requirements on the structure of the substrate and is not applicable to all types of organic molecules.[134]

The last type of halogenase is the nucleophilic halogenase, which mediates halogenation through a nucleophilic attack mechanism. The most widely studied example is the fluorinase (also known as 5′-fluoro-5′-deoxyadenosine synthase). This enzyme catalyses the reaction between fluoride ions and S-adenosyl-L-methionine (SAM), replacing the methylsulfonium group in SAM with a fluorine atom to form 5′-fluoro-5′-deoxyadenosine (5′-FDA) and L-methionine as a by-product.[135] The reaction proceeds via direct nucleophilic attack of the fluoride ion on the C5 carbon of the ribose moiety in SAM. The C5′ carbon is activated due to the excellent leaving group ability of the adjacent methylthioadenosine moiety. This results in a stereospecific displacement to form 5′-FDA. The enzyme's active site is tightly organised to stabilise the transition state, precisely orient the F^- ion, and shield it from bulk water, as free fluoride is normally a poor nucleophile in aqueous environments.[136,137] This enzyme is relatively rare in nature, but plays an important role in the production of specific fluorinated natural products, such as in the biosynthetic pathways of antibiotics and anticancer agents. However, due to their rarity, these enzymes can usually only accept and convert a few substrates, greatly limiting their range of applications.[138]

1.4.2. Flavin-dependent monooxygenases

In addition to halogenases, another important class of flavin-dependent enzymes widely utilised in biocatalysis are flavin-dependent monooxygenases (FMOs), which catalyse a diverse array of oxidative transformations.[139] FMOs are widespread in nature and are a key class of enzymes essential to the anabolism and catabolism of living organisms. The flavin is reduced by NAD(P)H, reacting with O_2 to form the flavin hydroperoxide. This intermediate then interacts with a substrate, incorporating one oxygen atom into it while reducing the other to water (Figure 16). These enzymes catalyse a variety of chemical reactions such as hydroxylation, epoxidations, halogenations and Baeyer-Villiger oxidations. These enzymes are classified based on their structure, protein sequence motifs, electron donor types, and the nature of the oxygenation reaction they perform. They are grouped into eight categories, each having unique mechanisms and properties. Some rely on external electron donors like NAD(P)H (Groups A and B), while others operate as two-component systems involving a monooxygenase and a flavin reductase (Groups C to F). There are also internal monooxygenases that utilise the substrate itself as an electron donor (Groups G and H).[140,141] Each group exhibits distinct features in terms of the type of reactions they catalyse, the substrates they utilise, and the mechanisms by which they activate O_2, making them integral to both natural and engineered biochemical pathways.[142]

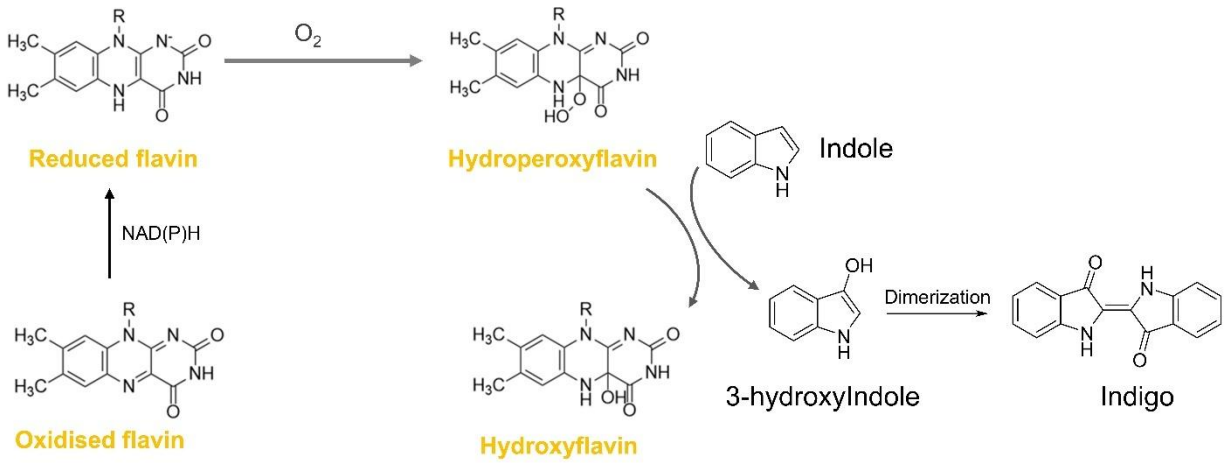


Figure 16. Catalytic mechanism of flavin-dependent monooxygenases.

In traditional chemical synthesis, a variety of methods are used to perform reactions like those catalysed by flavin-dependent monooxygenases. For example, hydroxylation often employs strong oxidisers like osmium tetroxide or palladium catalysts, offering controlled reactions but at the expense of severe conditions or over-oxidation risks.[143, 144] In addition, Baeyer-Villiger oxidations commonly use hazardous peracids such as meta-chloroperoxybenzoic acid (mCPBA) or employ catalytic methods that provide more sustainable alternatives with decreased peracid usage.[145,146] Moreover, epoxidation is typically done using peracids or through the Sharpless asymmetric method, which utilises titanium and tartrate under milder conditions for high enantioselectivity.[147] While these chemical methods are robust and effective, they often carry disadvantages such as environmental harm, stringent reaction conditions, poor selectivity and safety concerns. In contrast, biocatalytic processes with FMOs, despite being possibly slower and less scalable, offer greener alternatives by operating under milder conditions, demonstrating higher specificity, and producing lower

amounts of toxic waste, thus driving advancements towards more sustainable industrial chemical practices.[148]

1.5. Aims of this project

Halogenated compounds have wide applications in pharmaceuticals and agrochemicals. Traditional chemical halogenation methods rely on toxic reagents and harsh conditions, causing severe environmental pollution. While existing enzymatic methods are cleaner, they are complex and costly due to their dependence on expensive cofactors and auxiliary enzymes, making them difficult to apply widely in the industry. This project explores innovative methods for supplying reduced flavin cofactors using Hyd-1. The project aims to reduce oxidised flavins to their hydroquinone form, primarily utilising H_2 as the reductant. This method promises a more sustainable approach to using enzymes like flavin-dependent halogenases, monooxygenases, and haloperoxidases in chemical synthesis. As biocatalysis becomes increasingly important in producing pharmaceuticals, complex chemicals, and agrochemicals, the need for efficient cofactor recycling systems grows. Conventional systems often involve expensive cofactors, NAD(P)H, and produce significant waste, complicating scale-up efforts due to their fragility and complexity.

The focus of this project is on creating a simple, green, and economical cofactor recycling system to support halogenases. This research has developed a H_2-driven flavin recycling

system for coupling with flavin-dependent halogenases. It leverages the robustness of Hyd-1. This enzyme is O_2-tolerant and functions effectively across various temperatures, solvent conditions, and mild H_2 pressures. Therefore, it allows for direct reduction of important cofactor flavins using H_2 in the presence of safe O_2 levels. This method simplified the operation of halogenases by lowering reliance on expensive cofactors and auxiliary enzymes. At the same time, it demonstrated good conversions in halogenating substrates compared to the state of the art, making the halogenation process cleaner, cheaper and more sustainable. The implementation of this project has the potential to enhance the scalability and sustainability of enzymatic halogenation in industrial applications, leading to broader adoption of cleaner and more cost-effective biocatalytic technologies.

2

Chapter 2

2.1. Enzymes and chemicals

2.1.1. Overexpression and isolation of Hyd-1

This chapter describes the methodologies used for the overexpression, purification, and characterisation of key enzymes studied in this work (Hyd-1, FD-halogenase PyrH and flavin reductase Fre). Hyd-1 is composed of two subunits, HyaA and HyaB, which are encoded by the hyaA and hyaB genes, respectively. To enable efficient purification, all three proteins were engineered with N-terminal His-tags, allowing affinity purification via Ni-NTA (nickel-nitrilotriacetic acid) chromatography. Beyond purification, this chapter also details the analytical techniques used to assess enzyme activity and reaction outcomes such as UV-visible spectrophotometry, high-performance liquid chromatography (HPLC), and gas chromatography (GC).

The overexpression process began with the inoculation of LB medium containing transformed Hyd-1 cells from *E.coli* harboring the hyaA and hyaB genes. 50 mL LB medium was incubated overnight at 37 ℃, 220 rpm. Next, 100 µM of $FeCl_3$, 30 µM of $NiCl_2$ and 48 g of sodium fumarate were added to the 1L TB medium before the overnight starter culture was added to TB medium. The TB medium was then topped up with autoclaved water and incubated at 37℃ in stasis for 41 hours. Cells were collected by centrifugation at 4500 *xg* for 10 mins at 4 ℃. For the purification process, cell pellets were resuspended in Buffer A (Tris 100 mM, 350 mM NaCl, 3% Triton X-100, 1 mM DTT pH 7.5, DNase, lysozyme and a protease inhibitor tablet). Cells were disrupted by passage through a French press (2 times, 25000 psi) at 4 ℃. The

crude lysate was centrifuged at 18000 *xg* for 1 hour. The supernatant lysate was loaded into an AKTA purification system (3 x 5 mL HisTrap FF columns in series and attached to peristaltic pump). Buffer B (Tris 20 mM, NaCl 350 mM, imidazole 750 mM, Triton X100 0.02%, DTT 1 mM, pH 7.2) was used to elute the lysate. A dialysis tubing was used to exchange the purified enzymes into the storage buffer (Tris 50 mM, NaCl 350 mM, DTT 1 mM, pH 7.2, 10% glycerol) and the protein was concentrated by several cycles of in a 30 kDa Centricon Centrifugal Filter unit (8000 *xg*, 10 mins). The purified enzyme samples were separated into aliquots (30 mL) and snap-frozen in liquid nitrogen for long-term storage. The purity of the purified Hyd-1 was determined by SDS-PAGE analysis (Figure 17), and protein concentration was estimated by the Bradford assay.[149]

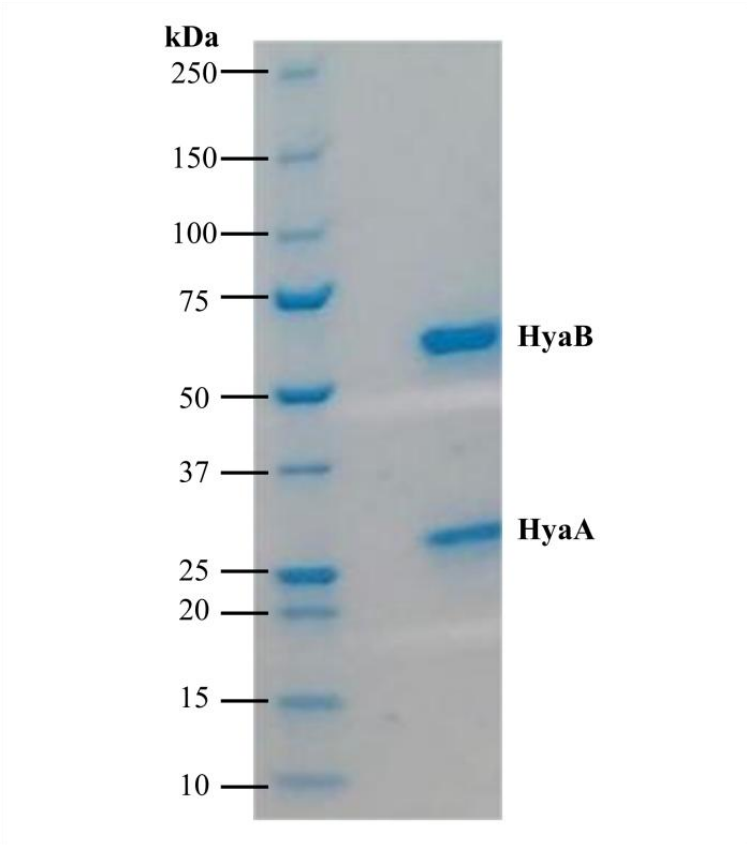


Figure 17. SDS-PAGE analysis of purified Hyd-1.

2.1.2. Overexpression and isolation of FD-halogenase PyrH and flavin reductase Fre

The gene for FD-halogenase *Streptomyces rugosporus* PyrH was synthesized (GeneArt, UK) with an N-terminal 6xHis-tag and enterokinase cleavage site and cloned in the expression vector pet100. The construct was then sequence verified and labeled p546_sg_PyrH. Transformation of *E. coli* BL21 (DE3) with this construct enabled the expression of tagged PyrH. The gene for the *E. coli* flavin reductase, Fre, had been previously cloned into plasmid pet45b-fre by Shepherd et al,[150] containing a N-terminus 6xHis tag. This plasmid was transformed into *E. coli* BL21 (DE3) cells. In each case, 50 µL transformed cells were cultivated overnight at 37 ℃, 220 rpm in LB medium containing ampicillin (100 µg/mL). The overnight starting culture was then added to 1 L TB medium containing ampicillin (100 µg/mL) and incubated at 37 ℃, 200 rpm until OD_{600} reached around 0.6. The culture was then cooled to room temperature and protein expression was induced by adding IPTG (to 0.3 mM) before incubating at 18 ℃ for a further 18 hours. Cells were collected by centrifugation at 6000 *xg* for 20 mins at 4 ℃. Around 10 grams of cells pellet was resuspended in 40 mL of lysis buffer (350 mM potassium phosphate buffer, pH 7.3, 300 mM NaCl, 20 mM imidazole). After disrupting the cells by sonication (2 sec. pulse, 5 sec. off, 5 minutes of total sonication) in an ice-water bath, the crude lysate was subjected to centrifugation at 16000 *xg* for 1 hour. The soluble lysate was loaded onto a Ni-NTA column purification, and the column was washed with lysis buffer. The target protein was then eluted with elution buffer (100 mM sodium phosphate buffer, pH 7.3, 300 mM NaCl, 200 mM imidazole). A 10 kDa cut-off centrifugal

filter unit was used to exchange the purified protein into storage buffer (50 mM potassium phosphate buffer, pH 7.3, 300 mM NaCl) and concentrate it (8000 *xg*, 10 mins). Purified protein samples were split into aliquots and snap frozen in liquid nitrogen for long-term storage. The purity of the purified proteins was determined by SDS-PAGE analysis (Figure S2). The concentration of PyrH and Fre was determined by Bradford assay (Figure 18).[150]

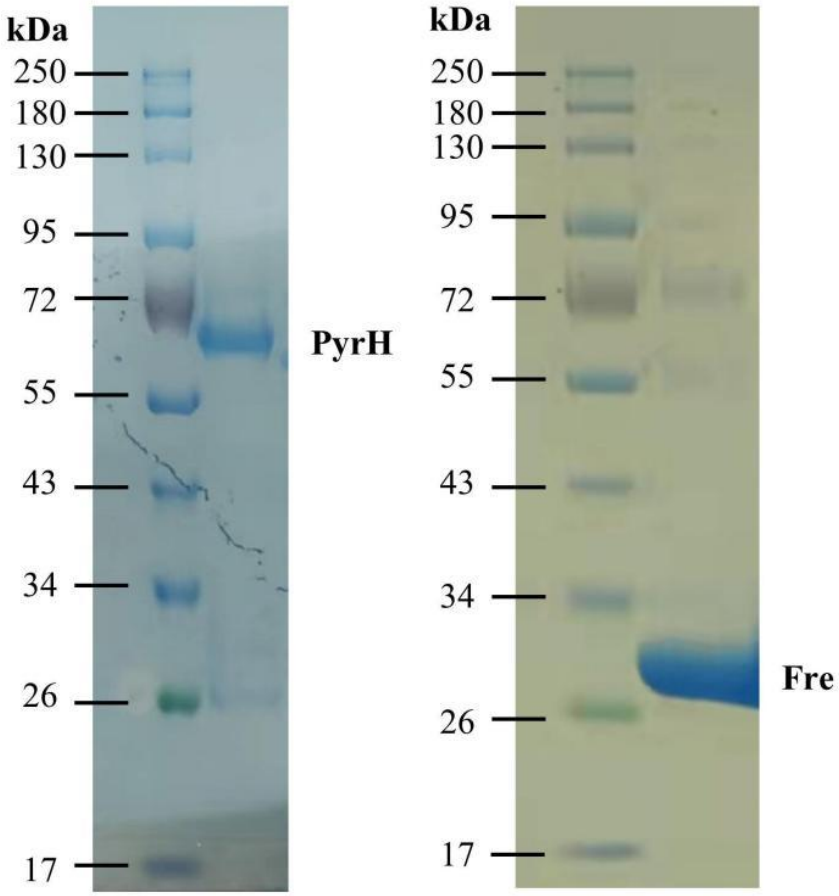


Figure 18. SDS-PAGE analysis of purified PyrH and Fre. After overexpression, the PyrH (58.14 kDa) and Fre (26.24 kDa) were purified by Ni-Affinity Chromatography. The concentration of PyrH and Fre was determined by Bradford assay.

2.2. Equipment, chemicals and experimental protocol

FAD (disodium salt, ≥98%, Cayman Chemicals), L-tryptophan (1, Fluorochem), 5-chloro-tryptophan (2, Carbosynth Ltd.). anthranilamide (4), potassium phosphate buffer salts, glucose, NAD+, Glucose dehydrogenase from Pseudomonas sp., NaCl, NaBr, *trans*-β-methylstyrene and catalase from bovine liver were purchased from Sigma-Aldrich. All the solutions and buffer were prepared with 50 mM potassium phosphate (MilliQ water).

High-performance liquid chromatography (HPLC) was employed to monitor biohalogenation reactions. Analyses were carried out using a Shimadzu HPLC system equipped with a LC-20AD dual-plunger parallel-flow pump, SIL-20A HT autosampler, CTO-10AS VP column oven, FRC-10A fraction collector, SPD-20A UV–vis detector, and CBM-20A system controller, with online degassing. Chromatographic separation was performed on a ZORBAX RR Eclipse Plus C18 column (Agilent, 95 Å, 4.6 × 100 mm, 3.5 µm particle size). The mobile phase consisted of an isocratic mixture of 60% water and 40% methanol, both containing 0.1% trifluoroacetic acid (TFA). The flow rate was maintained at 1.0 mL/min with a total run time of 15 minutes. The detection wavelength was 220 nm. All solvents used were of HPLC grade.

Gas chromatography (GC) was used to assess bioepoxidation products. Analyses were conducted using a ThermoScientific Trace 1310 GC system fitted with a CP-Chirasil-Dex CB chiral column (Agilent; 25 m length, 0.25 mm internal diameter, 0.25 µm film thickness),

protected by a 10 m undeactivated fused silica guard. The carrier gas was hydrogen (CP grade) supplied at a constant pressure of 170 kPa. The oven program began with an isothermal hold at 70 °C for 5 minutes, followed by a temperature ramp to 120 °C at 2 °C/min from 5 to 15 minutes, then a further ramp to 180 °C at 10 °C/min from 15 to 30 minutes, concluding with a 5-minute hold at 180 °C.

All samples were centrifuged using a 1.5 mL centrifuge (Eppendorf) at 13,000 rpm for 5 minutes before analysis to remove precipitated proteins. At different time points, 10 µL aliquots were taken from the reaction mixture and diluted by adding potassium phosphate buffer. The reaction mixture was quenched by heating to 95 ℃, followed by centrifugation at 14000 rpm for 5 minutes. The supernatant was then collected for HPLC analysis. For GC analysis, 400 µL aliquots were taken from the reaction mixture. Subsequently, ethyl acetate was used to extract the samples and anhydrous sodium sulfate was used to remove the water in the solution. Reactions were conducted according to a set of standard Procedures (A-D), with any modifications to these (eg variation in substrate or substrate concentration) specified in the text.

2.2.1 Procedure A (conventional PyrH operation with GDH/glucose)

A 200 µL reaction mixture was prepared in a 1.5 mL Eppendorf tube, and comprised 1 µM FAD, 30 mM NaCl, 0.5 mM L-tryptophan, 100 µM NAD^+, 200 mM glucose, 3 µM glucose

dehydrogenase (GDH), 5 μM Fre and 20 μM PyrH. The Eppendorf tube, open to air, was then placed in a thermomixer at 900 rpm and 30 ℃ for the duration of the reaction. These reaction conditions were adapted from previously optimised protocols reported in the literature.[150]

2.2.2. Procedure B (H_2-driven chlorination by PyrH with Hyd-1/H_2 with pulsed delivery of O_2)

The lid of a 1.5 mL Eppendorf tube was cut off to enable the vial to be capped with a Suba-Seal septum (Sigma-Aldrich). A 200 μL reaction mixture was first prepared, containing 0.5 mM FAD, 30 mM NaCl, 0.5 mM L-tryptophan and 5.8 μM Hyd-1. An inlet needle and an outlet needle were placed through the Suba-Seal septum, and the headspace of the Eppendorf tube was flushed with H_2 for one hour. Subsequently, 20 μM PyrH was injected using a Hamilton syringe. The Eppendorf tube was then placed in a thermomixer at 900 rpm and 30℃, with O_2 gas being regularly injected through the septum via a Hamilton syringe.

To conduct H_2-driven enzymatic halogenation over longer timecourses, an automated mode of delivery for pulsed O_2 was developed. This was used for data recorded using Hyd-1/H_2 with the pulsed O_2 delivery method at substrate concentrations above 0.5 mM. For this, a gas mass flow controller (BROOKS DELTA SMART 2) controlled by IGI Systems: BROOKS SMART Interface v1.0 software, was integrated with Python scripts to achieve programmed delivery of O_2 pulses against a constant background flow of H_2. Specifically, 0.5% O_2 in H_2 was injected into the reaction vessel's headspace every 5 minutes, and the headspace was

flushed with H_2 for 30 minutes every 2 hours. The following is the general Python script code for the delivery of O_2 and H_2:

```
import pyautogui
import time

setpoint_x, setpoint_y = *, *    # find the location of the Setpoint input box on the screen

def set_value(value):
    pyautogui.click(setpoint_x, setpoint_y)    # Click the input box
    pyautogui.write(str(value), interval=0.1)    # Enter the value
    pyautogui.press('enter')    # Press Enter to confirm

while True:
    set_value(*)    # Enter * and press Enter, the actual number depends on the unit
    time.sleep(*)    # Wait for * seconds
    pyautogui.press('backspace', presses=2)
    set_value(0)
    time.sleep(300)    # Wait for 5 minutes
    pyautogui.press('backspace')
```

2.2.3. Procedure C (H_2-driven bromination by PyrH with Hyd-1/H_2 with pulsed delivery of O_2)

The storage buffers of Hyd-1 and PyrH, containing 350 mM and 300 mM NaCl, respectively, were exchanged to potassium phosphate buffer (50 mM, pH 7.0) to minimise the NaCl concentration to less than 1 mM using a 10 kDa cut-off centrifugal unit. All other steps were

consistent with Procedure B, except that this procedure involved the addition of 30 mM NaBr instead of NaCl.

2.2.4. Procedure D (H_2-driven chlorination by PyrH with Hyd-1 and a safe mixture of H_2/O_2)

To run reactions under a constant atmosphere of 0.5% O_2 / 97.5% H_2, a gas mixture was prepared from 2.5% compressed air and 97.5% H_2 using two mass flow controllers (Sierra Instruments Inc, Smart-Trak 2 and Smart-Trak 100). This gas mixture was used to fill a balloon, which was connected to the top of the reaction vial; the reaction mixture was otherwise prepared as for Procedure B.

2.3. UV-vis measurement of flavins

As mentioned above, Hyd-1 can directly reduce flavin under a H_2 atmosphere. Thus, UV-vis spectroscopy was employed to test the H_2-driven reduction of flavin. First, UV-vis was used to obtain the UV spectrum of FAD and riboflavin. As shown in the Figure 19, the oxidised flavin moiety of FAD (left) has a λ_{max} at 450 nm, while riboflavin (right) shows a λ_{max} at 445 nm.

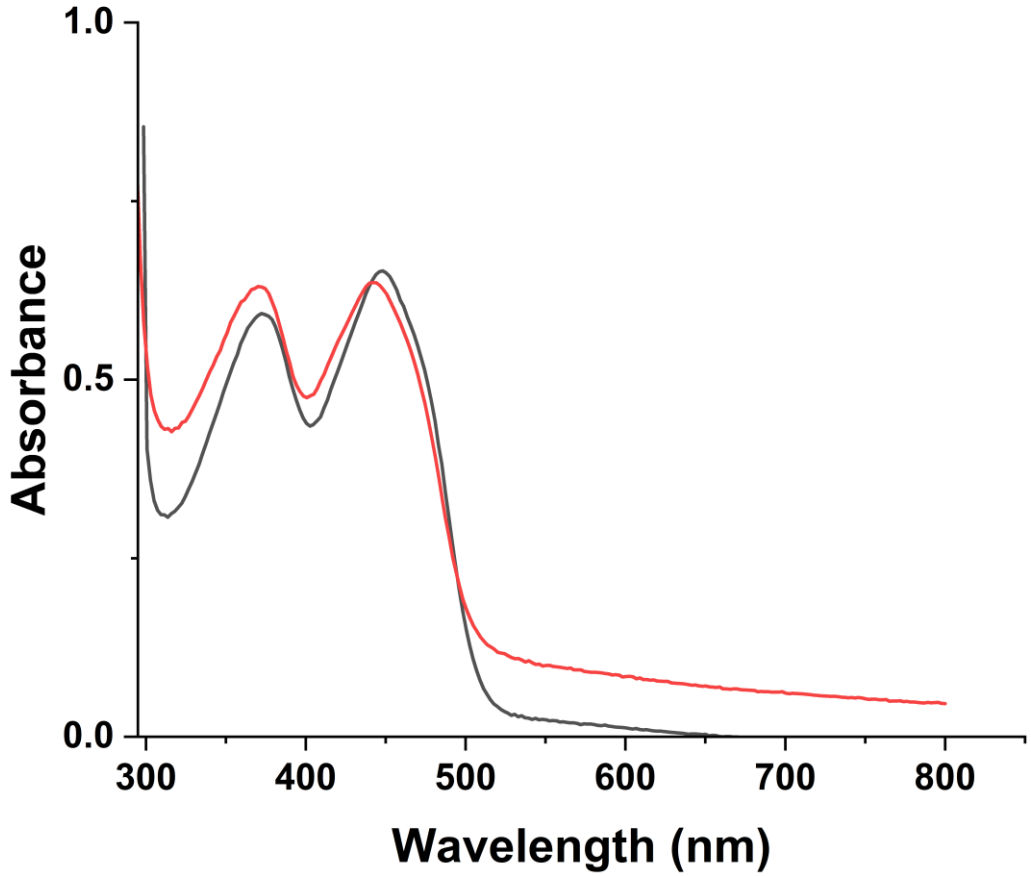


Figure 19. UV-vis absorption spectra of 0.05 mM FAD (black) and 0.05 mM riboflavin (red).

The initial reaction velocity (V_0) is calculated by the linear change in absorbance in the initial stage, and the experiment is repeated at different substrate concentrations to obtain a series of initial rate data. These V_0 are plotted against the substrate concentration ([S]) to form a Michaelis-Menten curve,[151] and the formula is:

$$v = \frac{V_{\max} \cdot [S]}{K_m + [S]}$$

Wherein, V_{max} is the maximum velocity of the reaction, and K_m is the Michaelis constant, which reflects the affinity of the enzyme for substrate. V_{max} and K_m values can be obtained by non-linear least square fitting of *V* vs. [S].

3

Chapter 3

3.1. Introduction

The catalytic mechanism of flavin-dependent halogenases relies on a complex enzymatic cascade that requires the regeneration of FAD and NAD(P)H. However, the complexity and the cost of the cofactors involved in this process have limited their practical applications. To address these challenges, various alternative strategies have been developed to simplify or replace the conventional cofactor recycling system, aiming to decrease cofactor consumption and enhance overall efficiency.

One promising approach involves the use of organometallic complexes, such as pentamethylcyclopentadienyl rhodium-bipyridine complexes, which utilise formate as an electron donor to regenerate $FADH_2$ directly. This system eliminates the need for both a reductase enzyme and NAD(P)H, providing a more simplified method for $FADH_2$ recycling. Experimental results indicate that this chemoenzymatic system can achieve conversion comparable to 85% of those obtained with the conventional cofactor recycling system. However, the efficiency of this system is limited by the concentration of both substrate and formate. High concentrations of formate can inhibit the activity of the halogenase, posing challenges for scaling up the process.[152]

Another notable alternative is a photochemical recycling system, which uses EDTA as a sacrificial reductant and light to recycle the $FADH_2$. This method avoids the use of expensive

NAD(P)H and operates under mild conditions, making it attractive for green chemistry applications. Despite these advantages, the photochemical system also suffers from efficiency issues, particularly during prolonged operations where FD-halogenases are prone to deactivation. Furthermore, by-products generated during photochemical reactions, such as reactive oxygen species, can negatively affect the stability of the enzymes.[153,154]

In addition to these methods, synthetic NADH analogs, such as BNAH, have been employed for the direct reduction of FAD. Unlike the natural NAD(P)H, these analogs provide $FADH_2$ through simplified chemical reactions, avoiding the need for a complex enzymatic system. Studies have shown that in some cases, these NADH mimics can achieve higher $FADH_2$ recycling rates than conventional enzymatic systems. The analogs BNAH is inexpensive and easily synthesised in just two chemical steps, making it an attractive option for practical applications. However, this approach also faces challenges. For example, particularly in the later stages of the reaction, the non-productive consumption of $FADH_2$ occurs due to the accumulation of hydrogen peroxide, which is generated as a by-product. Also, BNAH is converted into BNA^+, which is also a accumulated byproduct of the reaction itself.[155]

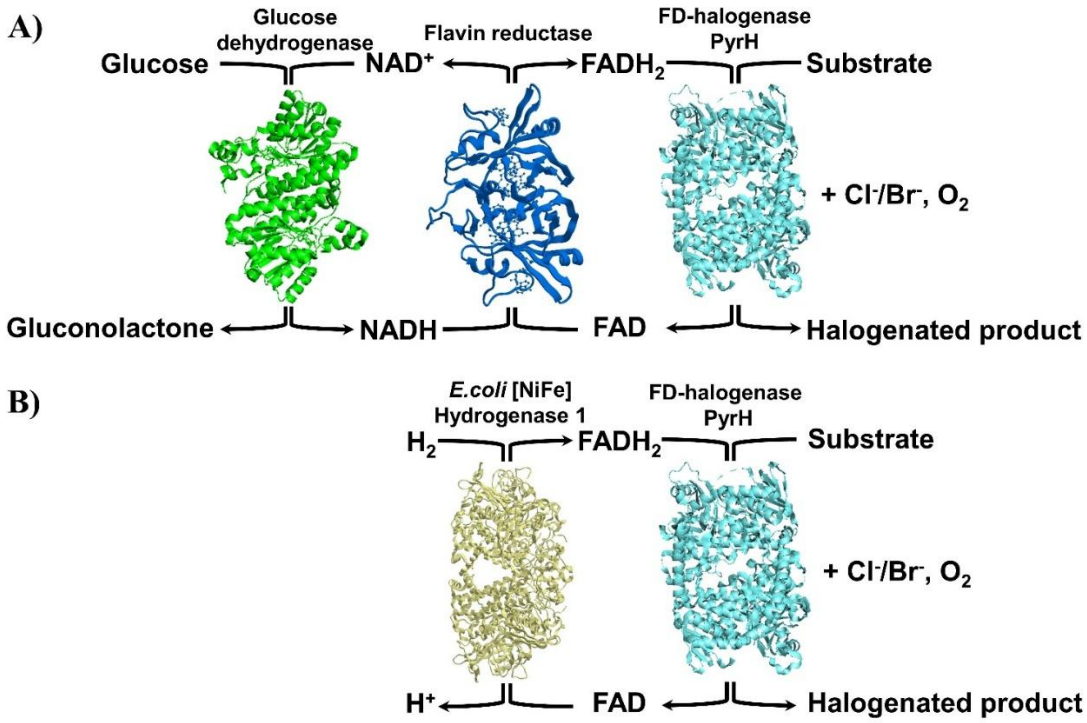
While these alternative systems provide certain improvements, they still suffer from obvious limitations. FD-halogenases generally demonstrate low activity and are prone to inactivation during extended operation due to its inherent instability, which restricts their scalability for industrial production.[156] Although photochemical and chemical regeneration systems

eliminate the need for NAD(P)H, their operational conditions must be optimised to ensure the stability and efficiency over prolonged periods. Thus, further exploration of new alternatives or optimisation of existing systems is essential to unlock the full promise of FD-halogenases in practical applications.

This chapter explores whether leveraging the direct reduction of FAD by hydrogenase under H_2, allows the use of FD-halogenases to be simplified without relying on a carbon-based electron donor, as illustrated in Scheme 4B. Although many hydrogenases are sensitive to O_2 exposure and would thus be inappropriate for such applications, several NiFe hydrogenases exhibit O_2 tolerance. Among them, the robust Hyd-1 stands out due to its ability to sustain H_2 oxidation even in the presence of O_2, alongside its stability across a broad spectrum of pH values and temperatures.[157]

While Hyd-1 retains functionality under aerobic conditions, its H_2 oxidation activity is somewhat compromised when O_2 is present, as some of the electrons generated from H_2 oxidation are shunted towards reducing O_2 to H_2O at the enzyme's active site. Despite this partial diversion, the enzyme maintains satisfactory activity at O_2 levels below approximately 3% in an H_2 atmosphere.[158] Importantly, mixtures of H_2 and O_2 are non-combustible when they are far from stoichiometric ratios. The explosive limits of H_2 and O_2 mixtures depend on the concentration of H_2 in the air or pure O_2. For H_2 in air, the lower explosive limit (LEL) is approximately 4% by volume, and the upper explosive limit (UEL) is about 75% by volume.

In pure O_2, the explosive limits are broader, with the LEL at around 4% and the UEL above approximately 94% by volume.[159] Thus, the safe operation can be allowed under H_2-rich, O_2-lean conditions. This approach aims to maximise electron transfer efficiency from the hydrogenase to FAD while minimising any undesirable direct re-oxidation of the reduced flavin by residual O_2. Moreover, the use of an H_2-rich environment will provide two key advantages: firstly, it could ensure a high availability of electrons for Hyd-1 for the reduction of FAD, critical for the proper functioning of FD-halogenases. Secondly, by maintaining an O_2-lean environment, non-productive side reactions that lead to the re-oxidation of the reduced FAD will be minimised, thus enhancing the efficiency of the entire catalytic process (Scheme 5).



Scheme 5. Operation of FD-halogenase. A) Conventional operation in which NADH and $FADH_2$ are recycled via catalysis of two enzymes, glucose dehydrogenase (PDB: 1GCO) and reductase Fre (PDB: 2ED4), to support catalysis by the FD-halogenase PyrH (PDB: 2WEU) which requires $FADH_2$, O_2 and halide source. B) This work: Hyd-1 (PDB: 6FPW) uses H_2 for the recycling of $FADH_2$ under safe H_2, O_2 mixtures to supply to PyrH.

3.2. Results

3.2.1 H_2-driven reduction of FAD and riboflavin by UV measurement

Direct H_2-driven FAD reduction by Hyd-1 was tested to reproduce work from Srinivasan et al.[56] In addition, this work was also extended to validate the feasibility of the direct riboflavin reduction by Hyd-1. The reaction assay consisted of Hyd-1, FAD (left, 0.05 mM) and riboflavin (right, 0.05 mM) under H_2 flow at 1 bar. Figure 20 shows the decrease in oxidised flavin concentration over time detected by UV-vis spectroscopy. Under the same experimental conditions, according to Beer Lambert law, the rate of the direct FAD reduction catalysed by Hyd-1 is 10.3 µmol/min/mg, and the rate of the direct riboflavin reduction catalysed by Hyd-1 is 16.7 µmol/min/mg, demonstrating that Hyd-1 is more effective in reducing riboflavin than FAD (Figure 21).

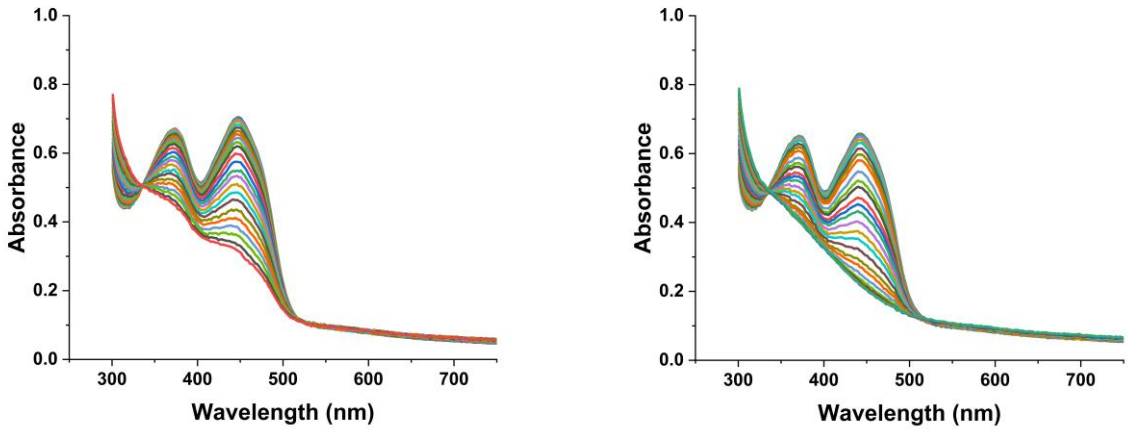


Figure 20. Results of UV/Vis spectrophotometric assays to explore H_2-driven FAD and riboflavin reduction by Hyd-1. The left spectrum is the decrease in absorbance of 0.05 mM FAD (ε= 11,300 M^{-1} cm^{-1} at the wavelength of 450 nm) over 13 minutes. The right spectrum is the decrease in absorbance of 0.05 mM riboflavin (ε= 12,100 M^{-1} cm^{-1} at the wavelength of 445 nm)

3.2.2. Calibration curves for HPLC

The calibration curve in HPLC is essential for accurate quantitative analysis. To construct the curve, a series of standard solutions with known concentrations are prepared and injected into the HPLC system. The corresponding peak areas are plotted against concentrations to generate a calibration curve via linear regression, from which the concentration of an unknown sample, could be calculated. It is important to ensure the HPLC system is stable, the sample preparation process is consistent with the standard solutions, and the curve is validated for precision, accuracy, and linearity. These steps help ensure that the results are reliable and accurate. The retention times of 0.5 mM of L-tryptophan (**1**), 5-chloro-tryptophan (**2**), 5-bromo-tryptophan (**3**), anthranilamide (**4**), and 5-chloro-anthranilamide (**5**) were determined using HPLC. Retention times may vary even when the same mobile phase composition is used. (Figure 21).

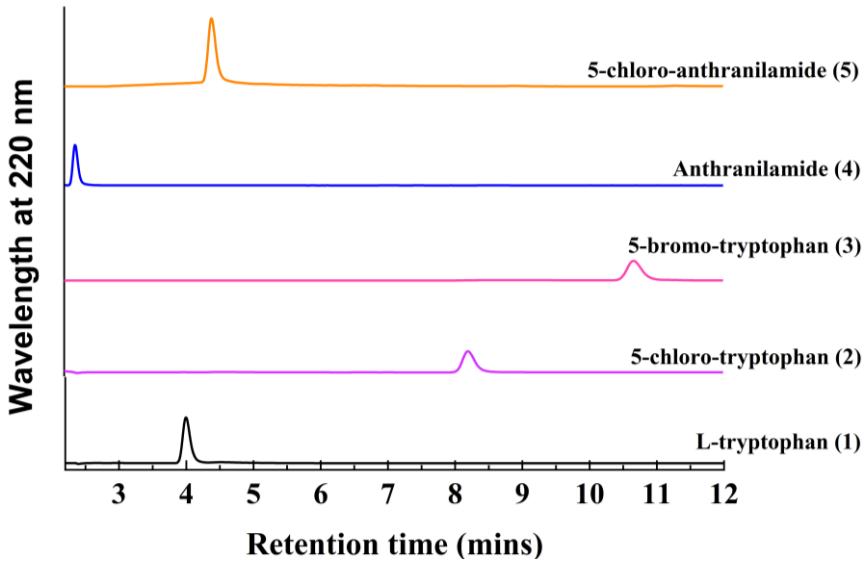


Figure 21. Retention times of L-tryptophan (**1**, retention time: 4 mins), 5-chloro-tryptophan (**2**, retention time: 4 mins), 5-bromo-tryptophan (**3**, retention time: 10.7 mins), anthranilamide (**4**, retention time: 2.3 mins), 5-chloro-anthraniliamde (**5**, retention time: 4.2 mins) monitored by HPLC. Column: ZORBAX RR Eclipse Plus C18, 95Å, 4.6 x 100 mm, 3.5 µm. Mobile phase: Isocratic flow of 60% water and 40% methanol and 0.1% trifluoroacetic acid. Detection wavelength: 220 nm.

The calibration curve for L-tryptophan is presented here as a typical calibration curve, and all conversions were obtained by comparison with the corresponding calibration curves. The calibration curve showed a strong linear relationship between concentration (0 - 2.0 mM) and peak area (mAu·s). The calibration points align closely with the regression line, demonstrating precision and reliability for quantitative analysis within the tested range (Figure 22).

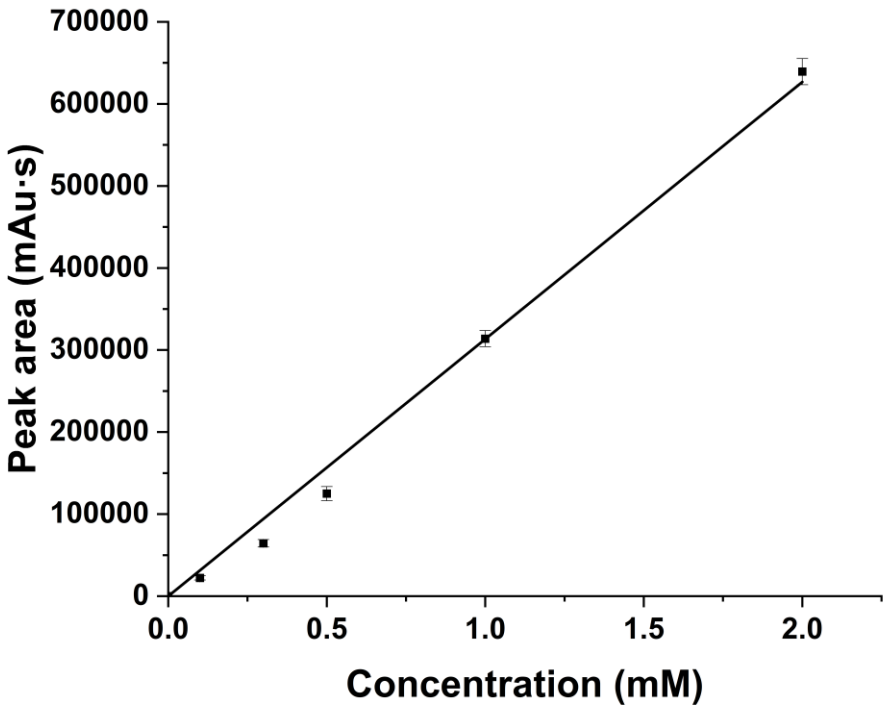


Figure 22. The calibration curve for L-tryptophan.

3.2.3. Testing of halogenases with conventional GDH system

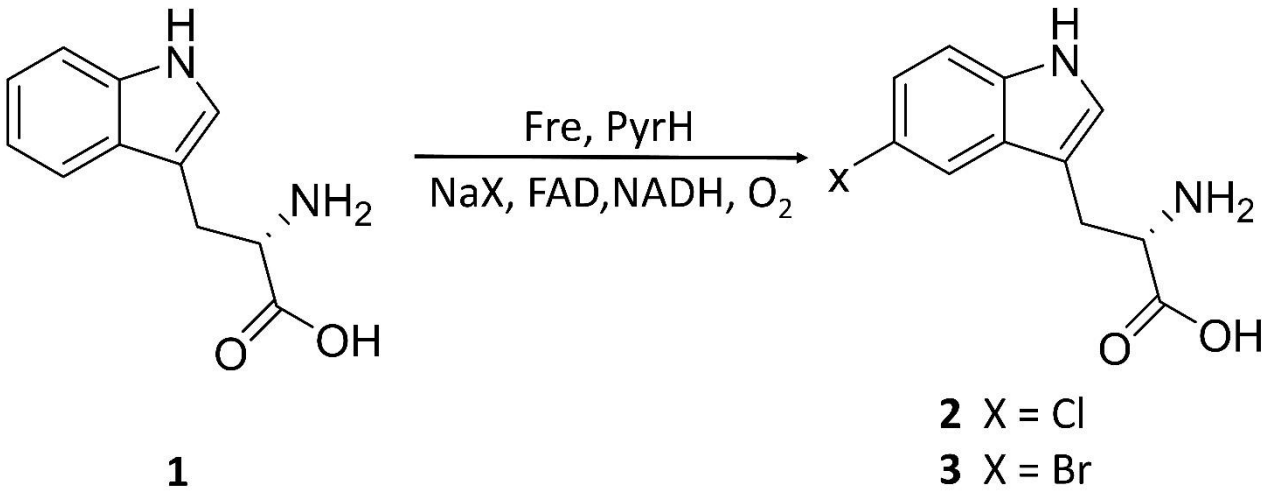
To validate the feasibility of the coupling between Hyd-1 with the FD-halogenase, the conventional cofactor recycling system consisting of flavin reductase, glucose dehydrogenase and FD-halogenase was initially tested. For the model reaction, the L-

tryptophan 5-halogenase PyrH was selected, which natively catalyses the site-selective chlorination of L-tryptophan to produce the target product 5-chloro-tryptophan as part of the biosynthesis of the antibiotic Pyrroindomycin B. Notably, PyrH also exhibits the capacity to catalyse the bromination of L-tryptophan, producing 5-bromo-tryptophan, albeit with a slower turnover compared to the chlorination activity. Both PyrH and flavin reductase, Fre, were heterologously expressed in *E. coli* and purified following established protocols (see chapter 2).[160,161]

In a preliminary setup, the halogenation reaction was carried out with the substrate L-tryptophan (0.5 mM) and cofactors including FAD (0.5 mM) and NADH (10 mM), in the presence of 0.03 mM PyrH, 0.01 mM Fre, and NaCl (50 mM). The 200 µL reaction mixture was incubated at 30 ℃ with shaking at 800 rpm in a 1.5 mL Eppendorf tube for 3 hours. The reaction was open to air for the supply of O_2. At the end of this period, the reaction was quenched by heating at 95 ℃ for 5 minutes to denature the proteins, followed by centrifugation to remove the precipitated protein. The supernatant was analysed by HPLC, with retention times, peak heights and peak areas compared against the analytical standards of L-tryptophan and 5-chloro-tryptophan.

Prior to applying the GDH-based recycling system, the reaction was tested by using NADH as the electron donor to Fre/FAD (Scheme 6). However, this approach was unsuccessful, as no detectable amount of the halogenated product was observed. Upon analysing the possible

causes, it was hypothesised that the issue stemmed from the excessive FAD concentration added to the PyrH. Since the Fre is responsible for reducing FAD to its reduced form using NADH, the excess FAD created a significant demand for reducing equivalents (NADH). This imbalance may lead to a rapid depletion of NADH in the reaction mixture, The $FADH_2$ was re-oxidised by O_2, thus preventing the recycling of FAD and stopping the halogenation process.



Scheme 6. Reaction scheme tested initially in this work for biocatalytic chlorination of L-tryptophan (Trp) by FD-halogenase PyrH.

To investigate the impact of FAD concentration on the halogenation reaction, a series of control experiments focusing on optimising both expression conditions and reaction parameters were conducted. During the expression phase, PyrH was expressed without the addition of FAD to the culture medium, thus avoiding the excess carryover of flavin into the reaction mixture. In the subsequent halogenation reactions, two different experimental setups were tested to evaluate the effect of FAD concentration. Both reactions were carried out under identical conditions except for FAD concentration, with 10 mM NADH as the electron

donor. The first experiment used a lower concentration of FAD (10 μM), while the second using a relatively high concentration (1 mM) to assess how varying FAD levels influenced the overall conversion rate (Figure 23). Notably, the FAD/PyrH ratios here is sub-stoichiometric.

In the reaction containing 10 μM FAD, the solution remained colorless throughout the 3-hour reaction period, indicating an ongoing reduction and brief oxidation cycle of FAD. This observation suggested that the NADH concentration was sufficient to continuously reduce FAD to its reduced form, allowing for sustained halogenation activity without premature depletion of NADH. In contrast, the reaction containing 1 mM FAD exhibited a different performance in terms of colour change. Within 30 minutes of initiating the reaction, the solution turned yellow. The accumulation of oxidised FAD, which represented the yellow colour, indicated that NADH was rapidly consumed in reducing the excess FAD. Consequently, the reaction quickly stopped as no further reduction of FAD could occur without NADH. This experiment confirmed that the high FAD concentration will overburden the available NADH pool and prematurely terminate the halogenation process.

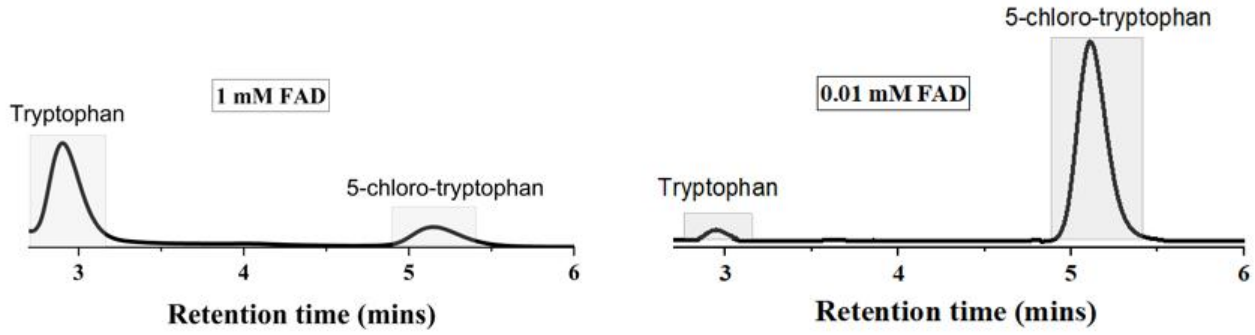


Figure 23. The left panel shows a conversion rate of 12% of 0.5 mM L-tryptpohan under conditions of 1 mM FAD, 10 mM NADH, 0.03 mM PyrH, 0.01 mM Fre, and 50 mM NaCl. The right panel demonstrates 95% conversion when the FAD concentration is decreased to 10 µM. The retention time may change due to column and mobile phase changes. The reactions were open to air for the supply of O_2.

For larger-scale and more practical applications, cost-effective recycling of the more expensive cofactors FAD and NADH is critical. PyrH was next tested with the conventional GDH / glucose / NAD^+ recycling system. An excess of glucose (100 mM) in the reaction mixture, along with GDH and NAD^+ (0.1 mM). In this setup, glucose serves as the electron donor for the regeneration of NADH, which in turn regenerates $FADH_2$ via Fre (Scheme 4B). This integrated recycling system ensures continuous availability of reduced cofactors, maintaining optimal reaction conditions for the halogenation process without requiring large quantities of expensive NADH. Since the reaction with the lower FAD concentration (10 µM) demonstrated significant substrate conversion. The FAD concentration was further decreased to 1 µM. Under these conditions, it was possible to achieve full conversion of L-tryptophan to 5-chloro-tryptophan within just 30 minutes, which is comparable to previously reported activities for this enzyme (Figure 24).[150]

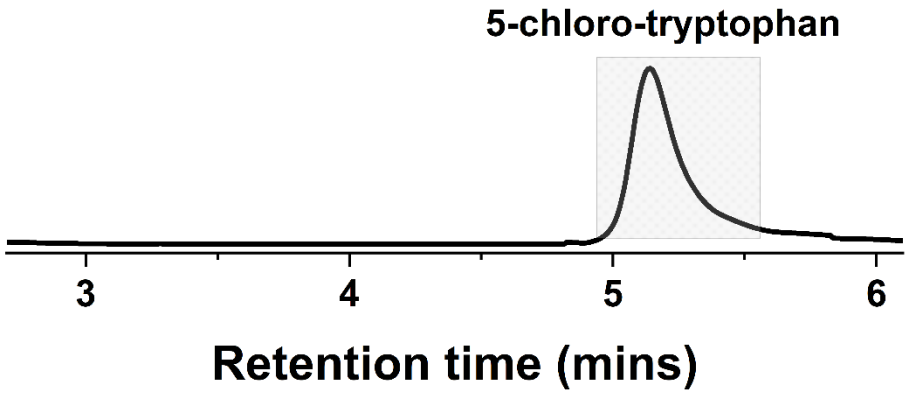


Figure 24. HPLC trace demonstrated full conversion of L-tryptophan with GDH-driven cofactor recycling system. Reaction conditions: 0.5 mM tryptophan, 1 μM FAD, 0.1 mM NAD^+, 0.03 mM PyrH, 0.01 mM Fre, 50 mM NaCl, 100 mM glucose and 0.01 mM glucose dehydrogenase. The reactions were open to air for the supply of O_2

3.2.3.1. Testing of halogenase with different flavins

In order to explore alternative flavin cofactors that could support halogenase activity, the possibility of FMN and riboflavin as substitutes for FAD was also investigated. These flavins differ in both structure and cost, with riboflavin being relatively inexpensive compared to FAD. Therefore, identifying a viable alternative could have significant economic and practical implications for large-scale or industrial biocatalytic applications. Since the chemical structures of FMN and riboflavin differ from that of FAD (most notably in the absence of the adenine moiety in FMN and the phosphoryl group in riboflavin), there was an initial hypothesis that these structural differences might influence the binding affinity and electron transfer efficiency with the FD-halogenase. However, Hyd-1 is able to directly reduce all three flavins (FAD, FMN, and riboflavin) under H_2. As riboflavin is the simplest and least costly of the three flavins, its possible acceptance by FD-halogenase could offer a cost-effective alternative if found to be functionally equivalent to FAD.

To test the feasibility of FMN and riboflavin as cofactors for halogenase activity, a series of comparative enzyme assays were designed. The experiments were set up under identical conditions to allow a direct comparison of the reaction efficiencies using 1 μM FMN, and riboflavin as cofactors. The experimental results demonstrated that neither FMN nor riboflavin could effectively substitute FAD as a cofactor for the halogenase under the tested conditions (Figure 25). This finding is consistent with previous literature reports which suggest that FAD is generally the only tolerated flavin cofactor for FD-halogenases.[107]

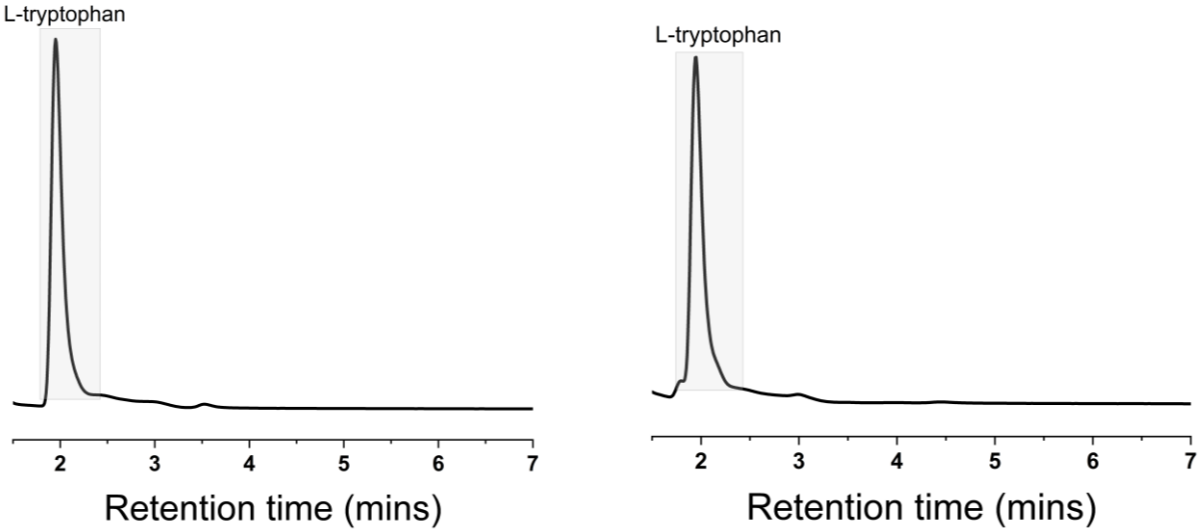


Figure 25. HPLC trace demonstrated no conversion of .05 mM L-tryptophan with GDH-driven cofactor recycling system using FMN (left) and riboflavin (right) as cofactors. Reaction conditions: 1 μM FMN / riboflavin, 0.1 mM NAD^+, 0.03 mM PyrH, 0.01 mM Fre, 50 mM NaCl, 100 mM glucose and 0.01 mM glucose dehydrogenase. The reactions were open to air for the supply of O_2.

Mechanistically, the results confirmed a high specificity of PyrH for FAD, which may be attributed to the precise interaction between the enzyme's active site and the cofactor's structure. All these halogenases, which strictly require $FADH_2$ for their activity, possess a

flavin-binding motif (GxGxxG) located near the N-terminal region.[162] Consequently, FAD remains the most suitable cofactor for such biocatalytic processes, despite its higher cost. Future research could focus on protein engineering approaches to modify the halogenase active site to enhance its compatibility with alternative, cheaper flavins.

3.2.4. Coupling Hyd-1 with FD-halogenase

3.2.4.1. Primary test

Following successfully establishing the GDH-driven halogenation system, the coupling of PyrH with Hyd-1 was explored. Typically, Hyd-1 requires an overnight pre-activation in an H_2 environment to achieve its catalytic function and to stay active under O_2. This was done by using a pressure vessel to saturate the Hyd-1 with 1 - 2 bar H_2. Then, the optimised conditions from the GDH system were initially replicated in the new setup. The reaction mixture, consisting of 50 mM NaCl, 0.01 mM FAD, 0.03 mM PyrH, and 5.8 µM Hyd-1, was prepared and mixed while H_2 was flowed through the headspace of a 1.5 mL microcentrifuge tube for an hour to facilitate the activation of Hyd-1. It is worth noting that one-third the stoichiometric amount of FAD compared to PyrH was used here.

While Hyd-1 is O_2-tolerant, it may still suffer from decreased activity when continuously exposed to O_2, possibly complicating the coupling reaction with PyrH. Therefore, it became necessary to carefully control the O_2 concentration to find a balance between providing

sufficient O_2 for PyrH activity without impairing the function of Hyd-1. To achieve this, the reaction was conducted in a sealed, H_2-filled reaction vessel, and a Hamilton syringe was used to inject controlled amounts of O_2. The precise volume of the solution relative to the total vessel volume was calculated to determine the appropriate air volume needed to achieve the desired O_2 concentration. Based on this calculation, 1% O_2 was introduced into the vessel at 24-hour intervals, with a total of two injections performed over a 48-hour period.

After 48 hours, the reaction mixture was quenched by heating at 95 ℃ and analysed by HPLC. However, no target product peak was detected, indicating no conversion of L-tryptophan to 5-chloro-tryptophan. In addition, in this analysis, peak splitting occurred during the HPLC detection of L-tryptophan (Figure 26). To find out the cause of the problem, factors that might affect the peak shape were systematically investigated. Firstly, the purity and stability of the sample were carefully examined. It was confirmed that it was high-purity L-tryptophan and there was no degradation or interference from impurities. Subsequently, the condition of the chromatographic column was evaluated. It was found that the column in use had shown signs of aging due to long-term use, which might have an impact on resolution. Meanwhile, the possibility of the solvent effect was taken into consideration. During the sample dissolution process, the difference between the solvent used and the mobile phase might lead to peak splitting. In addition, the stability of the instrument performance was comprehensively checked, including the pump flow rate, the accuracy of the injector and the signal stability of

the detector. After a series of analyses, it was confirmed that the instrument was in good working condition without any abnormalities.

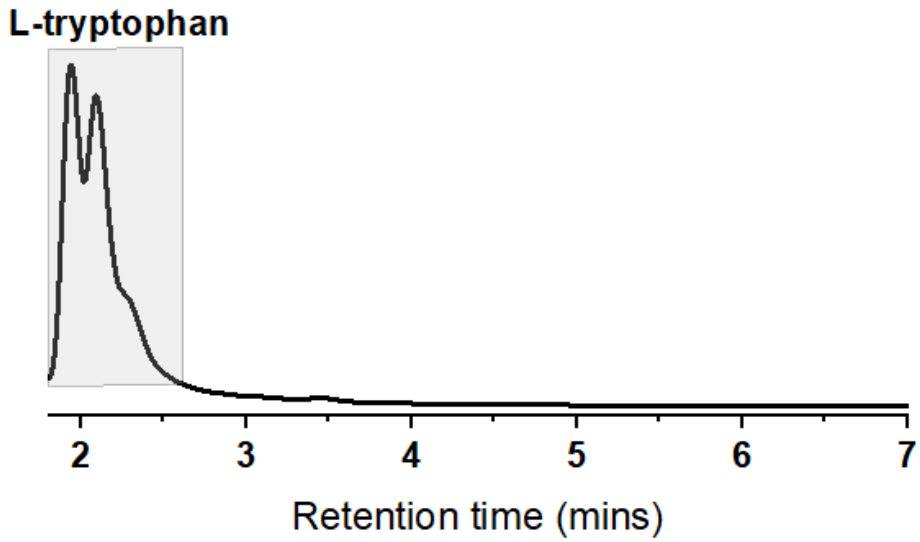


Figure 26. HPLC trace demonstrated no conversion when coupling Hyd-1 and PyrH. The splitting of the L-tryptophan peak was observed. Reaction conditions: 50 mM NaCl, 0.01 mM FAD, 0.03 mM PyrH, and 5.8 μM Hyd-1. The reaction was saturated of H_2 by a mass flow controlled. Controlled amount of air was injected into the reaction vessel by a Hamilton syringe.

In response to the above problems, the following solutions were implemented. The column was replaced with a new one, fundamentally solving the aging problem. The preparation of the sample solvent was optimised by using a solvent closer to the mobile phase, which significantly decreased the impact of the solvent effect on the peak shape. After the adjustment of the pH value and proportion of the mobile phase, they were more in line with the separation requirements of L-tryptophan. Eventually, through these measures, the peak shape of L-tryptophan was restored and a single peak was observed (Figure 27).

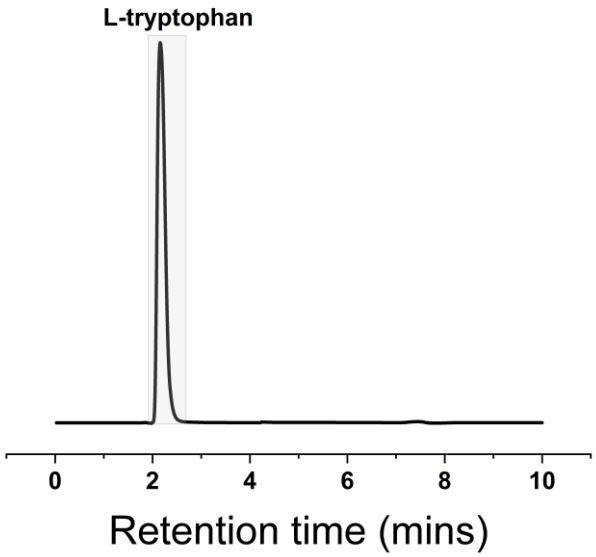


Figure 27. HPLC trace of L-tryptophan peak under altered conditions.

There are several hypotheses for the lack of product generation. One possibility is that Hyd-1 was inactivated due to the O_2 exposure over the course of the reaction. Although the O_2 concentration was controlled, the low concentration of reduced FAD concentration in the solution made it difficult to visually confirm if FAD was being properly reduced and re-oxidised, which is crucial for PyrH activity. Another possible issue could be suboptimal PyrH activity under the experimental conditions, which may not have been sufficient to drive the halogenation reaction. Additionally, the ratio of O_2 to H_2 might not have been properly balanced to support both enzymes simultaneously. Moreover, The O_2-tolerant NiFe hydrogenase primarily catalyses the four-electron reduction of O_2 to water, but a minor fraction undergoes the two-electron pathway, producing ROS such as hydrogen peroxide and superoxide. Given that Hyd-1 itself generates ROS during its interaction with O_2, and

$FADH_2$ also reacts with O_2 to produce ROS. These ROS may possibly damage PyrH, Hyd-1, or both, thereby impairing the catalytic cycle.

3.2.4.2. Optimisation of Reaction conditions

To address these challenges, a series of validation experiments were conducted. In order to further explore the coupling between PyrH and Hyd-1, the PyrH activity was initially assessed using the conventional GDH-based recycling system. To evaluate PyrH activity, two sets of tests were conducted. In one set, PyrH was used at the previously established concentration of 0.03 mM, while in the other, the concentration was decreased to 0.02 mM. Under these conditions, complete conversion of 0.5 mM L-tryptophan to 5-chloro-tryptophan was achieved within 30 minutes, confirming that PyrH was fully active and capable of efficient halogenation (Figure 28). However, the rate of FAD reduction by Hyd-1 is typically slower than that achieved by the GDH system. Additionally, high O_2 concentrations can impair the activity of Hyd-1. Meanwhile, the concentration of FAD, as a substrate for Hyd-1, can also influence its activity. Therefore, initial optimisation efforts focused on adjusting the concentrations of FAD and O_2 to ensure a better enzyme performance.

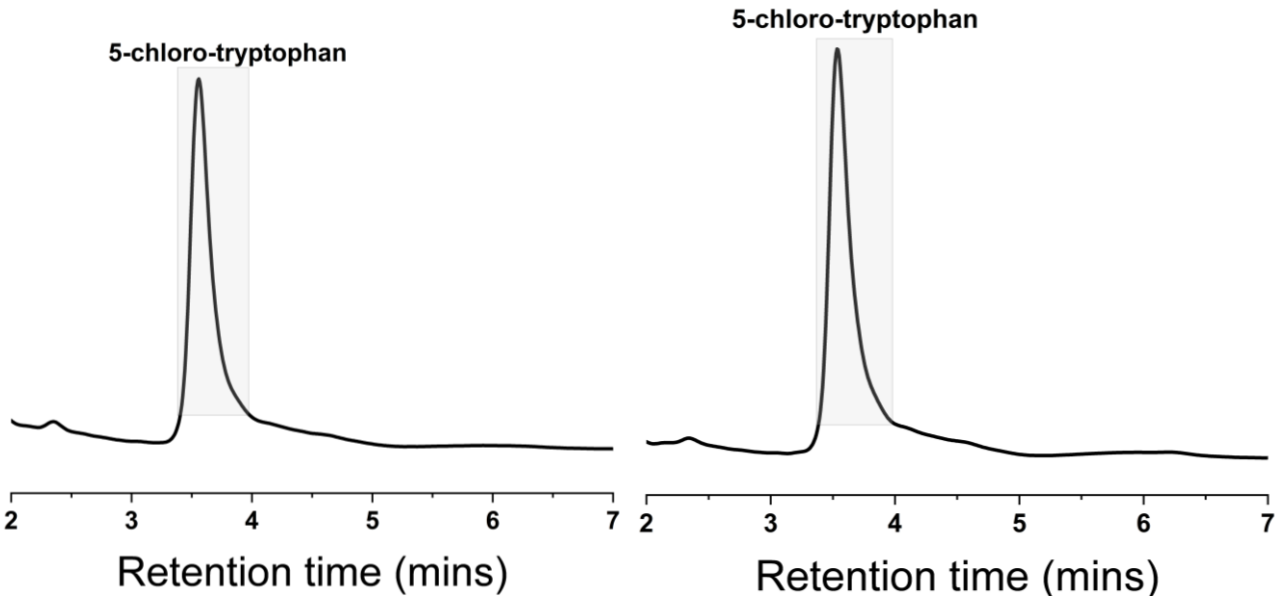


Figure 28. HPLC trace demonstrated full conversion when testing the activity of PyrH. Reaction conditions: 1 μM FAD, 0.1 mM NAD^+, 0.03 mM PyrH (left), 0.01 mM PyrH (right) 0.01 mM Fre, 50 mM NaCl, 100 mM glucose and 0.01 mM glucose dehydrogenase.

Subsequently, attention was turned to Hyd-1's effective affinity for FAD, since FAD is a non-natural substrate of Hyd-1. In previous trials, FAD was added at a low concentration (1 μM). Given that Hyd-1's effective Michaelis-Menten constant (K_M) for FAD has been previously measured as 0.86 ± 0.54 mM,[56] it was suggested that the initial concentration of 1 μM was insufficient for optimal Hyd-1 activity, possibly limiting its ability to reduce FAD effectively and contributing to the lack of product formation. To test this hypothesis, a set of comparative experiments was designed using two different FAD concentrations: 0.05 mM and 0.001 mM, while all other conditions were kept constant (Figure 29).

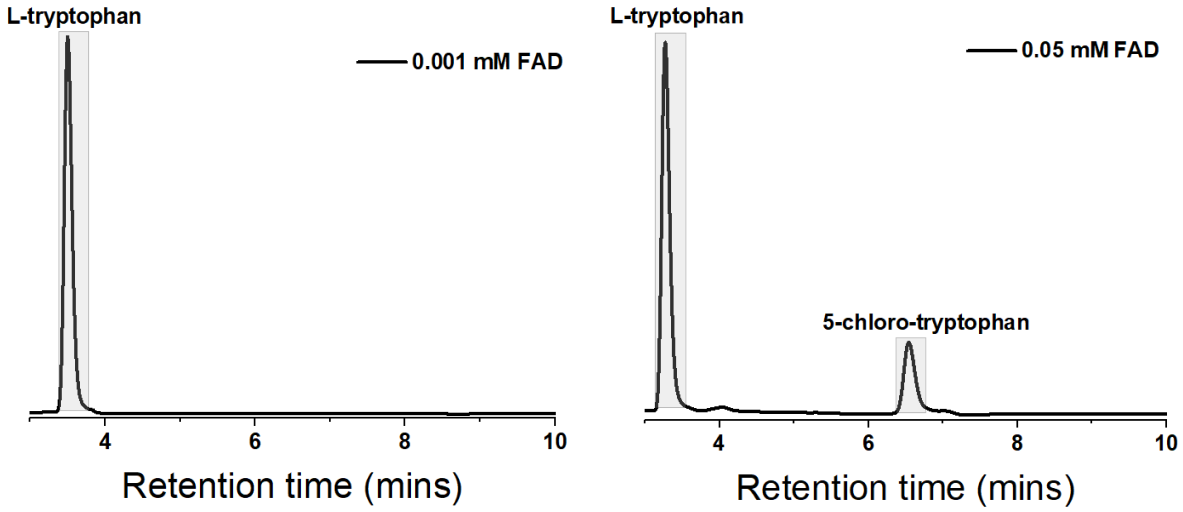


Figure 29. HPLC trace demonstrated the coupling of Hyd-1 with PyrH under different FAD concentrations. Reaction conditions: 0.001 mM FAD (left), 0.05 mM FAD (right), 50 mM NaCl, 0.02 mM PyrH, and 5.8 μM Hyd-1. The reaction was saturated of H_2 by a mass flow controlled. Controlled amount of air was injected into the reaction vessel by a Hamilton syringe.

The results clearly demonstrated the importance of FAD concentration in driving the H_2-driven halogenation reaction. At 0.05 mM FAD, the system successfully produced the desired halogenated product, achieving a conversion of approximately 13% L-tryptophan. This confirmed the feasibility of H_2-driven halogenation reaction via hydrogenase. In contrast, the reaction containing 0.001 mM FAD failed to produce any product, further validating that Hyd-1 requires higher FAD levels to maintain activity and driven the whole halogenation reaction.

With this understanding, the conversion of the H_2-driven halogenation was sought to be further improved. It was recognised that PyrH relies on O_2 for its halogenation activity, and that O_2 is concurrently consumed through its reaction with reduced flavin. Meanwhile, some of the O_2 will react with hydrogenase. Therefore, it was hypothesised that the sustained

progress of the reaction was limited by the availability of O_2. This limitation is particularly pronounced in the H_2-driven system, where the balance between O_2 and H_2 must be carefully managed to ensure continuous halogenation without impairing enzyme function. To address this, the frequency of O_2 injections into the H_2-filled reaction vessel was increased. Augmenting the O_2 supply was intended to maintain a better O_2 level in the solution to support PyrH activity while simultaneously providing enough FAD concentration for Hyd-1 saturation. In addition, this adjustment may be important to ensure a sufficient and steady supply of O_2 was provided to drive the halogenation process without overwhelming Hyd-1 or PyrH with unfavorable redox conditions.

The frequency of O_2 injections was first increased to once every 30 minutes, maintaining the injection volume at 1% of the reaction vessel volume. This continuous O_2 supplementation was applied over an 8-hour period. The results of these adjustments were promising. The conversion improved significantly, with the final conversion rate reaching 75% after 8 hours, indicating that a more frequent O_2 supply effectively enhanced the halogenation process.

However, analysis of the reaction mixture by HPLC revealed the appearance of an unknown by-product, indicated by unexpected peaks in the HPLC chromatogram (Figure 30). Therefore, a series of validation experiments were designed to determine the origin of the unknown peak and to investigate the underlying mechanisms responsible for their formation. Several hypotheses were considered: (1) the by-products might result from the unknown

reactions between the substrate and enzymes and (2) side reactions involving reactive oxygen species (ROS) could have altered the substrate or enzyme etc.

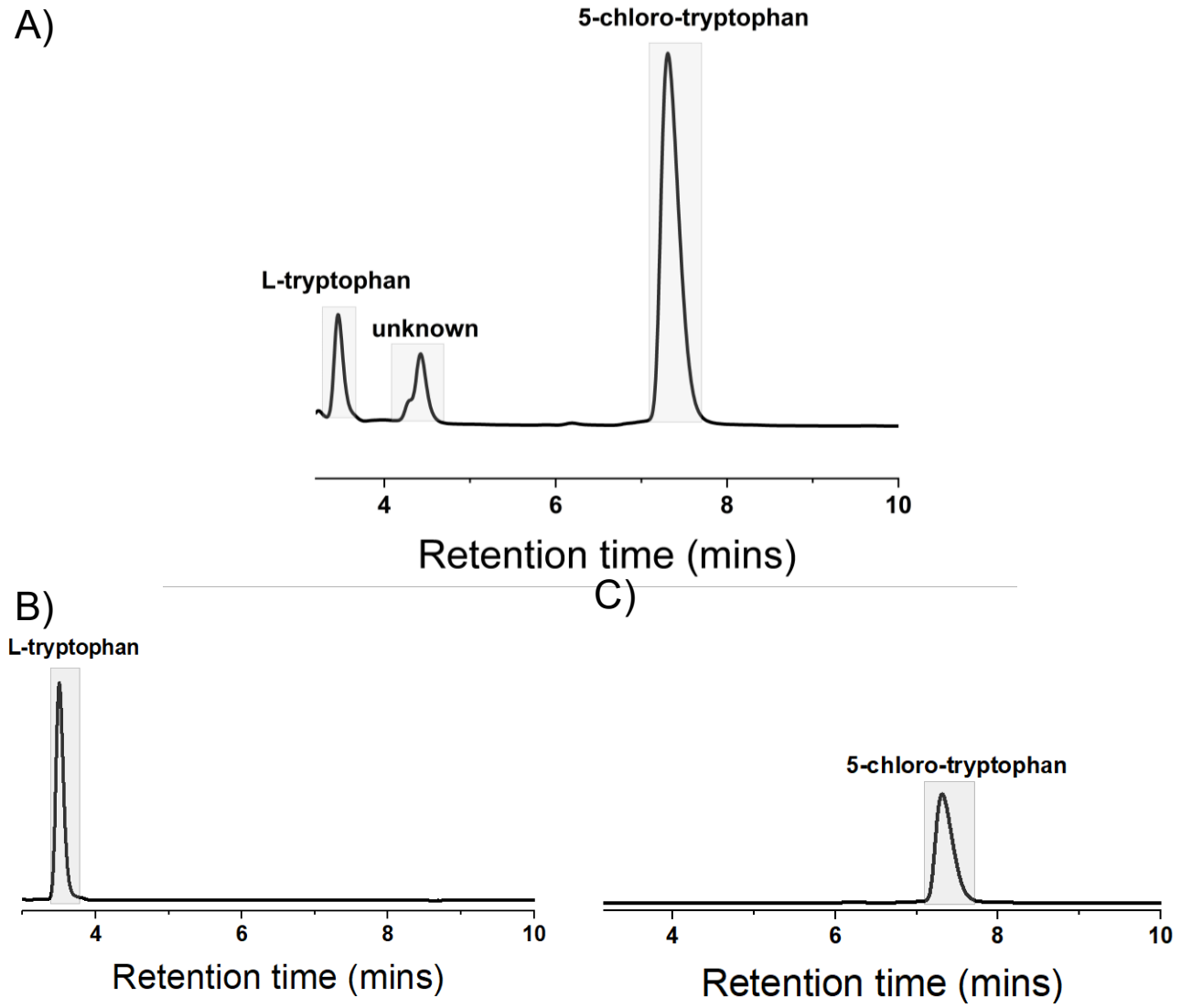


Figure 30. A): HPLC trace demonstrated 75% conversion for the coupling of Hyd-1 with PyrH, with 1% O_2 injected every 30 mins. B) HPLC trace for the analytic standard of 0.5 mM L-tryptophan. B) HPLC trace for the analytic standard of 0.5 mM 5-chloro-tryptophan. Reaction conditions: 0.05 mM FAD, 20 µM PyrH, 50 mM NaCl, 0.5 mM L-tryptophan and 5.8 µM Hyd-1. The reaction was saturated of H_2 by a mass flow controlled. Controlled amount of air was injected into the reaction vessel by a Hamilton syringe. The reaction was saturated of H_2 by a mass flow controlled.

To systematically investigate the origin of the unknown by-products, a series of experiments were conducted by removing individual components from the reaction one at a time to assess

their effects (Table 1). Reactions were first tested without FAD, NaCl, tryptophan, Hyd-1, and PyrH to determine if any of these components were directly responsible for the by-product formation. Additionally, the reaction was tested under different gas environments: pure H_2, nitrogen (N_2), O_2, and a combination of H_2 and O_2.

Table 1. Different reaction conditions to test the generation of by-product

	Test Condition	**By-product Formation**	**Interpretation**
1	No FAD	Yes	FAD is not responsible
2	No NaCl	Yes	NaCl is not responsible
3	No Tryptophan	No	Tryptophan is required
4	No Hyd-1	No	Hyd-1 is required
5	No PyrH	Yes	PyrH is not responsible
6	Only H_2 gas	No	Tryptophan and Hyd-1 interaction in H_2/O_2 likely responsible
7	Only N_2 gas	No	
8	Only O_2 gas	No	
9	H_2 + O_2 gas	Yes	

Reaction conditions: 0.05 mM FAD, 0.02 mM PyrH, 50 mM NaCl, and 5.8 µM Hyd-1.

The results from the different reaction conditions revealed key insights into the factors involved in by-product formation. The by-product was observed in reactions without FAD, NaCl, or PyrH, indicating that none of these components are directly responsible for by-product formation. However, when tryptophan or Hyd-1 was absent, no by-product was

generated, highlighting that both are essential for its formation. Furthermore, the absence of by-products in reactions exposed solely to H_2, N_2, or O_2 suggested that these gases alone did not facilitate by-product generation. The generation of by-product came from the reaction with a combination of H_2 and O_2, where by-products were formed, indicating that the interaction between these gases is essential for the process. These findings led to the hypothesis that reactive oxygen species, such as hydrogen peroxide or superoxide, might be involved.

To test this hypothesis, a direct reaction of tryptophan with hydrogen peroxide was conducted, expecting it to mimic the conditions under which the by-product might form. However, this experiment did not generate the target by-product. Additionally, reactions were conducted with catalase and superoxide dismutase (Cu / Zn-SOD) added to the same reaction mixture. Catalase breaks down hydrogen peroxide into H_2O and O_2, while SOD converts superoxide to hydrogen peroxide, mitigating ROS-related damage. If ROS were responsible for the by-products, the presence of these enzymes should have prevented their formation. However, even with these enzymes included, the by-products persisted, suggesting that the by-product formation was not solely dependent on ROS but might involve a more complex interaction between Hyd-1 and tryptophan (Figure 31).

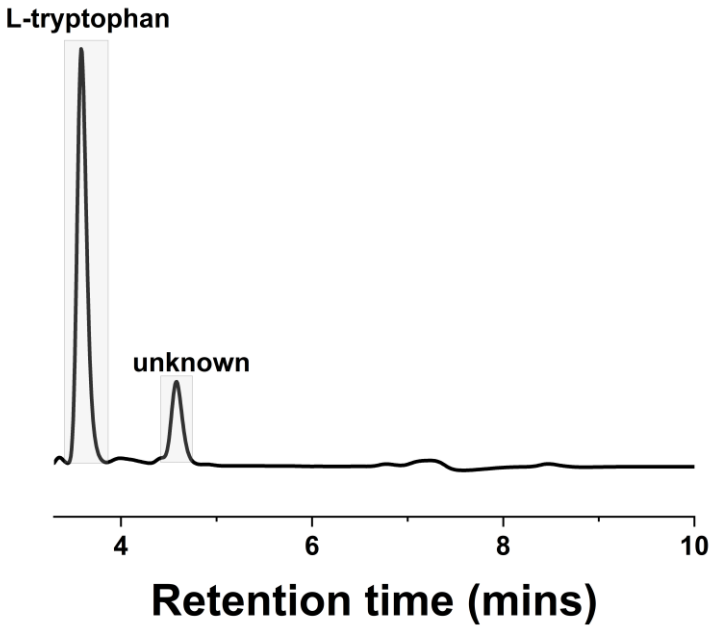


Figure 31. HPLC trace demonstrated unknown peak with the addition of catalase and SOD. Reaction conditions: 0.05 mM FAD, 20 μM PyrH, 50 mM NaCl, and 5.8 μM Hyd-1, 0.01 mM catalase, 0.01 mM SOD and 0.5 mM L-tryptophan. The reaction was saturated of H_2 by a mass flow controlled. Controlled amount of air was injected into the reaction vessel by a Hamilton syringe.

In an attempt to minimise the by-products, the enzyme concentrations were adjusted, increasing the concentration of PyrH to 30 μM. This adjustment aimed to shift the balance toward efficient halogenation by enhancing PyrH activity while minimising the possible side effects associated with Hyd-1. The results showed that the reaction proceeded efficiently with no detectable by-products. This suggested that higher PyrH activity might help suppress side reactions, possibly by reducing the time window for competing reactions to occur. The reaction time to achieve almost full conversion was further shortened by altering the O_2 injection time from 30 minutes per injection to 5 minutes per injection. Under these conditions, 95% conversion of 0.5 mM L-tryptophan to 5-chloro-tryptophan was achieved within 6 hours

(Figure 32). Due to the insufficient time, the identity of the byproduct was not investigated further.

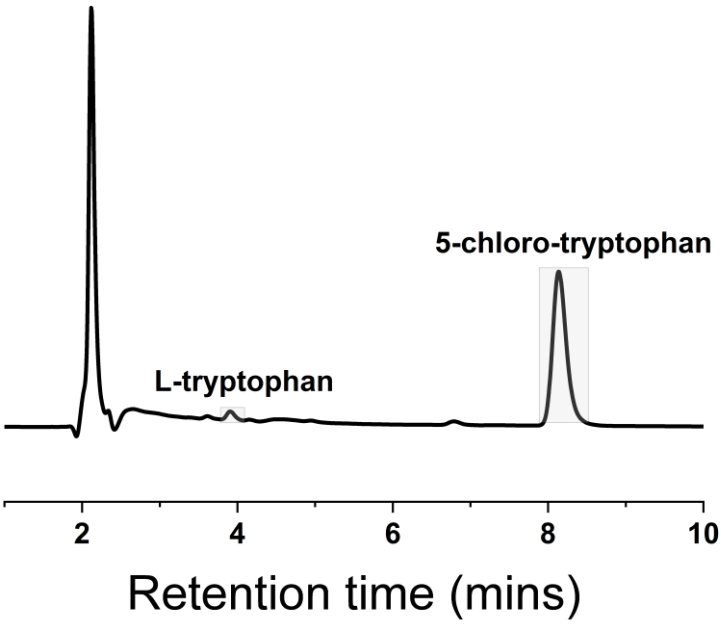


Figure 32. HPLC trace demonstrated 95% conversion of L-tryptophan to 5-chloro-tryptophan with no detectable unknown peaks. Reaction conditions: 0.05 mM FAD, 0.03 mM PyrH, 50 mM NaCl, 0.05 mM PyrH, 0.5 mM L-tryptophan and 5.8 μM Hyd-1. The reaction was saturated of H_2 by a mass flow controlled. Controlled amount of air was injected into the reaction vessel by a Hamilton syringe.

After achieving this result, attention was turned to the optimisation of the method of pulsed delivery of O_2. In terms of specific operation, the reaction was set up in a 1.5 mL mirocentrifuge tube sealed with a Suba seal. The headspace of the tube was flushed with H_2 to saturate the solution and further activate the hydrogenase. Subsequently, a 0.1 mL Hamilton syringe was used to inject a certain amount of O_2 (1%) every 5 minutes through the Suba seal to maintain a short O_2 pulse environment. This pulse method ensures that the

amount of O_2 injected each time is limited and does not lead to a loss of control of the redox balance.

During the pulsed injection process, after each injection of O_2, the colour of the reaction solution quickly changed from colorless to yellow, showing the re-oxidation of $FADH_2$ by O_2. After O_2 injection, the recovery of the solution colour (gradually from yellow to colorless) represents the reduction process of FAD, which is the result of Hyd-1 reducing FAD to $FADH_2$ using e^- from H_2. This is seen in the UV-vis response at 450 nm over time (Figure 33, 34). At the same time, PyrH will consume part of $FADH_2$ for the halogenation reaction, while the remaining $FADH_2$ may react with O_2 non-productively and be oxidised again. This redox cycle can make a better use of O_2 in each O_2 pulse cycle, thereby avoiding excessive O_2 waste and reducing the consumption of reducing equivalents, so that the entire reaction system remains in a dynamic balance. This phenomenon can be monitored by UV-vis spectroscopy at a wavelength of 450 nm, because of the strong absorption peak of the oxidised FAD at this wavelength. After O_2, the absorbance at 450 nm will increase significantly, reflecting the rapid oxidation of FAD.

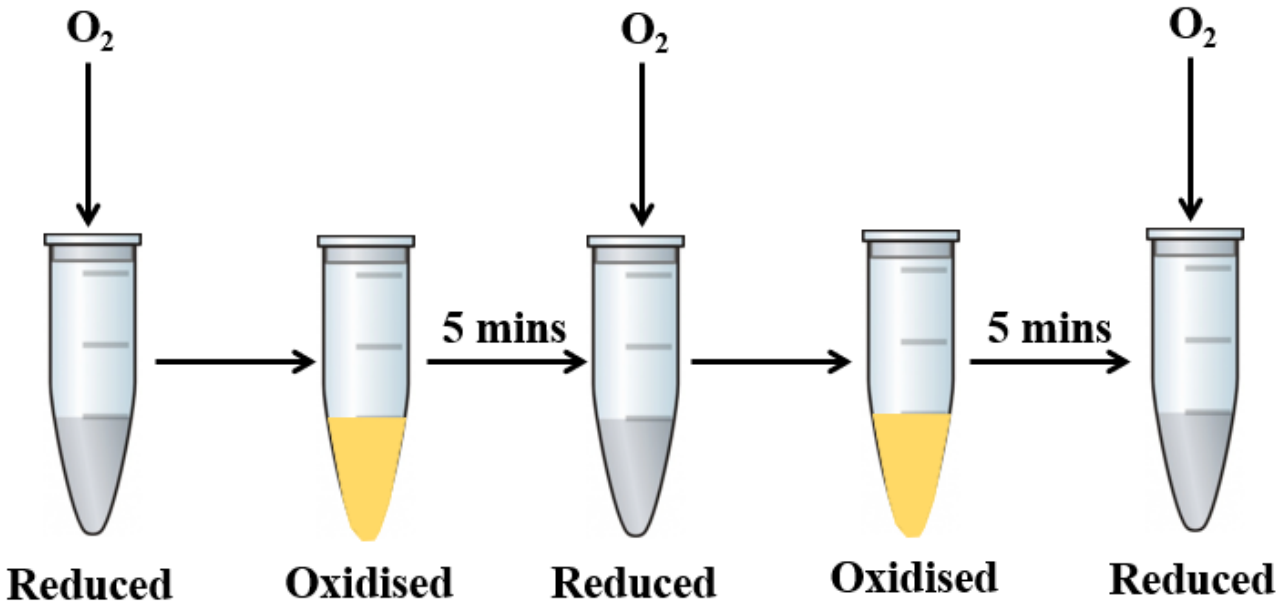


Figure 33. The FAD colour change in the solution during the pulsed delivery of O_2.

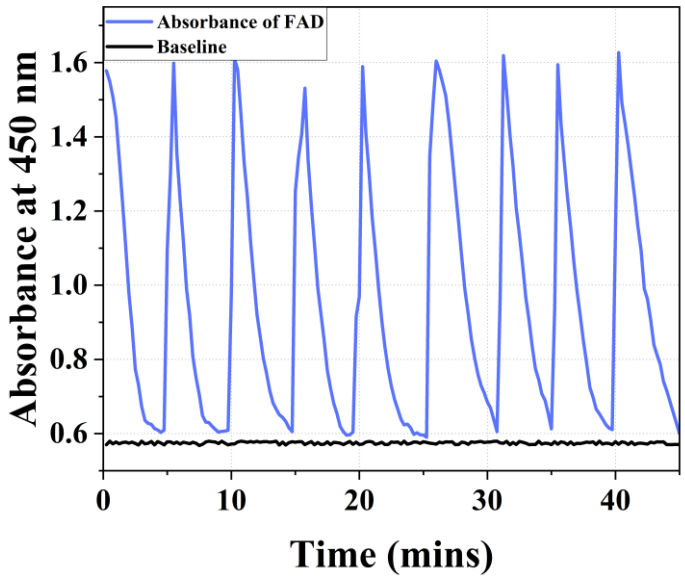


Figure 34. Oxidation state of FAD monitored via absorbance at 450 nm, during pulsed delivery of O_2 every 5 minutes during H_2-driven biohalogenation by PyrH, run in a cuvette. Reactions conditions: potassium phosphate buffer (50 mM, pH 7.0), 30 mM NaCl, 0.5 mM L-tryptophan, 5.8 μM Hyd-1 and 30 μM PyrH.

3.2.4.2.1. FAD concentration optimisation

According to the mechanism, O_2 is not only required for PyrH to catalyse the halogenation reaction, but also directly reacts with $FADH_2$, and this will result in the wasteful reoxidation of $FADH_2$, which in turn affects the effective utilisation of reducing equivalents in the system. Therefore, a fine balance is needed to provide enough FAD to Hyd-1 while minimising wasteful re-oxidation of $FADH_2$. Due to the key role of flavin and O_2 in the FD-halogenase reaction and its complex redox balance, it is important to accurately control the concentration of FAD and the ratio of O_2 inside the reaction solution to make sure the FAD could be effectively reduced by Hyd-1 and provide an appropriate amount of redox balance for PyrH without being consumed too much by the reoxidation by O_2. To optimise the reaction conditions for PyrH using the H_2-driven FAD recycling system, a series of comparative experiments were conducted to evaluate the effect of varying FAD concentrations.

In order to precisely control the supply of O_2 during the FAD concentration comparison experiment, O_2 was manually injected into the headspace of the reaction vessel every 5 minutes to maintain the O_2 concentration in the reaction system through this pulsed supplement of O_2. Furthermore, to systematically evaluate the effect of FAD concentration on conversion, experiments with different concentrations of FAD were set up, covering a range from 0.01 mM to 1 mM. At each concentration, the experimental conditions were consistent: the reaction was carried out in 50 mM potassium phosphate buffer (pH 7.0), containing 30 mM NaCl, 0.5 mM L-tryptophan, 5.8 µM Hyd-1, and 30 µM PyrH. The

experiments for FAD concentrations comparison and optimisation were conducted under 2% O_2 and the experiments for 0.5 mM of FAD concentration were conducted in triplicate.

During the experiment, timepoints samples were taken every 30 minutes and L-tryptophan and 5-chlorotryptophan in the samples were detected by chiral HPLC. By comparing with the analytical standards, the conversion efficiency at different FAD concentrations can be accurately determined (Figure 35, 36. HPLC traces in Figure A1 – A4).

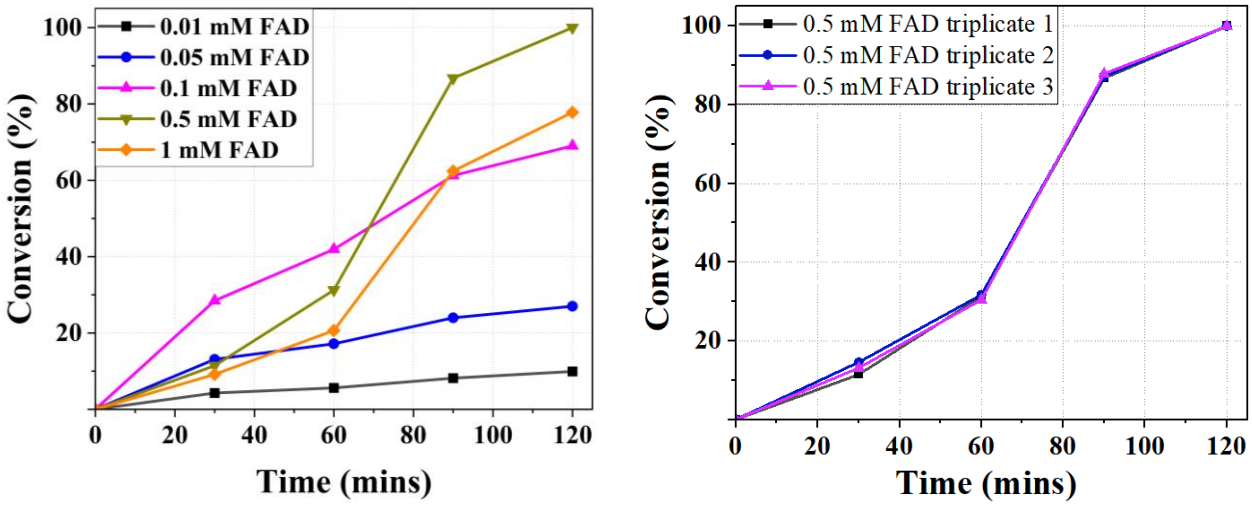


Figure 36. Time course conversion measurements for chlorination by PyrH and Hyd-1/H_2, used to determine optimal FAD concentration with 2% O_2 injection each 5 minutes (left); Conversion over time for triplicate 0.5 mM of FAD concentrations comparison (right).

The experimental results show that the FAD concentration of 0.5 mM is most beneficial to the reaction system, achieving full conversion within 2 hours (Figure 39). Further increasing the FAD concentration to 1 mM did not improve the conversion rate, but instead a short lag phase occurred, which may be due to the inhibition of the activity of Hyd-1 in the presence of a higher concentration of oxidised FAD.

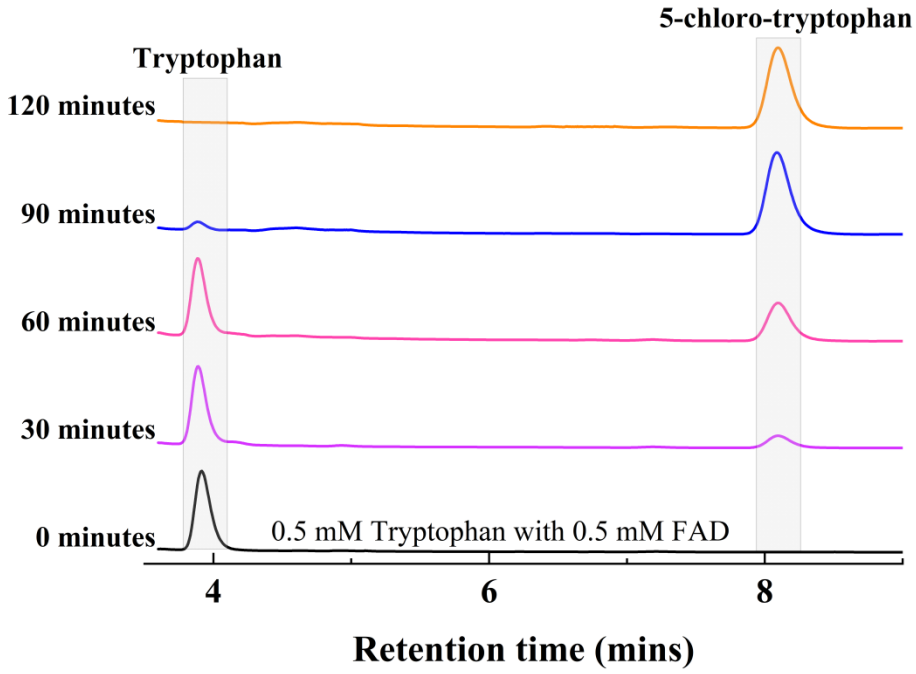


Figure 36. HPLC time point results for FAD concentrations comparison and optimisation with 0.5 mM FAD triplicate 1. Conditions: 30 mM NaCl, 0.5 mM L-tryptophan, 0.5 mM FAD, 5.8 μM Hyd-1, and 30 μM PyrH in 50 mM potassium phosphate buffer (pH 7.0)

Under the condition of 0.01 mM FAD, the conversion of L-tryptophan to 5-chlorotryptophan slowly increased with the extension of the reaction time, reaching 9.9% at 120 minutes. However, compared with the conversion under high-concentration FAD conditions, the reaction rate at this concentration was significantly lower. This suggested that 0.01 mM FAD is insufficient to sustain the optimal catalytic activity of Hyd-1, likely due to its concentration being significantly below the Hyd-1's effective K_M value for FAD, thereby constraining the efficiency of the reaction (Figure A1).

Under the condition of 0.05 mM FAD, the conversion of L-tryptophan to 5-chlorotryptophan increased significantly over time, reaching 27% at 120 minutes. Compared to the 0.01 mM

FAD condition, which achieved only 9.9% conversion within the same timeframe, the reaction rate at 0.05 mM FAD is markedly higher. This demonstrates that increasing the FAD concentration enhances the catalytic efficiency of Hyd-1 by providing more cofactor for the reaction. However, the conversion at 0.05 mM FAD still falls short of full conversion, indicating that further optimisation of FAD levels is necessary to achieve higher efficiency (Figure A2).

The reaction system with 0.1 mM FAD demonstrated a significant improvement in the conversion of L-tryptophan to 5-chlorotryptophan compared to lower FAD concentrations. Conversion began to increase rapidly, reaching 28% at 30 minutes and progressing to 69% at 120 minutes. This is a significant improvement compared to the lower concentrations (0.01 mM and 0.05 mM), where the conversion was below 10% and 30%, respectively, over the same period. This result confirmed that FAD concentration remained a key factor in driving reaction efficiency (Figure A3).

At 0.5 mM FAD, the conversion of L-tryptophan to 5-chlorotryptophan exhibited a distinct kinetic pattern, starting with a relatively slower rate compared to 0.1 mM FAD. At the 30-minute mark, the conversion was 11%, lower than the 28% achieved under 0.1 mM FAD. This slower initial rate can be attributed to a possible inhibitory effect of the higher FAD concentration on Hyd-1 activity. Additionally, it is possible that the reaction system required more time to reach equilibrium between the enzyme and the higher FAD concentration, thereby delaying the onset of maximum activity. Despite the slower start, the reaction under 0.5 mM FAD accelerated significantly after the initial lag phase. By 90 minutes, the conversion

reached 87%, substantially surpassing the rates observed at lower FAD concentrations, and full conversion was achieved within 120 minutes. This rapid increase in conversion suggests that once the system stabilised, the high availability of FAD allowed for efficient cofactor recycling and maximal catalytic turnover by Hyd-1. At this concentration, there is no substrate consumption or product inhibition. In contrast, at lower FAD concentrations, such as 0.1 mM, the early-stage conversion rate was higher. However, these lower concentrations ultimately failed to sustain the reaction rate, resulting in incomplete conversion. This limitation arises because the lower FAD concentration may fall below the K_M value for Hyd-1, leading to suboptimal enzyme saturation as the reaction progresses. As L-tryptophan is converted and FAD-dependent cofactor cycling increases, the limited availability of FAD likely becomes a bottleneck, preventing the reaction from achieving complete conversion.

Building on the observations at lower FAD concentrations, the results at 1 mM FAD further illustrates the diminishing returns of increasing FAD further. While 1 mM FAD provides sufficient cofactor availability to sustain the reaction, the conversion rate remains slower compared to 0.5 mM FAD throughout the reaction. The initial lag phase is more pronounced, with only 9% conversion at 30 minutes, suggesting that the excess FAD may exacerbate enzyme inhibition or disrupt the balance of enzyme-cofactor interactions. Although the reaction accelerates over time, it only reaches 78% conversion by 120 minutes. This result reinforces the notion that excessively high FAD concentrations do not enhance enzymatic efficiency and may instead hinder the system's overall performance (Figure A4).

The comparison of FAD concentrations suggested a subtle connection between cofactor availability, enzymatic activity, and system complexity for Hyd-1 driven FAD recycling. At lower FAD concentrations, the reaction was primarily limited by cofactor availability, and O_2 has a minimal influence since the hydrogenase cannot operate at full capacity. However, as FAD concentration increases, O_2 concentrations may become a critical factor because it introduced complexities such as oxidative stress that affects hydrogenase activity. At higher FAD concentrations, such as 1 mM, the excess oxidised FAD may exacerbate these effects and compete with O_2 for enzyme interaction, resulting in transient inhibition and a slower reaction start. The observed non-linear relationship between FAD concentration and system performance demonstrated the complex balance required to optimise both FAD and O_2 levels. Given these dynamics, optimising O_2 supplementation could further enhance the system's efficiency by minimising oxidative stress while ensuring adequate O_2 availability to support Hyd-1 activity.

3.2.4.2.2. O_2 concentration optimisation

In order to optimise the O_2 concentrations and decrease the effect of the 'Oxygen Dilemma', a series of experiments were conducted to confirm the best O_2 levels in the reactions. The 'Oxygen Dilemma' arises from the dual role of O_2 in enzymatic reactions. On one hand, a lot of enzymes (for example, FD-halogenases, FD-monooxygenases) require O_2 as a co-substrate. On the other hand, when O_2 reacts directly with reduced flavins, byproducts such as hydrogen peroxide and superoxide are generated, which will result in a waste of valuable

reducing equivalents. Although no obvious effects of adding catalase or SOD were found for short-time reactions, possible damage to the enzymes from ROS may still occur during a prolonged reaction process.[163,164]

The pulsed delivery of O_2 was applied to examine the effect of different O_2 concentrations in the headspace gas. The experiments for O_2 concentrations comparison and optimisation were then conducted under the optimal FAD concentration (0.5 mM; the experiments for 0.5% O_2 concentration were conducted in triplicate). The optimisation of the O_2 concentration was carried out by testing various O_2 injection levels, to give the following headspace %: 0.05%, 0.1%, 0.5%, 1%, and 2% (Figure A5 – A10).

Under 0.05% O_2 concentration, the conversion of L-tryptophan to 5-chlorotryptophan progressed slowly, with conversion rates increasing from 8% at 30 minutes to only 29% after 120 minutes. The gradual increase in conversion over time indicated that the system is operating under O_2-limited conditions.

At 0.1% O_2 concentration, the conversion of L-tryptophan to 5-chlorotryptophan improved only slightly compared to 0.05% O_2, reaching 35% at 120 minutes, probably due to slight alleviation of the severe O_2 limitation observed at 0.05%. allowing for a moderate enhancement in enzymatic activity.

At 0.5% O_2, L-tryptophan was fully converted to 5-chlorotryptophan within 90 minutes, demonstrating significantly improved reaction kinetics compared to 0.05% and 0.1% O_2 conditions. The early-stage reaction also demonstrated enhanced kinetics, with a conversion of 25% in just 30 minutes. This suggests that 0.5% O_2 not only sustains enzymatic activity over time but also supports a faster initiation of the reaction by providing sufficient O_2 for efficient turnover of the oxidation-reduction cycle. The absence of a slowdown in reaction rate, as seen in lower O_2 conditions, suggests that 0.5% O_2 provided sufficient O_2 to fully support the catalytic activity of FD-halogenase, allowing it to operate efficiently. This O_2 level aligned well with the O_2-tolerance of Hyd-1, ensuring that the enzyme remained stable and active.

At 1% O_2 concentration, the conversion of L-tryptophan to 5-chlorotryptophan still proceeded efficiently, achieving full conversion by 120 minutes, similar to the results observed under 0.5% O_2. However, the reaction rate was slightly faster during the early stages, with a conversion of 32% at 30 minutes compared to 25% under 0.5% O_2. By 90 minutes, the conversion reached 90%, slightly lower than the 100% achieved at the same time point under 0.5% O_2, suggesting that the higher O_2 concentration might introduce minor inefficiencies as the reaction progresses. The differences between 0.5% and 1% O_2 are subtle but important. At 1% O_2, the initial reaction may benefit from the increased O_2 availability, which may enhance the early turnover of the FD-halogenase. However, the slightly slower conversion after 60 minutes under 1% O_2 could indicate possible side effects of higher O_2 levels to hydrogenase,

such as the minor oxidative inhibition. In contrast, the 0.5% O_2 condition maintained a steady reaction rate throughout.

At 2% O_2 concentration, the conversion of L-tryptophan to 5-chlorotryptophan was slower compared to 1% O_2. By 120 minutes, the reaction reached 89% conversion, significantly lower than the full conversion achieved under 1% O_2. Similarly, the early-stage reaction rate was decreased. These results suggest that excessively high O_2 levels negatively impact the enzymatic system, which could slow the FAD recycling efficiency of Hyd-1 and FD-halogenase. The comparison between 1% and 2% O_2 also suggests a diminishing effect on increasing O_2 concentration beyond 0.5% level, indicating that further increases in O_2 concentration would likely exacerbate these effects and lead to even greater loss of efficiency.

3.2.5. Extending to biobromination

After confirming the optimal conditions for H_2-driven biochlorination and in order to further validate its feasibility of H_2-driven biobromination, a reaction was conducted in which NaBr was substituted for NaCl. The conditions were maintained consistent with previous FAD comparison experiments, including 0.5 mM L-tryptophan, 0.5 mM FAD, 5.8 μM Hyd-1, and 30 μM PyrH, with O_2 pulsing set at 0.5% every 5 minutes. The experiments for biobromination of 0.5 mM L-tryptophan were conducted in duplicate.

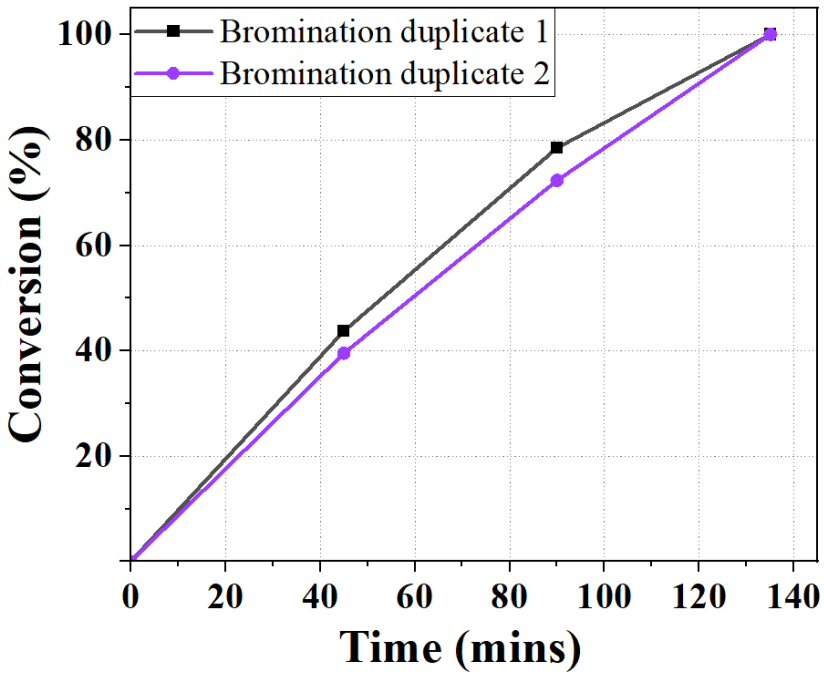
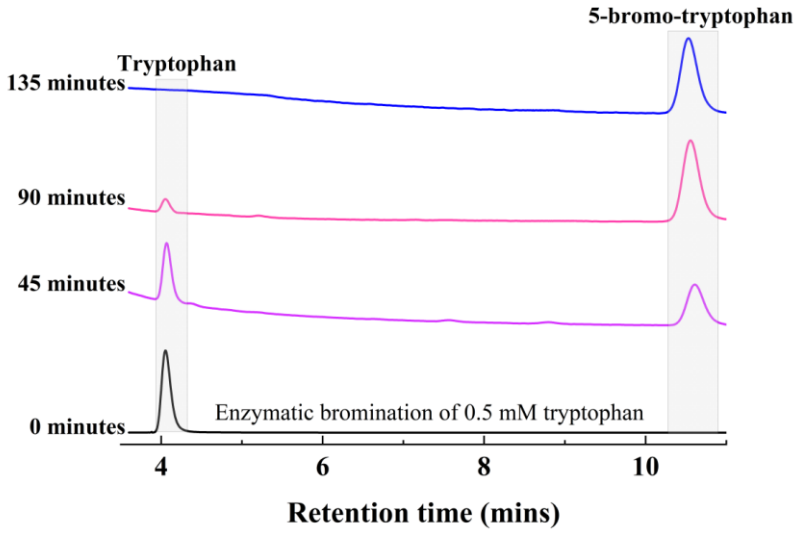
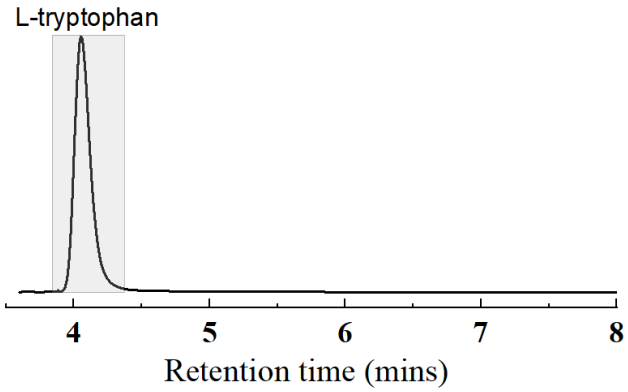


Figure 37. Conversion over time for duplicate biobromination reactions.

A)



B)



C)

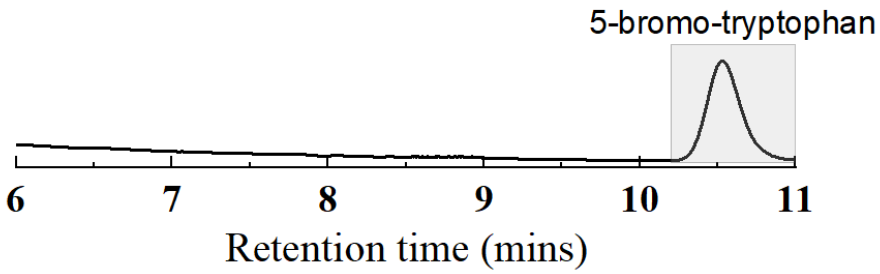


Figure 38. A): HPLC time point results for biobromination series 1 under optimal reaction conditions. B): HPLC trace of the analytic standard for L-tryptophan. C): HPLC trace of the analytic standard for 5-bromo-tryptophan. Conditions: 30 mM NaBr, 0.5 mM L-tryptophan, 0.5 mM FAD, 5.8 µM Hyd-1, and 30 µM PyrH with 0.5% O_2 in 50 mM potassium phosphate buffer (pH 7.0).

As shown in the Figure 37 and 38, by 45 minutes, the generation of the brominated product was obvious, achieving 40% conversion from L-tryptophan to 5-bromo-tryptophan. Full conversion was achieved within 135 minutes. The time course results demonstrated approximately 75% of the turnover frequency observed for the biochlorination reaction catalysed by PyrH under analogous conditions, consistent with previous findings.[184] The slower rate of bromination compared to chlorination is likely attributable to differences in the reactivity of halide ions, as bromide ions is larger and less electronegative, then it exhibits slightly lower reactivity in the active site of PyrH.

3.2.6. Increasing substrate concentrations

To test the feasibility of higher substrate concentrations for H_2-driven halogenation, manual syringe-based O_2 injection experiments were conducted using 1 mM, 2 mM, and 4 mM L-tryptophan as substrates. The results showed that at 1 mM L-tryptophan, full conversion to 5-chloro-tryptophan was achieved within 120 minutes. For 2 mM L-tryptophan, complete conversion required 240 minutes. At 4 mM L-tryptophan, approximately 90.6% conversion was achieved after 420 minutes. This decreased efficiency at higher substrate levels can be attributed to the inherent instability of FD-halogenase, which tends to lose activity within 3–6 hours, may have also contributed to the incomplete conversion observed in the 4 mM reaction (Table 2, Figure A11 – A13).

Table 2. Enzymatic chlorination by manual introduction of O_2 at increasing concentrations of L-tryptophan by PyrH coupled with Hyd-1/H_2 flavin recycling system.[a]

Entry	[**1**] mM	Time [mins]	Conversion [%][b]	PyrH TTN[c]
1	1	120	100	50
2	2	240	100	100
3[d]	4	420	90.6	181.2

[a] Reaction conditions: 30 mM NaCl, 5.8 µM Hyd-1 and 30 µM PyrH, in potassium phosphate buffer (50 mM, pH 7.0) at 0.5 mM FAD and 0.5 % O_2 in H_2. [b] Conversion to **2** monitored by HPLC. [c] Hyd-1 total turnover number (mol **2** per mol Hyd-1), PyrH total turnover number (mol **2** per mol PyrH). [d] 3.5 µM Hyd-1 was used instead of 5.8 µM.

3.2.7. Extending to other non-native substrate

To investigate the ability of PyrH to catalyse the halogenation of non-native substrates using the Hyd-1/H_2 FAD recycling system, anthranilamide (**4**) was selected as the substrate. PyrH has been previously shown to halogenate anthranilamide exclusively at the 5-position to produce 5-chloro-anthranilamide (**5**).[150] In the conventional cofactor recycling systems utilising GDH/glucose, NAD^+, and flavin reductase, 46% conversion of **4** to **5** was achieved after 30 minutes, compared to 100% conversion for the native substrate L-tryptophan under the same conditions. The experiments for biochlorination of 0.5 mM anthranilamide were conducted in triplicate, with consistent trends observed across all replicates. Under the established reaction conditions, full conversion was achieved within 180 minutes (Figure 39). This reaction speed is consistent with previous findings.[150]

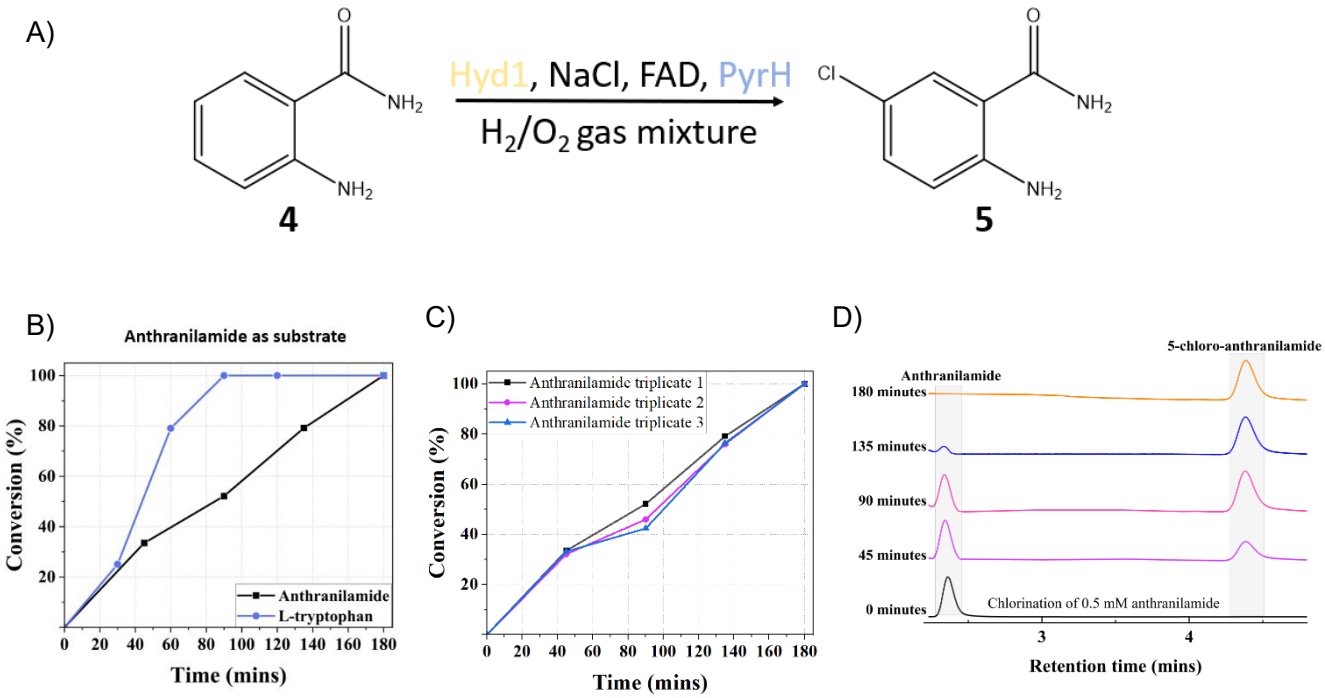


Figure 39. A)**:** Reaction scheme of the biochloriantion of anthranilamide to 5-chloro-anthranilamdie. B): Conversion of biochloriantion of anthranilamide over time compared to L-tryptophan. C): Conversion over time for triplicate chlorination of anthranilamide reactions. D): HPLC time point results for biochlorination with 0.5 mM Anthranilamide. Reaction conditions: 0.5 mM anthranilamide, 30 mM NaCl, 5.8 µM Hyd-1 and 20 µM PyrH, in potassium phosphate buffer (50 mM, pH 7.0) at 0.5 mM FAD and 0.5 % O_2 in H_2.

These results further demonstrate the versatility of the Hyd-1/H_2 FAD recycling system in supporting FD-halogenase activity on non-native substrates and its promise for broad applications in biohalogenation.

Despite the promising results, this method may not be the most optimal for several reasons. First, it could present challenges when scaling up the reaction. The pulse injection process relies on precise control of O_2 injection and careful monitoring of the reaction's colour changes, which might be difficult to achieve efficiently on a larger scale. The need for

continuous monitoring and injection of small amounts of O_2 could require complex equipment and constant adjustments, making it less practical for industrial applications. Secondly, while this method allows for a dynamic redox cycle that helps maintain a balance between oxidation and reduction, it is uncertain whether this approach truly maximises the catalytic efficiency of Hyd-1. The repeated cycles of oxidation and reduction of FAD might not be the ideal conditions for optimal enzyme activity. Therefore, further optimisation was explored subsequently in Chapter 4 to ensure that the reaction conditions fully support the highest catalytic efficiency of Hyd-1 and minimise any possible loss of activity.

In this chapter, a simplified system for H_2-driven halogenation was successfully established by coupling Hyd-1 with FD-halogenase. Building on initial benchmarks using the conventional GDH/glucose system, the Hyd-1/H_2 approach enabled efficient in situ flavin reduction using H_2 as the sole reductant, thereby eliminating the need for auxiliary enzymes and sacrificial cofactors. Systematic optimisation of flavin and O_2 concentrations, alongside careful modulation of gas delivery, achieved considerable conversion in both chlorination and bromination reactions. Moreover, the platform demonstrated adaptability to increased substrate loadings and non-native substrates, underscoring its potential for broader synthetic applications. These findings provide a strong experimental foundation for further refinement and extension of the system. In the following chapter, attention turns to enhancing operational robustness and expanding the enzyme repertoire.

4

Chapter 4

4.1. Optimisation of operations

To enable more efficient and consistent prolonged reactions, the manual injection method previously used was replaced with an automated system. This transition to automation aimed to improve reproducibility by minimising human error and allowed for precise control over reaction parameters. The automated O_2 delivery was integrated into the experimental setup using the BROOKS DELTA SMART 2 mass flow controller and IGI Systems: BROOKS SMART Interface software, programmed with Python scripts. The Python scripts used to control the BROOKS SMART Interface software for automated O_2 delivery were partially developed with the assistance of Jiachuan Peng (The code adapts to changing requirements).

The automation system integrates a Python script, control software, and a mass flow controller (MFC) to enable precise regulation of gas flow rates during enzymatic reactions. The MFC is crucial for maintaining consistent H_2 delivery, ensuring stable reaction conditions essential for reproducible results. A custom Python script dynamically interacts with the control software to set, monitor, and adjust gas flow rates in real time, eliminating the need for manual intervention and reducing human error. The automated system was designed to inject 0.5% O_2 in H_2 into the reaction vessel headspace every 5 minutes, with periodic flushing of the headspace with pure H_2 every 2 hours.

Table 3. Enzymatic chlorination at different concentrations of L-tryptophan (1), comparing catalysis by PyrH supported by GDH/glucose of Hyd-1/H_2.

Entry	Flavin recycling system	[**1**] mM	Time [mins]	Conv. [%][a]	PyrH TTN[b]	PyrH TOF[c] [min^{-1}]
1	GDH/glucose	0.5	30	100	25	0.83
2	Hyd-1/H_2	0.5	30 (90)	25 (100)	6.25 (25)	0.21
3	GDH/glucose	5.5	360	23.6	65	0.18
4	Hyd-1/H_2	5.5	360	100	275	0.76
5[d]	Hyd-1/H_2	11	720	90.4	270/ 255[e]	0.75/ 0.68[f]

[a] Conversion to **2** monitored by HPLC. [b] PyrH total turnover number (mol 2 per mol PyrH). [c] Turnover frequency of PyrH (mol 2 per mol PyrH per minute). [d] At 360 minutes, precipitated PyrH was removed by centrifugation, and an additional 20 μM PyrH was added, and the headspace was then flushed with H_2 for 30 minutes before re-commencing pulsed O_2 delivery. [e] Total turnover number for first addition of PyrH over 360 minutes/second addition of PyrH over another 360 minutes. [f] TOF PyrH in the first/second 360-minute phase. Entry 4 and 5 were conducted in triplicate.

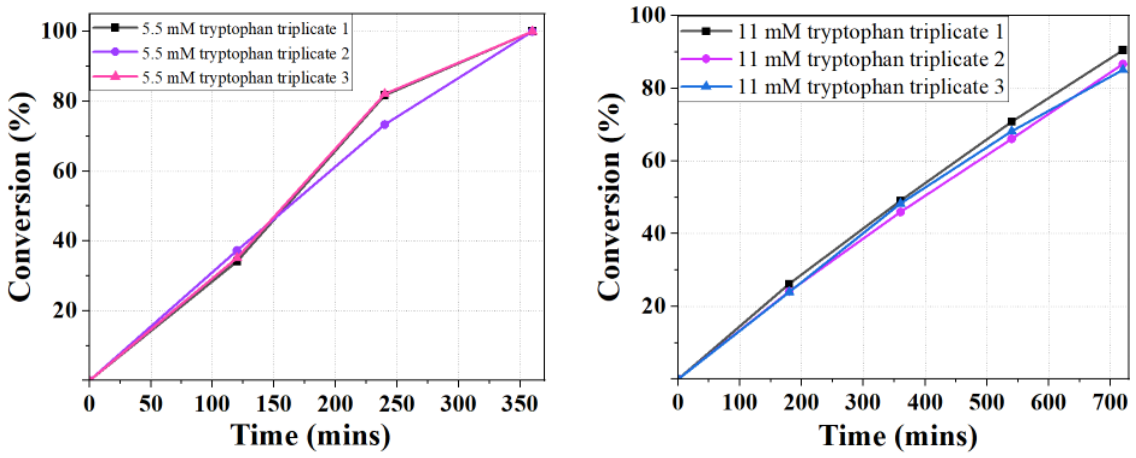


Figure 41. Conversion over time for triplicate biochlorination reactions of 5.5 mM tryptophan (left; entry 4). Conversion over time for triplicate biochlorination reactions of 11 mM tryptophan (right; entry 5).

The experiments for biochlorination of 5.5 mM and 11 mM L-tryptophan (1) to 5-chloro-tryptophan (2) were conducted in triplicate. The results were compared with the traditional GDH/glucose flavin recycling system (Table 3, Figure 41). The PyrH turnover frequency (TOF) for operation with Hyd-1/H_2 is 0.76 min^{-1} over the 6 hour reaction (Entry 4). This is close to rates measured over short reactions with the glucose/GDH system in this study (Entry 1) and in literature reports on PyrH[150], but the GDH/glucose system was unable to sustain this rate over more than 2.5 hours. In contrast, the H_2-driven Hyd-1/PyrH system achieved full conversion to 5-chloro-tryptophan under the same conditions (Figure 42, Figure A14). Notably, the H_2-driven system demonstrated a total turnover number (TTN) of 275 for PyrH, exceeding literature-reported values which are usually below 200.[165]

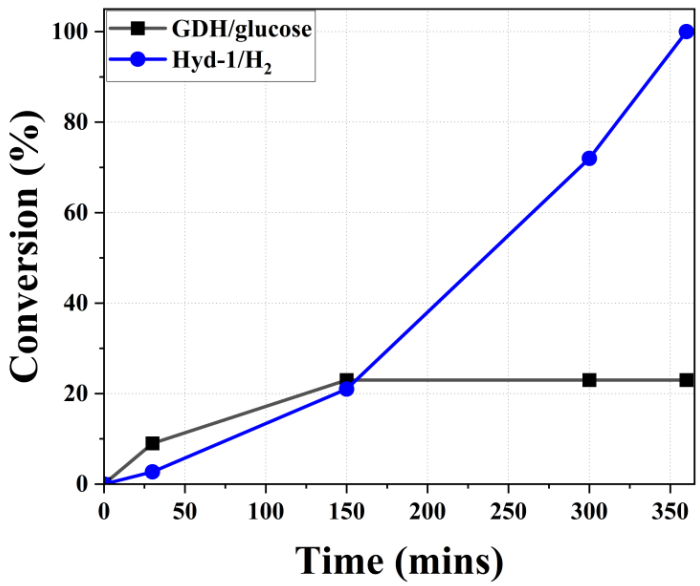


Figure 42. Timecourses for PyrH chlorination at 5.5 mM tryptophan using Hyd-1/H_2 vs GDH/glucose. Other conditions: see Chapter 2.

Encouraged by these results, the substrate concentration was further increased to 11 mM. During this reaction, precipitation of PyrH was observed after 6 hours due to its instability. The precipitated enzyme was removed by centrifugation, and an additional 20 µM PyrH was introduced into the reaction mixture. This intervention enabled the system to achieve a conversion rate of 90.4%, corresponding to 10.5 mM of 5-chloro-tryptophan (Figure A15). These results demonstrated the scalability of the H_2-driven Hyd-1/PyrH system, demonstrating its ability to outperform conventional flavin recycling systems at higher substrate concentrations.

It is important to note that the pH will change during the GDH-driven reaction due to the formation of gluconic acid and the constant re-oxidation of NADH and $FADH_2$ by O_2. Fluctuations in pH may contribute to the reduced enzymatic activity for prolonged reaction time. To find out whether significant pH shifts indeed occurred during the reactions, pH was monitored over time using a Thermo Scientific™ Orion™ ROSS™ PerpHecT™ Micro Glass Bodied Combination pH Electrode. Reactions with Hyd-1/H_2 were run according to Procedure B; reactions using GDH/glucose were run according to Procedure D. Data are summarised in Table 4.

Table 4. Time-dependent pH value changes for reactions run with either Hyd1/H_2 system or GDH/glucose system.[a]

Time [hours]	pH values of Hyd-1/H_2[a]	pH values of GDH/glucose[b]
0	7.4	7.4
1	7.4	6.7
2	7.3	5.9
3	7.2	5.2

[a] Reaction conditions: 1 mM L-tryptophan, 30 mM NaCl, 5.8 µM Hyd-1 and 20 µM PyrH, in potassium phosphate buffer (50 mM, pH 7.4) at 0.5 mM FAD and 0.5 % O_2 in H_2 at 30°C, 900 rpm for 180 mins. [b] Reaction conditions: 1 µM FAD, 100 mM NaCl, 1 mM L-tryptophan, 100 µM NAD^+, 200 mM glucose, 3 µM GDH, 5 µM Fre and 20 µM PyrH.

Over the 3 h, the Hyd1/H_2 system maintained a nearly constant pH (from 7.4 to 7.2), demonstrating high pH stability. In contrast, the GDH/glucose system became progressively more acidic, with pH dropping from 7.4 to 5.22 by 3 h, consistent with formation of gluconic acid as a by-product of glucose oxidation. In addition to pH monitoring, visual inspection of the reaction mixtures after 3 hours revealed that the Hyd-1/H_2 system remained visibly clear and homogeneous, while the GDH/glucose system exhibited significant turbidity and precipitation (Figure 43). The lowered pH may contribute to protein precipitation.

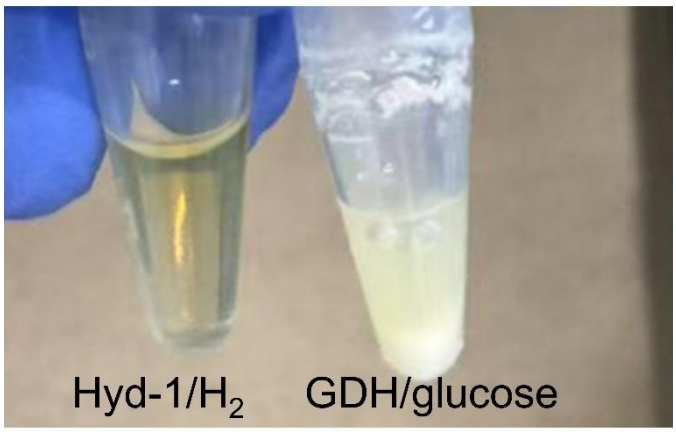


Figure 43. Visual comparison of reaction mixtures after 3 hours of biocatalysis using Hyd-1/H_2 and GDH/glucose systems.

Catalase is sometimes added to FD-halogenase reactions to remove hydrogen peroxide by disproportionation.[166,168,169] The Hyd-1/H_2-driven enzymatic chlorination was conducted with the addition of 650 U/mL of catalase to test whether the addition of catalase would make a difference. However, no change in conversion was seen when catalase was introduced into the halogenation reactions driven by Hyd-1/H_2 system. Therefore, the addition of catalase or SOD does not seem to be necessary (Figure 44).

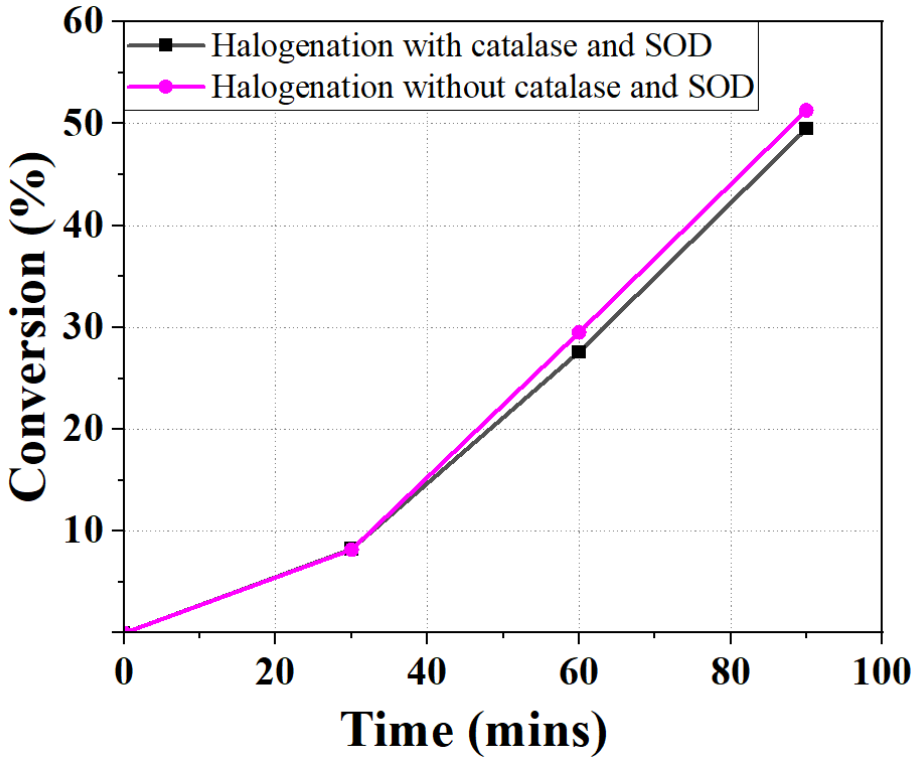


Figure 44. Time point results for H_2-driven enzymatic halogenation with and without catalase and SOD. Reaction conditions: 0.5 mM FAD, 30 mM NaCl, 1 mM L-tryptophan, 5.8 μM Hyd-1, 30 μM PyrH and one reaction is supplemented with 650 U/mL catalase and SOD, while the other is conducted without catalase and SOD.

To check whether the pulsed delivery of O_2 was responsible for improved activity of PyrH at higher substrate (5.5 mM) with the Hyd-1/H_2 system compared to the conventional system, PyrH with GDH/glucose system was tested under N_2 with pulsed delivery of 0.5% O_2 at 5-minute intervals for 2 hours. However, the conversion was almost identical to that observed in air. The results confirm that the improved performance of PyrH under the H_2-driven Hyd-1 system is not solely attributable to the pulsed delivery of O_2 but rather to the efficient and sustained FAD recycling facilitated by Hyd-1 (Figure 45). In addition, the Hyd-1-driven system does not generate gluconic acid like the traditional GDH/glucose system, avoiding the pH fluctuation of the solution,

and this may further stabilise the activity of the enzyme. These findings highlight the unique advantage of the Hyd-1 system in maintaining the catalytic activity of PyrH over extended reaction durations, even at elevated substrate concentrations. However, it should be noted that the conditions are not entirely comparable due to differences in FAD concentration, which may also contribute to the observed effects.

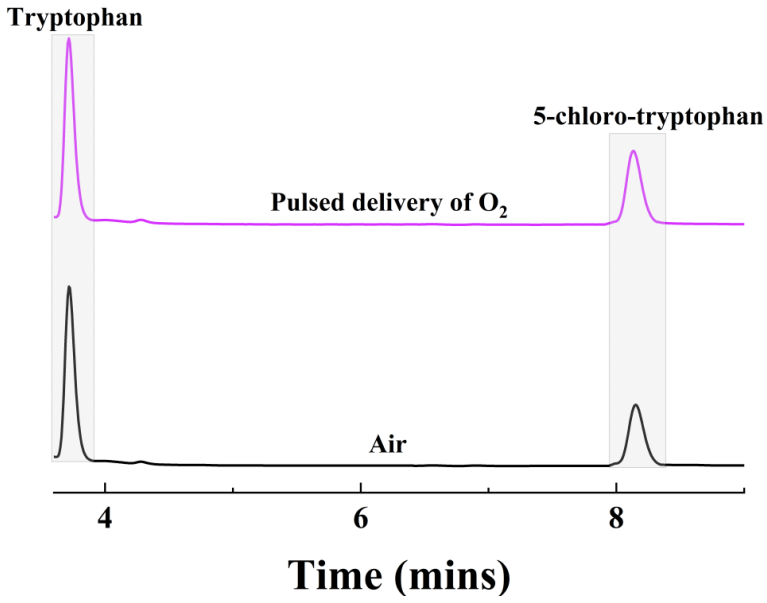


Figure 45. HPLC traces showing conversions for GDH-driven chlorination with air and pulsed delivery of O_2. GDH system conditions:1 μM FAD, 30 mM NaCl, 5.5 mM L-tryptophan, 100 μM NAD^+, 300 mM glucose, 5 μM glucose dehydrogenase, 10 μM Fre, and 30 μM PyrH. Hydrogenase system: 0.5 mM FAD, 30 mM NaCl, 5.5 mM L-tryptophan, 5.8 μM PyrH, and 30 μM PyrH, 0.5% O_2 in H_2, 2-hour reactions.

Notably, the catalytic efficiency achieved with the H_2-driven Hyd-1 system surpasses that of alternative flavin recycling strategies commonly employed in FD-halogenase-catalysed biohalogenation reactions. PyrH achieved a catalytic rate of 0.76 min^{-1} under the H_2-driven system, significantly outperforming photochemical flavin recycling (0.012

min^{-1}),[125] chemoenzymatic recycling using a rhodium-bipyridine complex (0.0023 min^{-1}),[152] and synthetic NADH analogues like BNAH (0.20 min^{-1}).[155] Moreover, the H_2-driven system achieves these improvements without the need for sacrificial reductants or precious metal catalysts, further underscoring its sustainability and cost-effectiveness. Compared to traditional biohalogenation systems, the H_2-driven Hyd-1/PyrH platform offers a greener and more atom-efficient alternative, avoiding the reliance on costly cofactors and minimising chemical waste. This system's robustness, coupled with its compatibility with a simple safe gas mixture of H_2 and O_2, makes it highly suitable for scalable industrial applications. Future research may focus on enhancing the stability and catalytic efficiency of PyrH, possibly through enzyme engineering or directed mutagenesis, to further optimise the system for long-term industrial use.[170.171] Additionally, the promise of the Hyd-1 system to support a broader range of flavin-dependent enzymes, such as monooxygenases, opens new avenues for sustainable biocatalysis.

4.2. Hyd-2 for flavin recycling system

To assess the capability of NiFe hydrogenase-2 (Hyd-2) from *E. coli* in supporting H_2-driven flavin recycling and its compatibility with PyrH, a series of experiments was conducted. Hyd-2, which plays a critical role in H_2 oxidation under anaerobic conditions, was initially tested for its ability to reduce flavin directly. A H_2 atmosphere was applied, and the color change of the reaction mixture (from yellow to colorless), as shown in

Figure 46 provided visual evidence of flavin reduction. This result confirmed that Hyd-2 can perform the essential function of flavin reduction, demonstrating its possible utility in biohalogenation systems.

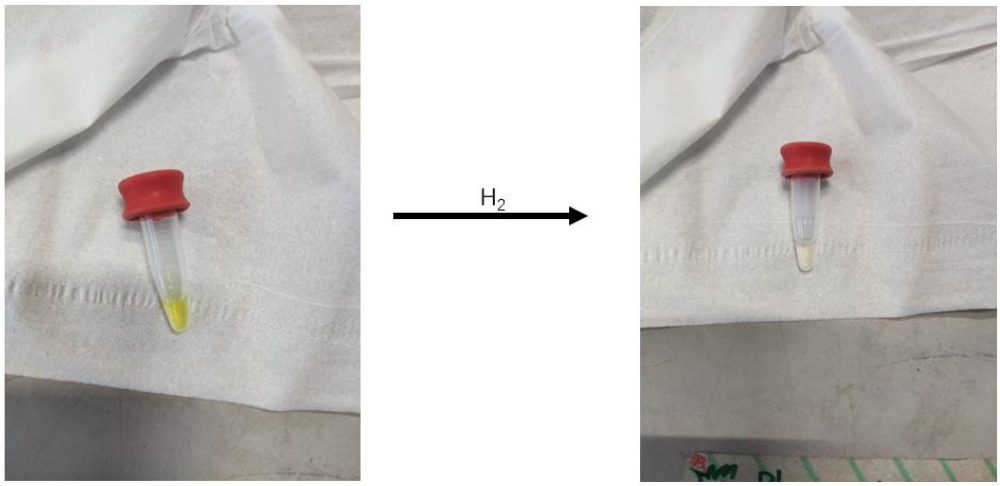


Figure 46. Direct FAD reduction of 0.5 mM FAD by 5.8 μM Hyd-2 under the H_2 atmosphere, making the color change from yellow to colorless.

Following the flavin reduction tests, Hyd-2 was coupled with PyrH for the H_2-driven halogenation of L-tryptophan under conditions identical to those previously used with Hyd-1. These conditions included 0.5 mM L-tryptophan, 0.5 mM FAD, 30 μM PyrH, and pulsed O_2 delivery at 0.5% every 5 minutes.

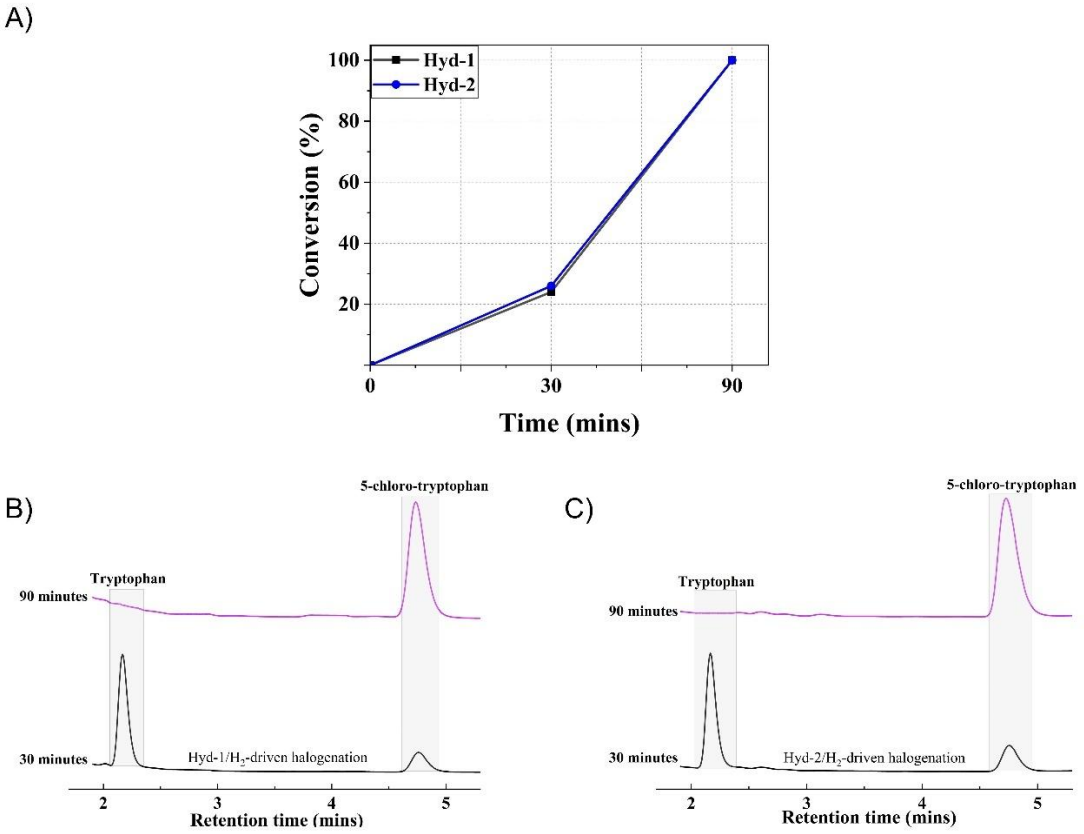


Figure 47. a): The comparison of the timepoint results between Hyd-1-driven and Hyd-2-driven halogenation reactions. b): HPLC traces for the Hyd-1-driven halogenation reactions. c): HPLC traces for the Hyd-2-driven halogenation reactions. Reaction conditions: 0.5 mM L-tryptophan, 0.5 mM FAD, 30 μM PyrH, 5.8 μM Hyd-1/Hyd-2, 20 mM NaCl and pulsed O_2 delivery at 0.5% every 5 minutes.

Surprisingly, the Hyd-2/PyrH system achieved complete conversion of L-tryptophan to 5-chloro-tryptophan within 90 minutes, identical to the performance of the Hyd-1/PyrH system. This was unexpected because Hyd-2 is classified as an O_2-sensitive hydrogenase,[195] whereas Hyd-1 is known for its O_2 tolerance. The comparable performance suggests that under the reaction conditions employed, the O_2 sensitivity of Hyd-2 did not limit its catalytic efficiency, demonstrating the importance of the precise control of H_2/O_2 ratio in the solution (Figure 47).

The comparable rates observed between Hyd-1 and Hyd-2 systems strongly indicate that hydrogenase activity is not the rate-limiting factor in this H_2-driven halogenation system. This result also highlighted two insights. First, the electron transfer facilitated by both Hyd-1 and Hyd-2 is sufficient to make sure that the reduced FAD is available to drive PyrH-catalysed halogenation at high rates. Second, it suggested that PyrH itself, rather than the hydrogenase, may impose limitations on the overall reaction rate under these conditions, particularly due to its natural low turnover rate and possible structural instability during prolonged reactions.[172]

Moreover, the success of Hyd-2 in this system emphasises the robustness of the H_2-driven flavin recycling system. Despite its sensitivity to O_2, Hyd-2 still operates effectively when O_2 is delivered in a controlled manner and recovers rapidly under H_2 flow. The structural arrangement of Hyd-2, particularly its interaction with the electron transport chain via quinone pools, may also contribute to its ability to handle fluctuating O_2 levels without significant loss of activity. Future work should delve deeper into understanding the interplay between hydrogenase structure, O_2 handling, and electron transfer dynamics in flavin recycling systems. For Hyd-2 specifically, exploring how its interaction with PyrH is influenced by variables such as redox potential, and subunit coordination may unfold its unexpected performance. Additionally, further optimisation of O_2 delivery mode could extend the operational lifetime of both hydrogenase and

PyrH, enhancing the catalytic efficiency of the whole halogenation system. The research on Hyd-2 driven halogenation was stopped due to lack of Hyd-2.

4.3. Exploring constant gas environment for the halogenation system

After achieving the automated operation mode, it was hypothesised that H_2 and O_2 could be more effectively utilised by the enzyme under a constant environment without wasting the valuable reducing equivalents, which would better maintain the redox balance of the system. A balloon connected to the headspace was chosen for its ability to provide a stable gas atmosphere and facilitate scalability for possible industrial applications (Figure 48).

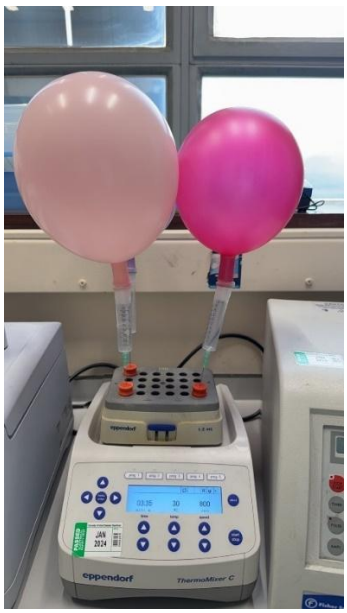


Figure 48. Proposed Hyd-1-driven halogenation under constant flow via a balloon.

To test this hypothesis, a gas mixture of 0.5% O_2 and 99.5% H_2 was prepared using a mass flow controller and delivered above the reaction headspace via a balloon. This setup ensured safety by keeping the gas mixture well-outside the combustion limit while maintaining a consistent gas environment. The reaction was initially tested with around 5 μM Hyd-1, the concentration used in previous experiments. Under these conditions, the solution quickly turned yellow in the early stage of the reaction, corresponding to the characteristic color of 0.5 mM FAD, and remained yellow throughout the whole experiment. The final conversion was low, achieving 22% after 2-hour reaction (Figure 49).

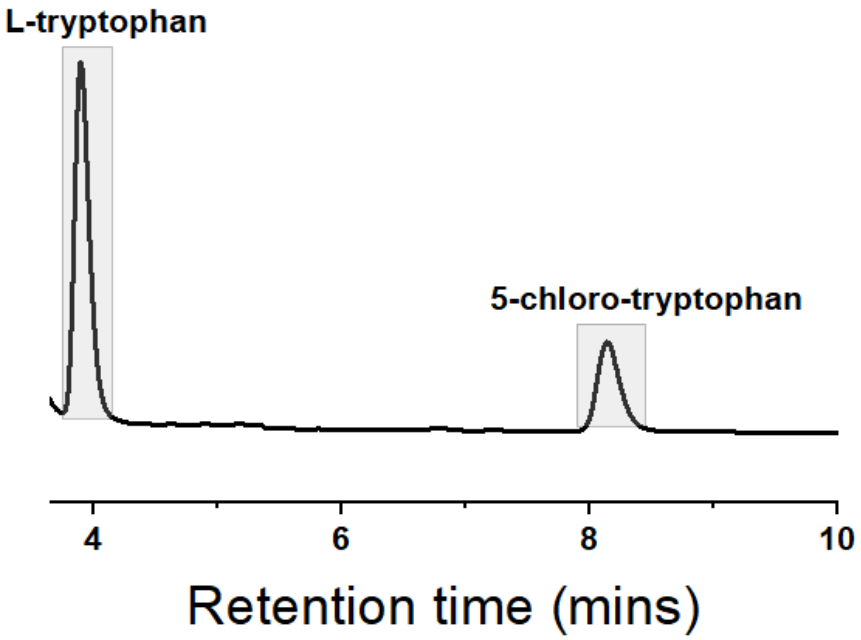


Figure 49. H_2-driven halogenation under constant flow with 5 μM Hyd-1. Reaction conditions: 0.5 mM L-tryptophan, 0.5 mM FAD, 30 μM PyrH, 5 μM Hyd-1, 20 mM NaCl and constant gas environment at 0.5% O_2 / 99.5% H_2.

To test if the reaction performance could be enhanced, the concentration of Hyd-1 was gradually increased to 6.5 μM, 8 μM, and 10 μM. The results showed a clear

improvement in conversion rates, reaching 42%, 71%, and 96%, respectively (Figure A16 – A18).

The visual appearance of the reaction solutions provided further insights into the redox dynamics of the system. Specifically, at 5 μM Hyd-1, the solution rapidly turned yellow at the beginning of the reaction and retained this colour throughout the process. This yellow coloration corresponds to the presence of 0.5 mM FAD, indicating that $FADH_2$ was not being sufficiently regenerated. The inability to sustain FAD reduction under these conditions resulted in low reaction efficiency. In contrast, at 10 μM Hyd-1, the solution displayed a stable and consistent pale yellow color, lying between the deep yellow of 0.5 mM FAD and a colourless state (Figure 50). This intermediate coloration persisted for several hours, reflecting a steady-state redox balance where the rates of FAD reduction and $FADH_2$ oxidation were effectively matched. This equilibrium allowed the reaction to proceed efficiently, achieving a conversion rate of 96%. However, under prolonged constant O_2 flow, the system eventually exhibited a decline in enzymatic activity. This decline is possibly attributed to the gradual inactivation of Hyd-1 due to the constant supply of O_2. Importantly, the system could be fully reactivated by introducing a H_2 flow for 30 minutes. This optimised method offers significant advantages over previous approaches. It is not only easier to operate and control but also provides a more reliable foundation for the kinetic study of the reaction. More importantly, the method facilitates scalability, making it a practical choice for

industrial applications. As a result of its demonstrated effectiveness, all subsequent H_2-driven halogenation reactions in this study were conducted using this optimised setup.

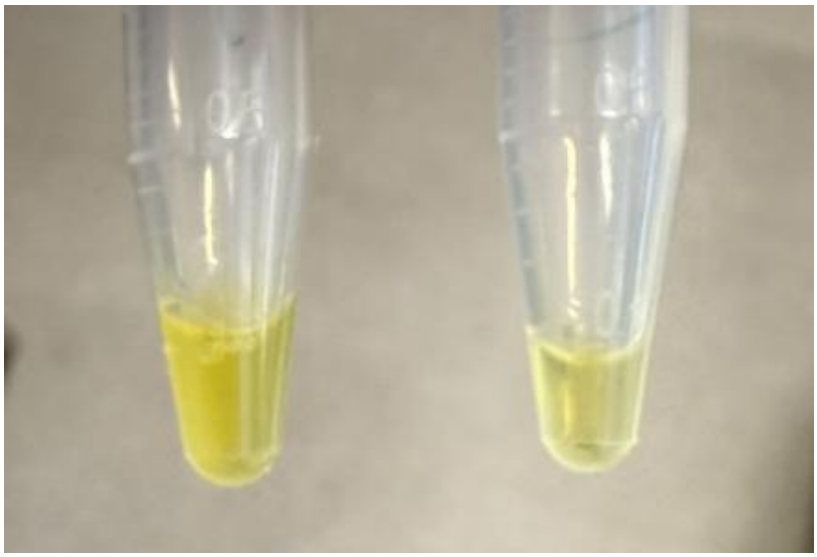


Figure 50. Solution color of 5 μM Hyd-1 reaction (left) and 10 μM Hyd-1 reaction (right).

4.4. Extending to FD-halogenase PrnA

The work of this section as done with a Part II student who expressed PrnA with assistance from Dr Stephen Carr. All subsequent experiments were conducted jointly or under my direct supervision, with my primary responsibility including experimental design, troubleshooting, data analysis, and interpretation. As a flavin-dependent halogenase, PrnA is a tryptophan 7-halogenase. It catalyses the chlorination reaction of the 7-position of L-tryptophan to produce 7-chloro-L-tryptophan. PrnA exhibits remarkable regioselectivity through a sophisticated interplay of its active site structure and electronic properties. The specificity for the 7-position arises from the precise

spatial orientation of L-tryptophan within the enzyme's substrate-binding pocket. This pocket stabilises the amino and carboxyl termini of the substrate, positioning its indole ring in a conformation that exposes the 7-position directly to the catalytic machinery (Figure 13). Structural studies suggest that steric hindrance from side chains near the 5- and 6-positions of the indole ring blocks access to alternative halogenation sites, leaving the 7-position as the sole target. Additionally, the electronic density at the 7-position is lower than at other positions, making it more susceptible to electrophilic attack by hypochlorous acid (HOCl), generated from the reaction of chloride ions with the flavin peroxide intermediate. The unique channel-like structure in PrnA directs the HOCl produced in the active site specifically to the 7-position, ensuring high regioselectivity and efficiency. This regioselectivity is further reinforced by stabilising interactions between active site residues and the transition state, which lower the energy barrier for the reaction at this specific site.[173,174,175]

To test the compatibility of PrnA with the H_2-driven flavin recycling system, the enzyme was coupled with both Hyd-1 and Hyd-2 under the optimised constant gas atmosphere method. The reactions were conducted with 0.5 mM FAD, 0.5 mM L-tryptophan, 25 μM PrnA and 10 μM Hyd-1 / Hyd-2 with a balloon of gas mixture of 0.5% O_2 / 99.5% H_2, 30 ℃. The results showed that both Hyd-1 and Hyd-2 supported PrnA activity, achieving approximately 10% conversion of L-tryptophan to 7-chloro-L-tryptophan within 1 hour. These results demonstrated that PrnA can operate within the H_2-driven

system and the comparable performance of Hyd-1 and Hyd-2 further reinforces the observation that hydrogenase activity is not the primary limiting factor in this system (Figure 51).

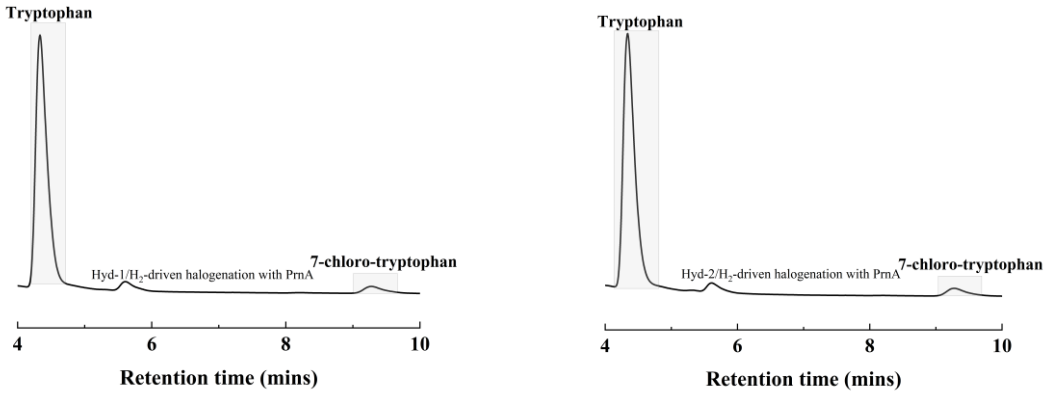


Figure 51. HPLC trace of Hyd-1 (left) and Hyd-2 (right) driven chlorination of L-tryptophan catalysed by PrnA, achieving around 10% conversion. Reaction conditions: 0.5 mM FAD, 0.5 mM L-tryptophan, 25 μM PrnA and 10 μM Hyd-1 / Hyd-2 with a balloon of gas mixture of 0.5% O_2 / 99.5% H_2, 30 ℃.

Following the initial experiments with PrnA, which achieved a relatively low conversion of 10%, a series of optimisation steps were undertaken to enhance the system's efficiency. Recognising that enzyme concentration might be a limiting factor, the concentration of PrnA was doubled. In addition, in order to further refine the reaction conditions, we investigated the optimal temperature for PrnA activity within the H_2-driven system，ranging from 30 ℃ to 50 ℃. The reactions were conducted with 0.5 mM FAD, 0.5 mM L-tryptophan, 30 μM PrnA and 10 μM Hyd-2 with a balloon of gas mixture of 0.5% O_2 / 99.5% H_2, 2 hours (Figure A19 – A23). The peak around 6 minutes is a background peak, because this peak also appears in the analytical reference spectrum of the substrate and product.

The results demonstrated a 7-chloro-tryptophan conversion of 20% at 30 ℃, which significantly increased to 39% at 35 ℃. Hyd-1 is known to exhibit exceptional robustness, with its activity increasing with temperature up to about 50 ℃ range. Unlike PyrH, which begins to lose activity at 35 – 40 ℃ and rapidly denatures around 50 ℃, PrnA showed enhanced activity and stability at elevated temperatures. Consequently, the reaction temperature was further increased to 40 ℃, 45 ℃, and 50 ℃ to determine the optimal temperature range.

The results at 40 ℃, 45 ℃, and 50 ℃ demonstrated a significant temperature-dependent enhancement in the catalytic performance of PrnA within the H_2-driven system, highlighting its exceptional thermostability and catalytic efficiency under elevated temperatures. At 40°C, the conversioin of 7-chloro-tryptophan increased to 51%, a significant improvement compared to 35 ℃ (39%). This upward trend continued at 45°C, where the conversion enhanced to 86%, and at 50 ℃, a remarkable 96% conversion was achieved. Such results indicated that PrnA operates optimally within this high-temperature range, maintaining catalytic activity without apparent denaturation. This is a contrast to enzymes like PyrH, which rapidly lose activity above 35 ℃.

The synergy between PrnA and Hyd-1 is central to these observations. Hyd-1, known for its robustness, facilitates efficient and continuous FAD recycling across a broad

temperature range, providing a stable redox environment essential for sustained enzymatic activity. Generally, elevated temperatures not only enhance enzymatic reaction rates by increasing molecular kinetic energy but may also improve substrate diffusion and binding efficiency. Additionally, the H_2-driven system eliminates the pH fluctuations commonly seen in conventional systems (e.g., gluconic acid production in GDH/glucose systems), further stabilising PrnA activity at high temperatures.

The superior thermostability of the flavin-dependent halogenase PrnA over PyrH can be explained by several specific structural features. Experimentally, PrnA retains full catalytic activity from 30 °C up to at least 50 °C, while PyrH begins to aggregate and lose activity above 35 °C. This contrast is likely rooted in differences in their domain architecture, surface electrostatics, and quaternary structure. Structurally, PrnA appears to possess a more tightly packed hydrophobic core that minimises internal cavity volume, reducing the likelihood of thermal unfolding.[176] Additionally, PrnA has a higher density of stabilising salt bridges and hydrogen bonds at its surface, particularly between charged residues such as Glu, Asp, Arg, and Lys, which form a more extensive electrostatic interaction network than in PyrH. These interactions have been shown in other halogenases, like Thal and RebH, to significantly raise thermal tolerance.[174] The loop regions connecting PrnA's FAD-binding and tryptophan-binding domains are also shorter and more structured than those in PyrH, which contains an extended, flexible loop that may increase conformational entropy and act as a

destabilising element under heat stress.[177] Notably, PrnA also contains conserved residues such as Ser347 and Glu346 that participate in long-range hydrogen bond chains reaching into the active site, stabilizing both structure and function. In contrast, PyrH lacks equivalent stabilising contacts in corresponding positions.[178]

Beyond the enzymatic performance, the experimental design incorporating the balloon method with a constant gas atmosphere represents a scalable and industrially relevant approach. In an industrial context, constant gas atmosphere or gas flow are more suitable for continuous processes, enabling precise control over gas concentrations, decreasing variability, and supporting prolonged reaction durations. This compatibility with scalable setups, combined with the stability of both PrnA and Hyd-1, positions the system as a promising platform for industrial biocatalysis. Future explorations such as stabilising PyrH at higher temperatures through protein engineering or using thermostable variants could allow the system to operate even more efficiently under conditions more favorable to hydrogenase.

4.5. Ni-complex for flavin recycling system

To extend the H_2-driven flavin recycling system to new reductive catalysts, a DuBois-type nickel bis-diphosphine complex (Ni-complex) was tested for its ability to support flavin reduction and drive halogenation reactions (Figure 52). This was kindly provided

by Professor Vincent Artero. The Ni-complex employed in this study provides a robust system for catalytic H_2 oxidation and flavin reduction. Its nickel bis-diphosphine core is designed for exceptional redox stability. This substitution enhances the electronic properties of the complex, optimising its ability to facilitate electron transfer during H_2 activation and flavin reduction. The complex has been employed in nitro hydrogenation reactions under mild conditions, demonstrating robustness and tunability for various reductive transformations (see Dr. Maya Landis DPhil thesis). Unlike hydrogenases, this molecular catalyst operates independently of a proteinaceous environment and offers synthetic versatility while maintaining high catalytic turnover. These catalysts feature a Ni(II) metal centre coordinated by diphosphine ligands bearing pendant amines, which mimic key features of the active site in [FeFe]-hydrogenases. At the outset of the catalytic cycle, the nickel centre typically adopts a +2 oxidation state, existing as a stable complex. Upon exposure to molecular hydrogen, the complex initiates catalysis through heterolytic cleavage of H_2, enabled by the synergistic interaction between the Ni centre and the pendant amine groups. This results in the formation of either a Ni–H/N–H intermediate (where one hydrogen becomes a metal hydride and the other protonates a pendant amine), or a fully reduced Ni(0) species with two protonated amines. Both intermediates are observed by low-temperature NMR and are rapidly interconvertible via proton transfer. This process reduces the Ni(II) center to Ni(0), while maintaining charge balance through protonation of the ligands.[179,180,181]

In the latter stages of the catalytic cycle, the Ni(0) species transfers its electrons to FAD. Electron transfer may proceed in a stepwise fashion, where Ni(0) first donates one electron to FAD, generating the flavin semiquinone ($FAD^{\bullet -}$) and forming Ni(I), followed by a second electron transfer to yield fully reduced $FADH_2$ and regenerate Ni(II). In parallel, protons are delivered from the protonated pendant amines to the flavin, enabling the net transfer of two electrons and two protons from H_2 to FAD, in a mechanism known as proton-coupled electron transfer (PCET). Alternatively, the mechanism may proceed via hydride transfer from the Ni–H species directly to the flavin, forming $FADH^-$ intermediates that are subsequently protonated to $FADH_2$.[182,183]

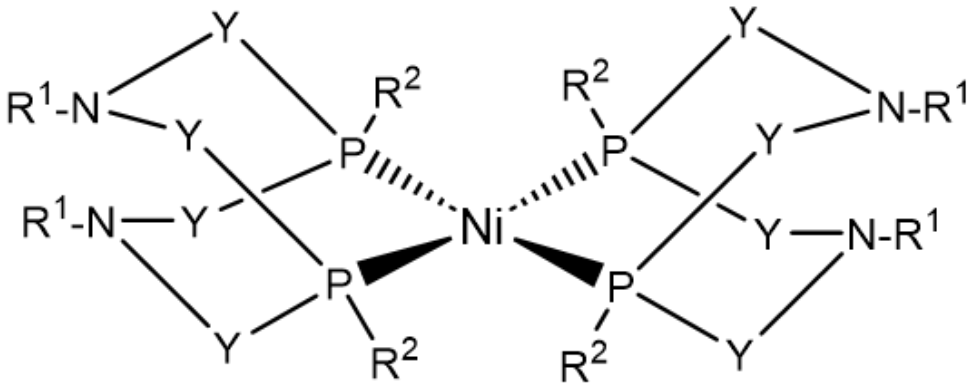


Figure 52. Structure of Ni-complex used in this study. R^1 is arginine, R^2 is phenyl.

Initial tests with the Ni-complex were performed to evaluate its ability to reduce flavin under H_2 flow. Using the same H_2 atmosphere and reaction setup as the Hyd-1 and Hyd-2 systems, visual analysis confirmed successful flavin reduction, similar to the

enzymatic systems. Following this, the Ni-complex was integrated into the H_2-driven halogenation reaction system with PrnA as the FD-halogenase. The reaction conditions included 0.5 mM FAD, 0.5 mM L-tryptophan, 20 μM PrnA, and a balloon with 0.5% O_2 / 99.5% H_2, 30 ℃ for a preliminary and qualitative test. After 1 hour, the reaction achieved approximately 10% conversion of L-tryptophan to 7-chloro-L-tryptophan, matching the results obtained using Hyd-1 and Hyd-2 under identical conditions (Figure 53). Future work could focus on expanding the substrate scope to assess the full promise of this catalyst in diverse valuable halogenation reactions. Additionally, mechanistic studies could provide deeper insights into the electron transfer dynamics between the Ni-complex and flavin, offering opportunities for further tuning and enhancement of the catalytic system.

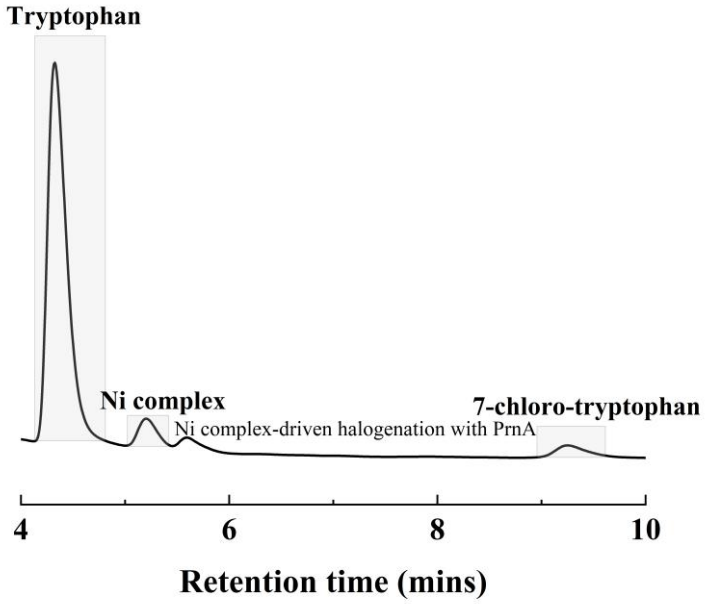


Figure 53. HPLC trace of Ni complex-driven chlorination of L-tryptophan catalysed by PrnA under 30℃, achieving around 10% conversion after 1 hour. Reaction conditions: 5.8 μM Ni-complex, 0.5 mM FAD, 0.5 mM L-tryptophan, 20 μM PrnA, 20 mM NaCl and a balloon with 0.5% O_2 / 99.5% H_2, 30 ℃.

This chapter extended the H_2-driven flavin reduction platform through systematic exploration of enzyme alternatives and gas delivery strategies. By comparing the performance of different hydrogenases (Hyd-1 vs. Hyd-2), incorporating synthetic flavin reductants, and optimising O_2 concentrations under varied delivery regimes, a broader, more robust halogenation framework was developed. Furthermore, testing with additional flavin-dependent halogenases such as PrnA confirmed the system's generality. While the focus thus far has been on halogenases, the potential of this H_2-driven flavin recycling system extends to other classes of flavin-dependent enzymes. Chapter 5 explores this possibility by adapting the system for use with flavin monooxygenases to achieve selective epoxidation.

5

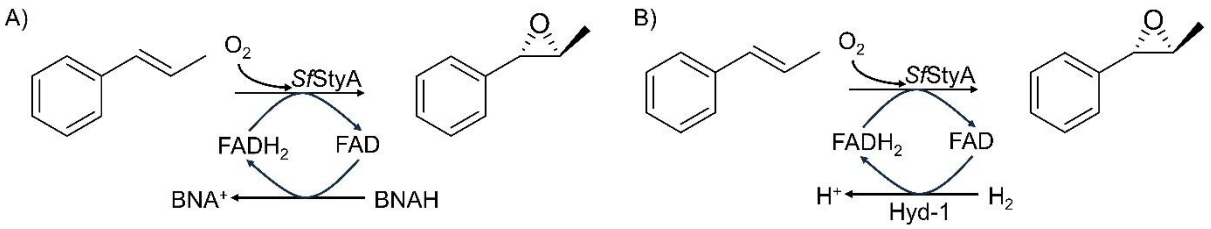
Chapter 5

5.1. Introduction

This work was done in collaboration with Aster van Noord and Professor Caroline Paul and the flavin-dependent monooxygenase *Sf*StyA was also provide by them. This study sought to expand the application of our H_2-driven flavin recycling system to flavin-dependent monooxygenases (FMOs), a versatile class of enzymes known for their ability to catalyse a wide range of oxidative transformations under mild and environmentally friendly conditions. Specifically, this study focused on the FMO Styrene Monooxygenase (*Sf*StyA), which natively catalyses the epoxidation of *trans*-β-methylstyrene to its corresponding epoxide. Styrene monooxygenase (StyA), a flavin-dependent monooxygenase, catalyses the enantioselective epoxidation of styrene to (*S*)-styrene oxide through a two-component system comprising a reductase and an epoxidase. In the initial step, the reductase uses NADH to reduce flavin adenine dinucleotide (FAD) to $FADH_2$, which is subsequently transferred to the epoxidase component. Within the epoxidase, $FADH_2$ reacts rapidly with molecular oxygen to generate a C4a-hydroperoxyflavin intermediate. This intermediate facilitates the epoxidation of styrene via a concerted electrophilic addition mechanism. Specifically, the π-electrons of the styrene double bond attack the terminal oxygen of the hydroperoxyflavin, forming a three-membered oxirane (epoxide) ring in a stereoselective fashion. Simultaneously, the oxygen-oxygen bond of the hydroperoxyflavin cleaves, and the flavin is returned to its oxidised form. This oxygen transfer step is highly regio- and enantioselective, favouring formation of (S)-styrene

oxide due to the well-organised active site that orients the substrate precisely relative to the oxygenating species.[184,185]

This reaction is of industrial interest due to the high demand for epoxides as intermediates in the production of pharmaceuticals, agrochemicals, and as polymer precursors.[186,187,188] Traditional FMO-catalysed reactions rely on the expensive cofactor NADH or stoichiometric levels of analogs, such as BNAH (Scheme 7A), for flavin reduction, presenting significant cost and sustainability challenges for large-scale applications.[201] By coupling *Sf*StyA with our H_2-driven flavin recycling system, facilitated by hydrogenase Hyd-1, this study aimed to provide a greener and more cost-effective alternative for enzymatic epoxidation (Scheme 8B). Through this integration, trans-β-methylstyrene was used as the model substrate to evaluate the system's efficiency and compatibility with FMOs.



Scheme 7. Reaction scheme of BNAH-driven bioepoxidation and H_2-driven bioepoxidation.

5.2. Results

5.2.1. BNAH-driven bioepoxidation

Flavin monooxygenases are typically operated in air (~21% O_2), which provides ample oxygen for their activity. However, such high O_2 concentrations pose significant challenges when combined with hydrogenase-dependent systems. Excess O_2 can rapidly inactivate hydrogenase enzymes, making it crucial to determine whether the biocatalyst can function under lower O_2 levels. Therefore, the *Sf*StyA was first tested for its tolerance to lower O_2 levels with the BNAH-driven flavin recycling system. The results showed that, at 10% O_2, the conversion for the epoxidation of trans-β-methylstyrene by *Sf*StyA was nearly identical to that observed under air (21% O_2), achieving around 90% conversion. However, when the O_2 level was at 1%, the conversion dropped significantly, similar to the no-O_2 control. This result strongly supported the conclusion that *Sf*StyA activity is significantly compromised as O_2 levels fall below 10%. While *Sf*StyA demonstrated near-optimal activity at O_2 levels of 10% and above, the H_2-driven flavin recycling system introduces additional constraints, as higher O_2 concentrations lead to rapid inactivation of the hydrogenase (Figure 54). Even though Hyd-1 is O_2-tolerant, the exposure to O_2 concentrations this high could significantly impair its ability to catalyse the reduction of flavins. Furthermore, 10% O_2 in H_2 would be a combustible mixture. Therefore, achieving a balance between sufficient O_2 to sustain *Sf*StyA activity and low O_2 levels to preserve hydrogenase functionality and safety becomes a critical challenge in optimising the H_2-driven

bioepoxidation system. To address this, precise control of the gas composition is essential.

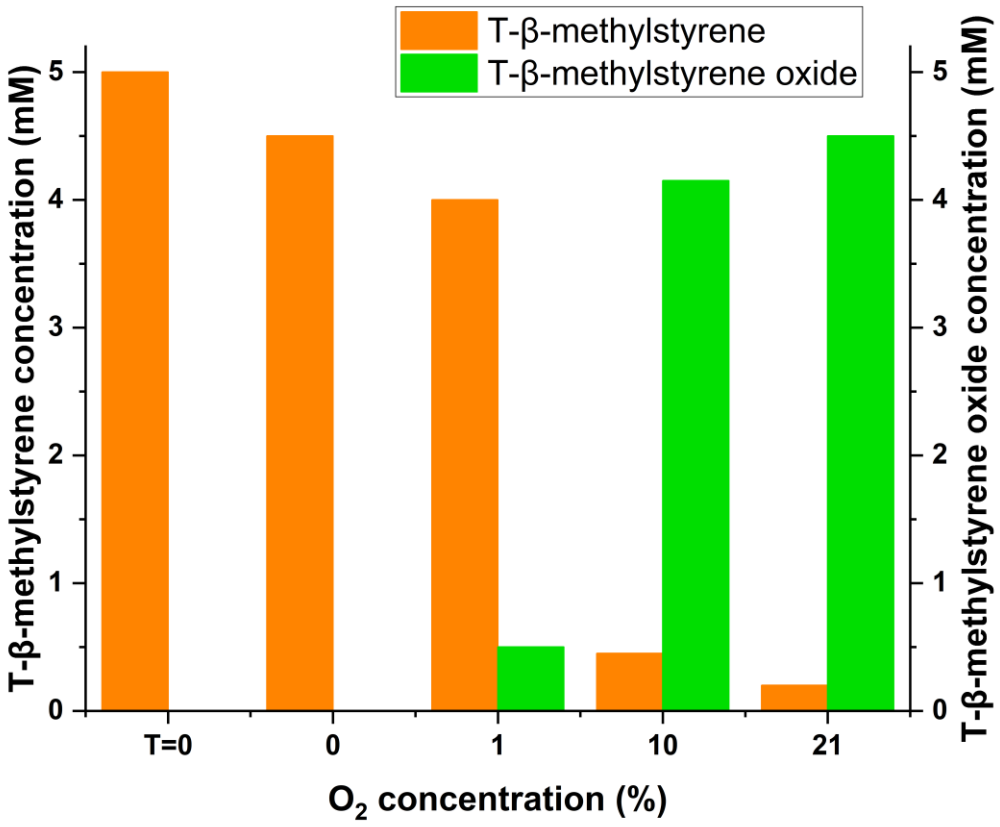


Figure 54. The results of O_2 tolerance test for *Sf*StyA with BNAH-driven flavin recycling system. The reactions were performed in glass 2 mL GC vials, each reaction had a final assay volume of 400 µL containing 15 mM BNAH, 650 U/mL catalase, 3 µM *Sf*StyA, 5 mM trans-β-methylstyrene and 0.05 mM FAD in 50 mM Tris-HCl (pH = 7.0, 30 ℃). The reaction was open to air and incubated at 30 °C, 900 rpm shaking for 1 h. Substrate and product peak areas were determined by GC (2µL injection).

5.2.2. Substrate evaporation test

To investigate discrepancies between substrate amounts remaining at the end of the reaction and the observed conversion rates, the volatility of trans-β-methylstyrene was identified as a possible factor. It was hypothesised that substrate evaporation during

the reaction could lead to underestimation of the actual reaction efficiency. To test this, a series of experiments was conducted using different sealing methods, comparing the effects of substrate evaporation and absorption. Four sealing methods were evaluated: (1) a used Suba Seal, (2) a new Suba Seal, (3) an Eppendorf tube lid with a punctured hole covered by Parafilm, and (4) Parafilm alone (Figure 55). The amount of substrate remaining at the end of the reaction was quantified by GC analysis and compared to the initial substrate concentration (t=0).

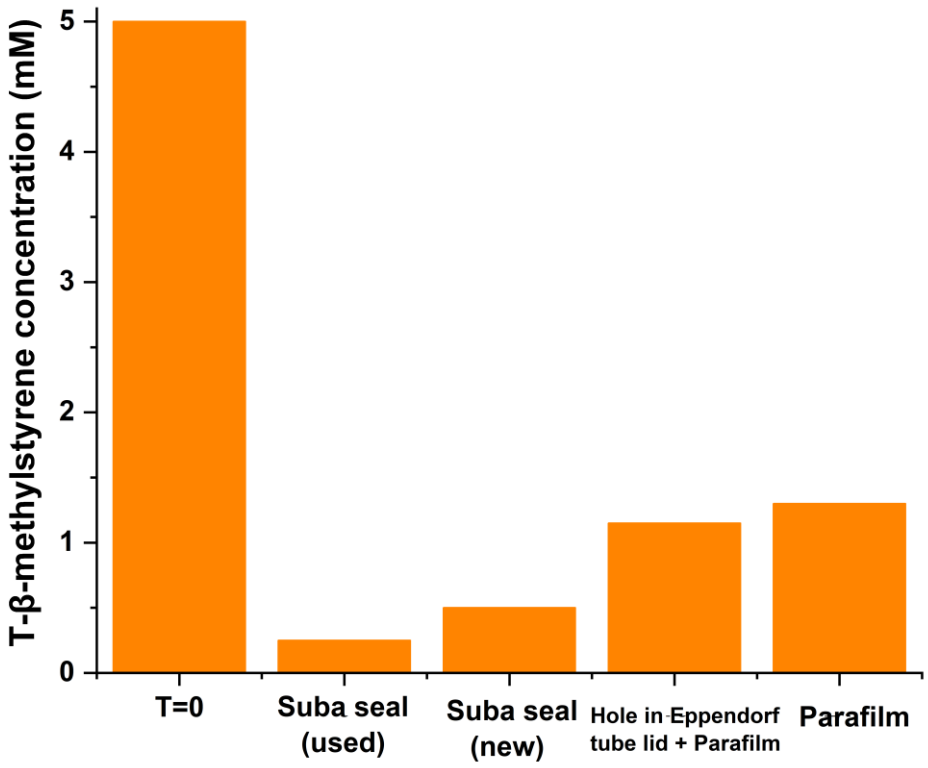


Figure 55. The results of evaporation test for different sealing method with 5 mM trans-β-methylstyrene. The reactions were performed in glass 2 mL GC vials, each reaction had a final assay volume of 400 µL containing 5 mM trans-β-methylstyrene in 50 mM Tris-HCl (pH = 7.0, 30 ℃), 4-hour reactions.

The results confirmed that evaporation and absorption significantly impact the measured substrate amounts. When using the used Suba Seal, almost no substrate was detected by the end of the reaction. Similarly, the new Suba Seal also showed a significant loss of substrate, though to a slightly lesser extent. In contrast, the configurations involving Parafilm, either alone or in conjunction with a punctured Eppendorf tube lid, exhibited considerably less substrate loss. These findings indicated that despite its intended role as a secure sealing material, the Suba Seal likely interacts with volatile substrates, absorbing them during the reaction.

Following the observed substrate loss due to evaporation and absorption in initial setups, alternative methods were explored to mitigate these issues and ensure accurate reaction conditions. Hyd-1 was also coupled with the *Sf*StyA to compare with the BNAH-driven epoxidation reactions. A balloon was placed over the reaction vessel to maintain a controlled and constant gas environment, while a gas-tight pressure vessel was also tested to minimise substrate loss. However, despite these modifications, substantial evaporation of the volatile substrate persisted, particularly when compared to the faster reactions driven by BNAH (Figure 56). The prolonged reaction times required for the H_2-driven flavin recycling system amplified the evaporation issue, as a faster reaction generally shows less evaporation. Because the substrate evaporation under the constant gas environment method was still severe, the subsequent method used was pulsed delivery of O_2.

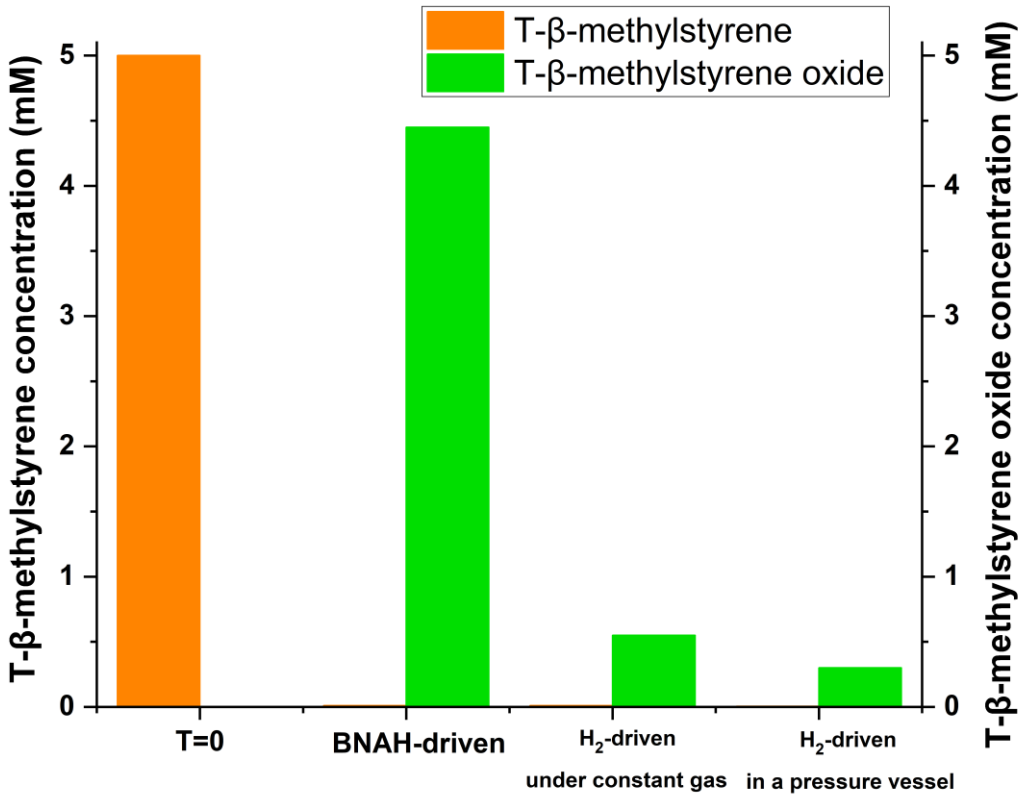


Figure 56. The results of evaporation test for the balloon and pressure vessel methods. T4H: 4-hour reactions. The reactions were performed in glass 2 mL GC vials, BNAH-driven reaction had a final assay volume of 400 µL containing 15 mM BNAH, 650 U/mL catalase, 0.05 mM FAD, 3 µM *Sf*StyA, 5 mM trans-β-methylstyrene in 50 mM Tris-HCl (pH = 7.0, 30 ℃). H2-driven reaction had a final assay volume of 400 µL containing 5.8 µM Hyd-1, 650 U/mL catalase, 3 µM *Sf*StyA, 0.05 mM FAD, 5 mM trans-β-methylstyrene in 50 mM Tris-HCl (pH = 7.0, 30 ℃).

5.2.3. Reaction conditions optimisation

To optimise the reaction conditions, different concentrations of FAD (0.05 mM, 0.1 mM, 0.3 mM, and 0.5 mM) were tested (Figure 57), as well as evaluating the impact of different O_2 levels (Figure 58). To ensure comparability of the conditions, a comparative analysis of the reaction performance using both Hyd-1 and BNAH-driven systems was also conducted.

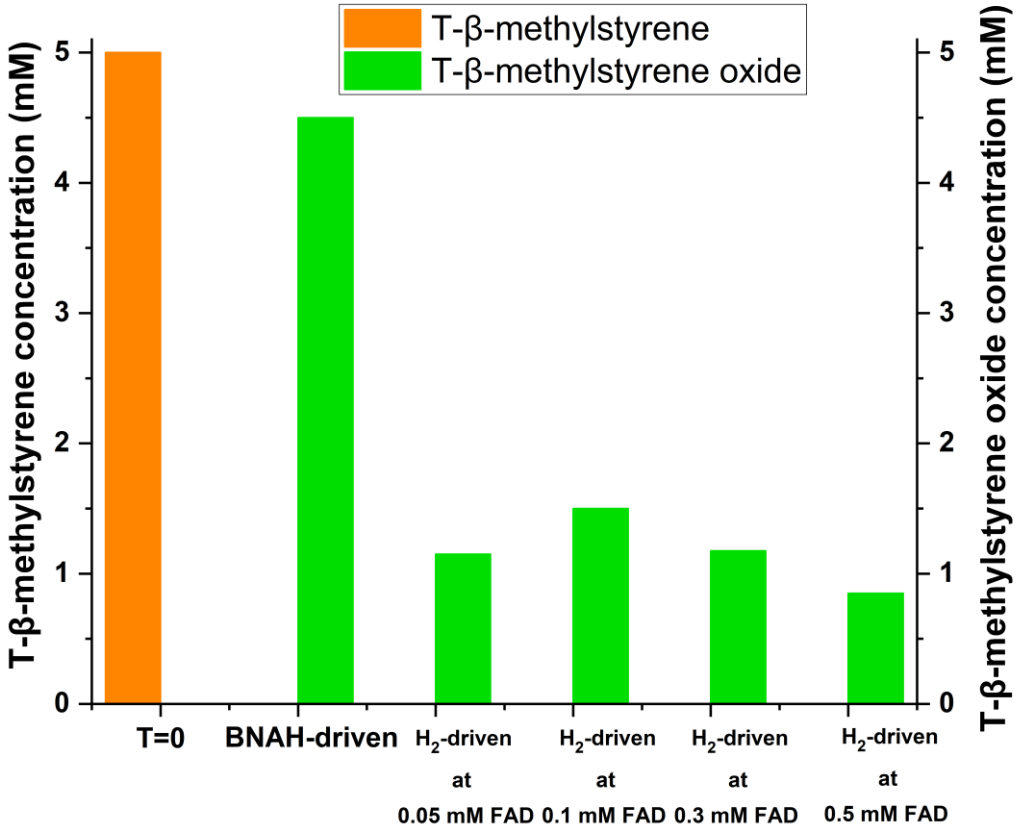


Figure 57. The results of FAD concentrations comparison. Reaction conditions: 0.05 / 0.1 / 0.3 / 0.5 mM FAD, 650 U/ml catalase, 5 mM trans-β-methylstyrene, 5.8 μM Hyd-1, 3 μM *Sf*StyA, 1% O_2, 4 injections, 4-hour reacion, 30℃, 900 rpm shaking in a GC vial sealed with parafilm. Samples were placed on the ice for 5 minutes before extraction.

It is important to note that no detectable substrate remains under any of the reaction conditions tested. However, due to substantial and variable evaporation observed across different setups, this does not indicate complete conversion.

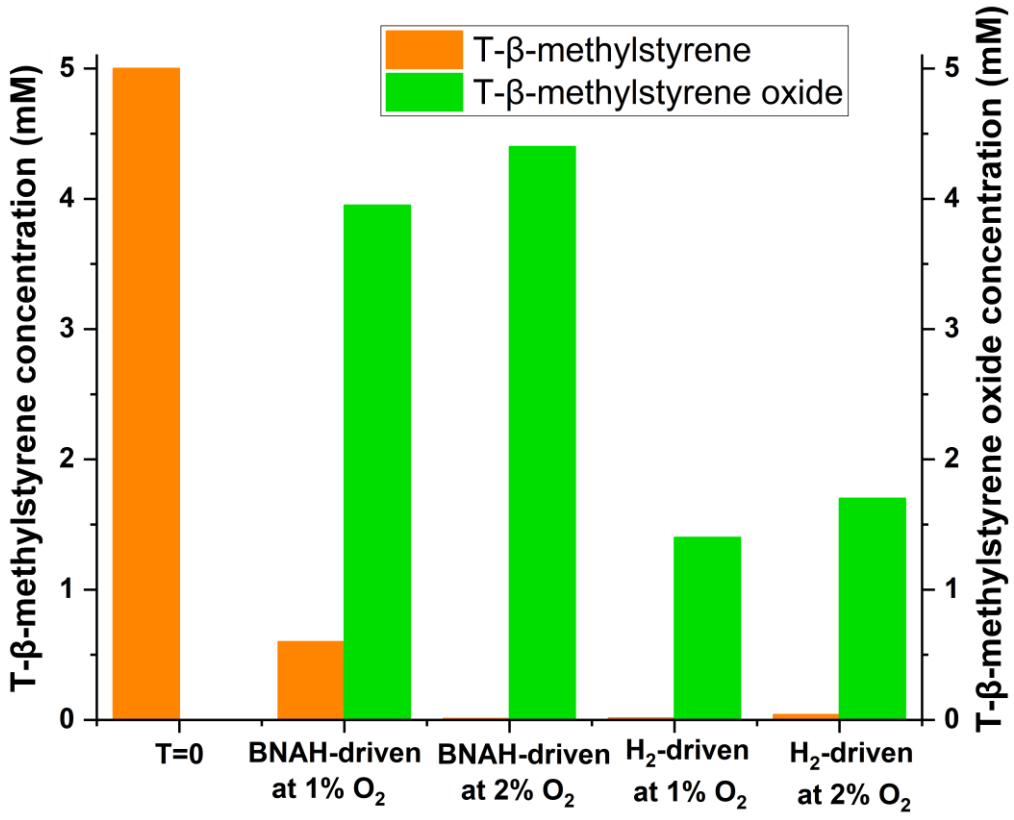


Figure 58. The results of O_2 concentrations comparison. Hyd-1 reaction conditions: 0.1 mM FAD, 650 U/ml catalase, 5 mM trans-β-methylstyrene, 5.8 μM Hyd-1, 3 μM *Sf*StyA, 1%/2% O_2, 4 injections, 4 hours, 30℃, 900 rpm shaking in a GC vial. BNAH reaction conditions: 15 mM BNAH, 0.1 mM FAD, 650 U/ml catalase, 5 mM trans-β-methylstyrene, 3 μM *Sf*StyA, 1%/2% O_2, 4 injections, 4 hours, 30℃, 900 rpm shaking in a GC vial. Samples were placed on ice for 5 minutes before extraction.

The results showed the highest product conversion was achieved at an FAD concentration of 0.1 mM. At lower concentrations of FAD (0.05 mM), the reaction rate was presumably limited by insufficient electron donors. Conversely, at higher FAD concentrations (0.3 mM and 0.5 mM), product formation decreased, likely due to ithe consumption of reducing equivalents by flavin which gets re-oxidised by O_2. For O_2 optimisation, the Hyd-1-driven system under 2% O_2 demonstrated significantly higher

product conversion compared to 1% O_2. This suggests that 2% O_2 provides sufficient supply for *Sf*StyA activity while remaining below the threshold that siginificantly inhibits hydrogenase activity. However, given that all conditions resulted in considerable substrate evaporation, it is uncertain whether one condition is inherently superior to another. Although higher product formation might suggest a faster reaction, the significant evaporation observed across different reaction conditions introduces uncertainty in this interpretation.

5.2.4. Addressing the evaporation problem

To further address the issue of substrate evaporation, the addition of co-solvents was evaluated as a possible solution. The selection of dimethyl sulfoxide (DMSO) as a co-solvent for these experiments was based on prior findings that demonstrated both *Sf*StyA and Hyd-1 exhibit tolerance to DMSO.[56] Evaporation tests were carried out with varying concentrations of DMSO (1%, 5%, 10%, 15%, and 20% by volume), and the residual substrate was measured after a two-hour reaction time (Figure 59).

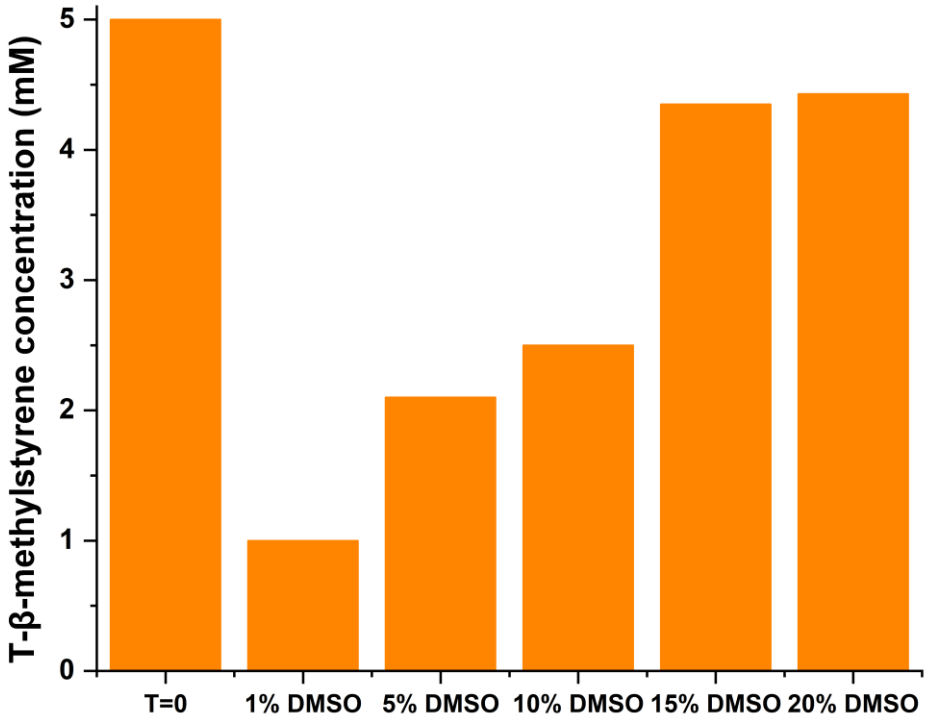


Figure 59. The results of evaporation test with DMSO as the co-solvent. Conditions: 5 mM trans-β-methylstyrene in DMSO, Tris-HCL buffer with 1 / 5 / 10 / 15 / 20% DMSO, open to air.

The results demonstrated that higher concentrations of DMSO, particularly at 15% and 20%, significantly decreased substrate evaporation compared to lower concentrations and the no-co-solvent control. The observed reduction in evaporation with higher DMSO concentrations can be attributed to the fact that DMSO is known for its high boiling point (189 ℃) and low volatility, which can stabilise the substrate in the solution when used as a solvent or co-solvent.[189] While the use of DMSO offers a practical solution for reducing evaporation, possible effects on enzyme activity and system

performance must also be considered. Future experiments will be investigated to test the compatibility of DMSO with both hydrogenase and FMO systems to confirm that catalytic efficiency and reaction rates remain largely unaffected.

Following the completion of DMSO volatility assessments, the available stock of *Sf*StyA enzyme was fully consumed. As a result, no further investigations were performed to assess the effect of DMSO as a co-solvent on the catalytic performance of the system.

5.3. Discussion and future direction

FMOs present a promising catalyst for the industrial applications in biocatalysis due to their ability to catalyse diverse oxidation reactions with chemo-, regio-, and stereoselectivity. Their promise for synthesising natural products and modifying various substrates has made them possible tools in biotechnology and pharmaceutical synthesis.[190] However, several challenges still remain such as the volatility of certain substrates and the enzyme catalytic efficiency. To address these challenges, several strategies have been explored. One approach involves the application of Pickering emulsions in biocatalysis. Pickering emulsions provide a large interfacial area for the biocatalytic system by converting the two-phase system into an emulsion. This could promote efficient contact between substrate and biocatalyst while reducing exposure

of substrate to the environment without the need for the consistent stirring, thereby possibly reducing volatile losses. In addition, the particles used for stabilisation in the emulsion will form a barrier at the oil-water interface, which may effectively limit the volatility of the substrates. In addition, Pickering emulsions can be designed to encapsulate the organic or the aqueous phase as needed to further isolate the reaction environment and protect the substrate from evaporation (Figure 60).[191]

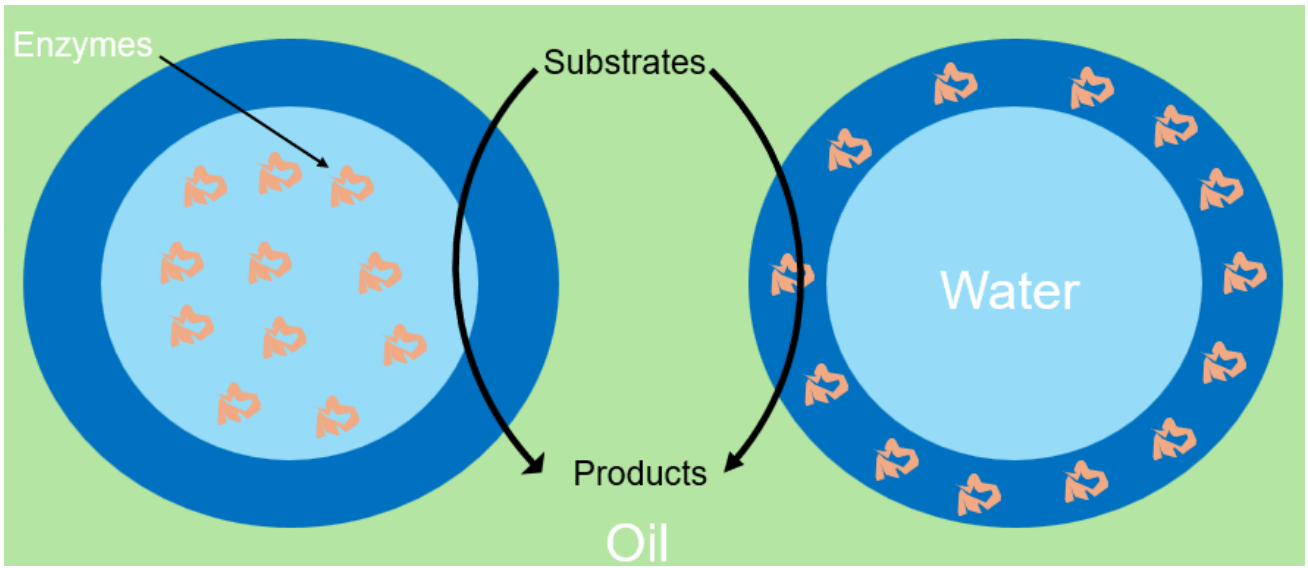


Figure 60. Biocatalysis in and on the Pickering emulsion.

Substrate engineering has also been applied to P450 monooxygenases, which, like FMOs, belong to the hydroxylase family. This approach usually adds protective or anchoring groups, like ester or phosphate groups. These groups can help substrates get positioned accurately within the active site of the enzyme and stop any unwanted side reactions that might involve sensitive functional groups. Both the natural anchoring groups (such as amines or carboxyl groups) and the groups designed

synthetically (for example, long-chain alkyl or aromatic rings) can greatly improve the enzyme's affinity for substrates (Figure 61). When combining this strategy with molecular dynamics simulations and structural analysis, the interactions between the substrate and the enzyme can be optimised further. As a result, the catalytic efficiency can be enhanced and the selectivity can be improved, which also helps to decrease unnecessary substrate evaporation. For instance, phosphorylated phenol substrates have made it possible for bacterial P450 enzymes to selectively oxidise non-native C-H bonds. Modified cyclopentanecarboxylic acids have also boosted the stereoselectivity and conversion rates in the synthesis of antiviral drug precursors.[192,193]

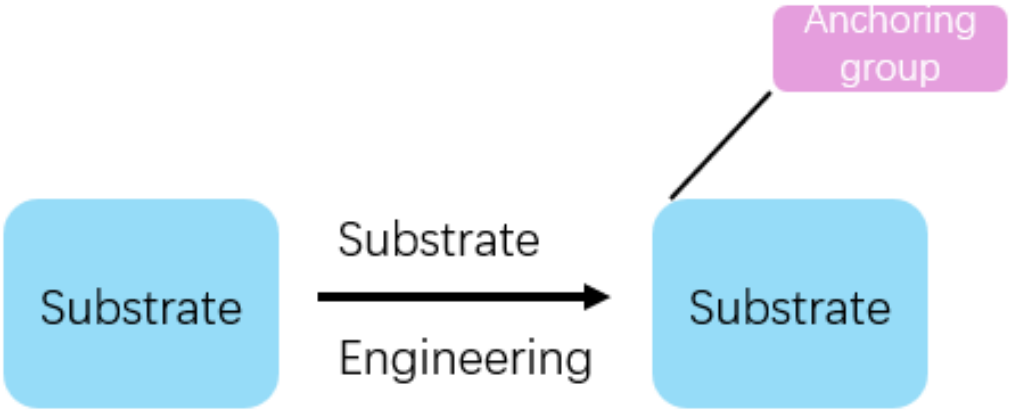


Figure 61. Substrate engineering to enhance catalytic efficiency and unnatural substrate affinity.

To increase the conversion of substrates and decrease the waste caused by substrate evaporation, efforts can also be made from five aspects: optimising the reaction medium, enhancing the stability and activity of enzymes, controlling reaction conditions,

adopting auxiliary strategies, and optimising process design. Firstly, choosing an appropriate reaction solvent is of great importance. By using unconventional solvent systems, such as biphasic solvent systems, micro-aqueous reaction systems (MARS), or pure substrate systems, the substrate concentration and conversion rate can possibly be effectively increased, while the evaporation waste of substrates can be significantly decreased. In a biphasic system, enzyme catalysis mainly occurs in the aqueous phase, while substrates and products are mostly distributed in the hydrophobic organic phase, which decreases evaporation losses and also helps with product separation. The MARS system, by adding a small amount of water into the organic solvent, can not only maintain the activity of the enzyme but also decrease the amount of solvent used and the generation of waste. However, improving the stability and activity of enzymes is the key. The structure of enzymes can be modified through protein engineering or surface modification to make them more tolerant to the environment of organic solvents. Or enzymes can be immobilised on carriers by immobilisation techniques, thus enhancing their stability and decreasing the risk of inactivation. In addition, the control of reaction conditions is also crucial. By adopting the fed-batch method of adding substrates step by step, the situation where high substrate concentration leads to evaporation or enzyme inhibition can possibly be avoided. Meanwhile, optimising the reaction temperature can minimize substrate evaporation while maintaining the activity of the enzyme to the greatest extent. Finally, through reasonable process design, for example, using continuous flow reactors, the utilisation rate of substrates and the conversion of products can be optimised.[194]

6

Chapter 6

6.1. Conclusion and future work

In chapter 1, the concept of a H_2-driven flavin recycling system operating in H_2/O_2 mixtures was introduced as a promising strategy for flavin-dependent biocatalysis. This system could decrease the dependency on expensive cofactors NADH/NAD^+ and minimise the possible chemical waste generated by the conventional GDH-driven flavin recycling system. The motivation for this work was built on addressing the challenges in the industrial application of FD-halgoenases due to their dependence complex and expensive cofactor recycling methods.

Chapter 3 demonstrated the combination of Hyd-1 with PyrH to achieve H_2-driven halogenation. Initial tests established on the conventional GDH-driven system, confirming PyrH's activity for site-selective chlorination of L-tryptophan. Subsequent coupling with Hyd-1 required optimisation of key parameters such as flavin concentration and precise control of O_2 delivery. A pulsed O_2 injection method at safe H_2/O_2 mixtures was first established for balancing the flavin recycling and the system's stability and activity. Conditions of 0.5 mM FAD and 0.5% O_2 were proved as the optimal reaction conditions. This system demonstrated scalability and versatility by catalysing higher substrate concentrations (up to 5.5 mM) and extending halogenation to bromination reactions with comparable efficiency.

Building on the successful combination of Hyd-1 with PyrH, the robustness of the system with Hyd-1/H_2 was further tested with non-native substrates, which exhibited slower conversion rates. Chapter 4 also explored a more scalable and controlled operation mode, a constant gas atmosphere method via a balloon of H_2/O_2. Moreover, this chapter extended this constant gas method to the application of another FD-halogenase, PrnA, a 7-position chlorinase. Initial experiments successfully showed the conversion (~10%). After systematic optimisations including increased enzyme concentrations and temperature profiling, the conversion achieved significant improvements. A reaction temperature of 50 ℃ was identified as optimal, enabling 96% conversion within 2 hours. O_2-sensitve Hyd-2 was also introduced as an alternative recycling enzyme for $FADH_2$. Surprisingly, Hyd-2-driven halogenation performed comparably to Hyd-1 under controlled conditions, suggesting that the hydrogenase activity is not the limiting factor in reaction rates. This chapter also concludes with experiments combining Ni-complexes as synthetic reductants, successfully demonstrating its promise for flavin recycling and halogenation reactions.

Chapter 5 extended the application of the H_2-driven system to flavin-dependent monooxygenases, focusing on *Sf*StyA for biocatalytic epoxidation reactions. Initial tests with a conventional BNAH-driven system established the O_2 tolerance for the *Sf*StyA. This revealed *Sf*StyA's activity at around 10% O_2 levels, which required careful balancing of O_2 and H_2 to maintain safety and the activities of both hydrogenase and

monooxygenase. The Hyd-1 system demonstrated lower rates to the BNAH system while operating under similar conditions. Reaction conditions were further refined, with 0.1 mM FAD and 2% O_2 emerging as the optimal settings for *Sf*StyA activity. Around 40% conversion was found during the reaction. However, substrate evaporation posed a significant challenge, particularly with trans-β-methylstyrene. The co-solvent optimisations with 15-20% DMSO successfully mitigated evaporation. Further efforts of addressing substrate evaporation and enhancing the system's rates will should be conducted in the future.

6.2. Discussion

Traditional chemical halogenation reactions usually require high temperature, high pressure or specific free radical initiators to proceed. These harsh conditions raise the requirements for the materials and structures of production equipment, increase costs and make the operation more complicated. On the contrary, biocatalytic halogenation reactions can be carried out under mild conditions at normal temperature and normal pressure. This greatly decreases the hardware requirements and energy consumption costs, and also cuts down the safety risks related to high temperature and high pressure. Besides, biocatalytic reactions are highly regioselective. They can accurately identify the specific positions of substrate molecules and efficiently introduce halogens at those positions, thus producing single products. This simplifies the subsequent separation and purification processes, decreases costs and lessens the burden on the

environment. In terms of environmental impact, the halogenated pollutants generated by traditional chemical halogenation reactions are difficult to degrade in the environment and pose a long-term threat to the ecosystem. Therefore, biocatalytic halogenation reactions are gradually becoming a promising alternative.

Therefore, the H_2-driven flavin recycling system demonstrated in this study holds promise for advancing sustainable flavin-dependent biocatalysis. This system has already proven its compatibility with multiple flavin-dependent enzymes with a range of substrates. However, although this system has effectively simplified the flavin recycling, the stability and catalytic efficiency of flavin-dependent halogenases themselves still need to be further improved. Since flavin-dependent halogenases are not essential for survival and growth in natural microorganisms, they have less evolutionary pressure, resulting in lower catalytic reaction efficiency.[195] Besides, although these enzymes offer high regioselectivity, their stereospecificity towards substrates and reaction selectivity also need to be optimised to broaden their application range. The integration and optimisation of the system towards larger-scale production, are also challenges. Moving forward, the plan should focus on enhancing the performance of halogenases, including their stability, activity, substrate scope, and the oxygen tolerance and flavin reduction capability of hydrogenases. Efforts should also concentrate on scaling up the system. This includes methods such as immobilization, protein stabilisation, and optimisation of overexpression. Such

improvements are essential for transitioning from laboratory-scale experiments to industrial applications, where efficiency and robustness are critical.

6.2.1. Future scope for the scale-up

In the field of biocatalysis, scaling up halogenase-catalysed reactions is crucial for their practical application in chemical synthesis, pharmaceuticals, and agrochemicals where halogenated organic compounds are extensively utilised. FAD-dependent halogenases, like RebH, present a promising alternative due to their efficiency and selectivity, yet their preparative synthesis applications have been underexplored. Payne *et al*. demonstrated significant advancements in overcoming these challenges by optimising the expression and reaction conditions of RebH in *E. coli*. Low yields and poor solubility of these proteins were initially problematic. [196] However, co-expression of RebH with the chaperone proteins GroEL / ES and the fusion of RebF with maltose-binding protein (MBP) substantially enhanced protein solubility and production levels. These modifications enabled sufficient production of RebH and MBP-RebF without the need for specialised fermentation equipment or bioreactors. The enhanced process also expanded the substrate scope of RebH, enabling halogenation of a variety of medicinally relevant indoles and naphthalenes, including substrates that are typically less reactive under conventional chemical catalysis. This approach has proven effective even on a preparative scale, with successful chlorination and bromination reactions with high conversion. This work advanced the understanding of FAD-

dependent halogenases like RebH in biocatalytic applications and set a foundation for further scale-up efforts in the synthesis of halogenated compounds.[196] In addition, the fusion protein in this study may also be applied to hydrogenase-halogenase in the future by adding a linker between them to improve the stability of halogenases (Figure 62). However, this approach requires careful consideration of several factors: the compatibility of the folding and function of the two enzymes when they are linked; the impact on the catalytic activity of each enzyme as a fusion construct, and the selection of an optimal linking sequence that can maintain the flexibility and functional independence of each enzyme domain.

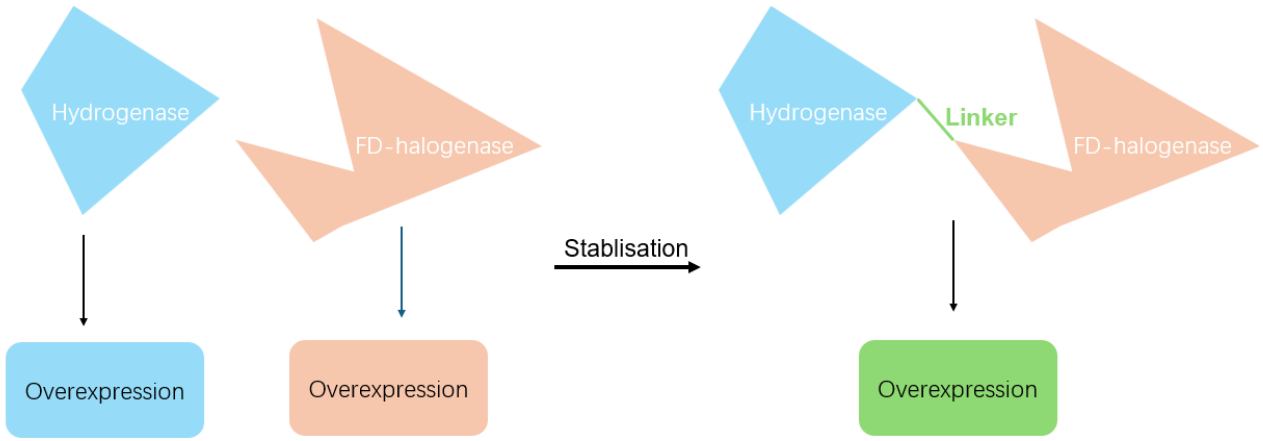


Figure 62. Proposed fusion protein between hydrogenase and FD-halogenase to enhance stability.

Another method for scale-up involved the use of enzyme immobilization technology, for example, through the integration of cross-linked enzyme aggregates (CLEAs), to achieve efficient halogenation in biocatalysis. A new immobilised enzyme system, referred to as combiCLEAs, was developed by Frese *et al.*, which incorporated the

halogenase RebH and its auxiliary enzymes, significantly enhancing enzyme stability and activity. The results demonstrated that this immobilised enzyme system can be stably stored at 4 ℃ for over four months, with only a decline in activity after 12 weeks. Using this system, an average conversion rate of 81% was achieved for 3 mM of L-tryptophan in batch reactions, and the enzymes could be reused at least 10 times. Under optimised immobilisation conditions, an immobilisation yield of 99% and an activity recovery of 30% were achieved for the three enzymes. Furthermore, the highest enzyme activity was observed when lower concentrations of glutaraldehyde were used for cross-linking, indicating that moderate cross-linking helps maintain enzyme activity. Using this method, L-tryptophan was completely converted within 8 days, producing 1.813 g of 7-bromo-L-tryptophan. Considering the application of this method to a H_2-driven FAD recycling system with FD-halogenase might further simplify the operational process. This system, combining hydrogenase and halogenase, does not require additional glucose as the reducing equivalents or NADH as cofactors, relying solely on H_2 as the energy source.[165]

Scaling up and industrial application of enzymatic processes significantly benefit from the development of continuous flow systems. Liu *et al*. demonstrated the construction of a continuous catalytic system for the halogenation of L-tryptophan. The system incorporated a tri-enzyme fusion, consisting of tryptophan halogenase, glucose dehydrogenase, and flavin reductase, immobilised on Ni-NTA material. By integrating

the immobilised enzymes into a column within a continuous flow reactor, the system facilitates the controlled and steady conversion of L-tryptophan to 6-chloro-L-tryptophan. The enzyme system operated under optimised conditions with a reaction mixture containing 0.5 mM L-tryptophan, 20 mM glucose, 10 mM $MgCl_2 \cdot 6H_2O$, 0.5 mM NADH, and 0.1 mM FAD, processed at a flow rate of 1 mL/min. This system achieved 97.6% conversion of L-tryptophan to 6-chloro-L-tryptophan in 12 hours (Figure 63). Continuous flow processes offer substantial advantages over traditional batch reactions by improving reaction safety, decreasing time, and providing better control over reaction kinetics, crucial for safe, scalable, and economically viable industrial applications.[197] Moreover, the development of H_2-driven halogenation system in this thesis, operating under a constant flow of a gas mixture of H_2 and O_2, could be possibly applied to this continuous flow system. This integration points toward enhanced industrial applications, leveraging the unique advantages of continuous flow setups to achieve efficient and controlled halogenation reactions at scale.

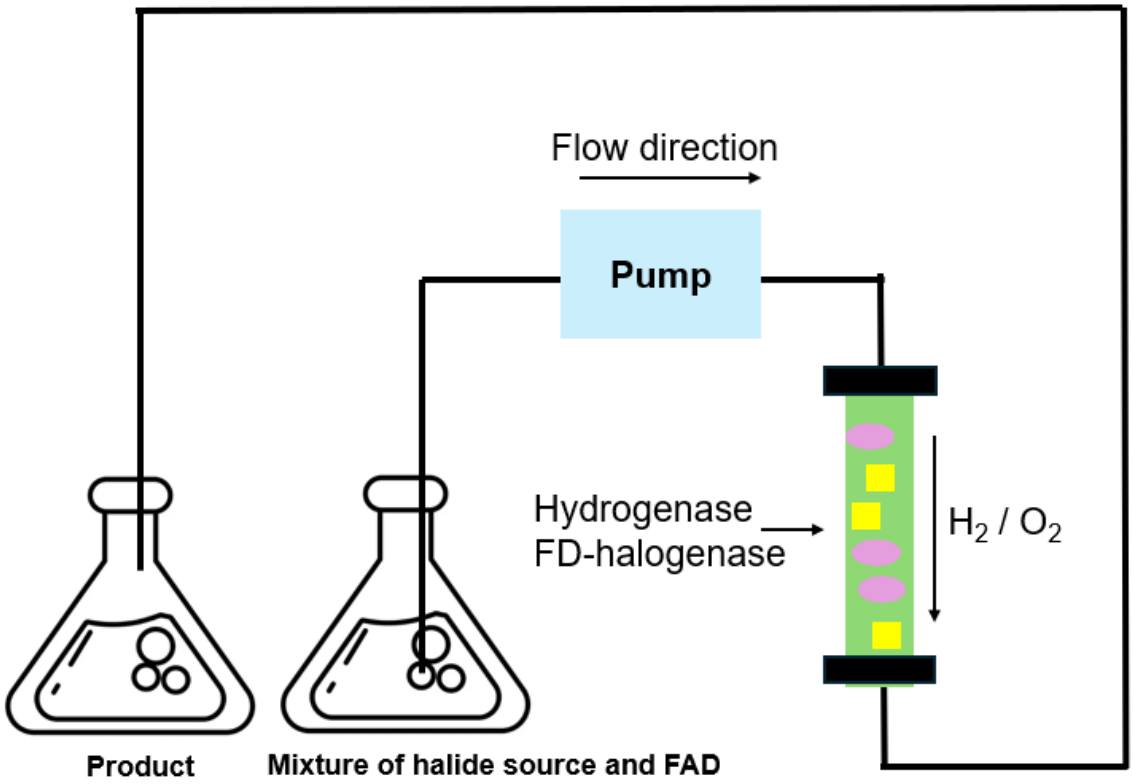


Figure 63. Proposed flow reaction mode for H_2-driven halogenation.

6.2.2. Future scope of the H_2-driven flavin recycling system

The integration of H_2-driven flavin recycling systems with a variety of flavin-dependent enzymes, such as halogenases and monooxygenases, holds tremendous promise for advancing sustainable chemical synthesis across multiple industries. For example, VirX1, a flavin-dependent halogenase, demonstrates unique capabilities in iodination of diverse substrates, a process essential for synthesizing compounds with enhanced molecular properties like higher bioavailability. This enzyme's specificity and efficiency make it particularly valuable for targeted synthesis in pharmaceutical and agrochemical

applications.[198] In addition, FD-halogenase FasV plays a pivotal role in the biosynthesis of naphthacemycins through its ability to catalyse five successive chlorinations. This emphasises its importance in generating highly effective pharmaceutical agents through precise molecular modifications.[199] Rifampicin monooxygenase (RIFMO) is instrumental in biodegrading and altering antibiotics, thereby playing a crucial role in addressing antibiotic resistance. By modifying the molecular structure of rifampicin, RIFMO can possibly restore the efficacy of this critical therapeutic against resistant strains of bacteria.[200] Baeyer-Villiger Monooxygenases (BVMO), known for facilitating the Baeyer-Villiger oxidation, transform ketones into esters and lactones, processes vital in the synthesis of various fine chemicals and pharmaceuticals.[201] Some BVMOs accept reducing equivalents from free flavin.

The integration of these enzymes into an H_2-driven flavin recycling system could possibly increase the sustainability and efficiency of these processes. By using H_2, a clean and abundant reductant, to regenerate flavin cofactors necessary for these enzymatic activities, the system promises to decrease the dependency on expensive and environmentally harmful reagents. Such advancements could provide more sustainable pathways for producing complex molecules, combating antibiotic resistance, and enabling the greener production of a broad range of high-value chemical products in industrial biocatalysis. Continued research and development will

be key to overcoming challenges related to enzyme stability and system integration, paving the way for widespread industrial adoption of these technologies.

References

[1] Vardanyan, Ruben, and Victor Hruby. *Synthesis of essential drugs*. Elsevier, **2006**.

[2] Wright, Peter M., Ian B. Seiple, and Andrew G. Myers. "The evolving role of chemical synthesis in antibacterial drug discovery." *Angewandte Chemie International Edition* 53.34 (**2014**): 8840-8869.

[3] Vane, J. R., and R. M. Botting. "The mechanism of action of aspirin." *Thrombosis research* 110.5-6 (**2003**): 255-258.

[4] Vogel, I. *Practical organic chemistry*. **1974**.

[5] Abdussalam-Mohammed, Wanisa, A. Qasem Ali, and A. O. Errayes. "Green chemistry: principles, applications, and disadvantages." *Chem. Methodol* 4.4 (**2020**): 408-423.

[6] Anastas, Paul, and Nicolas Eghbali. "Green chemistry: principles and practice." *Chemical Society Reviews* 39.1 (**2010**): 301-312.

[7] Nestl, Bettina M., et al. "New generation of biocatalysts for organic synthesis." *Angewandte Chemie International Edition* 53.12 (**2014**): 3070-3095.

[8] Winkler, Christoph K., Joerg H. Schrittwieser, and Wolfgang Kroutil. "Power of biocatalysis for organic synthesis." *ACS Central Science* (**2021**): 55-71.

[9] Alcántara, Andrés R., et al. "Biocatalysis as key to sustainable industrial chemistry." *ChemSusChem* 15.9 (**2022**): e202102709.

[10] Manzoni, M., and M. Rollini. "Biosynthesis and biotechnological production of statins by filamentous fungi and application of these cholesterol-lowering drugs." *Applied Microbiology and Biotechnology* (**2002**): 555-564.

[11] Hollmann, Frank, and Roberto Fernandez-Lafuente. "Grand challenges in biocatalysis." *Frontiers in Catalysis* (**2021**): 633893.

[12] Merino, Sandra T., and Joel Cherry. "Progress and challenges in enzyme development for biomass utilization." *Biofuels* (**2007**): 95-120.

[13] Yang, Haiquan, et al. "Microbial production and molecular engineering of industrial enzymes: challenges and strategies." *Biotechnology of microbial enzymes* **2017**. 151-165.

[14] Nelson, David L., Albert L. Lehninger, and Michael M. Cox. *Lehninger Principles of Biochemistry* **2008**.

[15] Hashim, Onn H., and Nor Azila Adnan. "Coenzyme, cofactor and prosthetic group—ambiguous biochemical jargon." *Biochemical Education* 22.2 (**1994**): 93-94.

[16] Mander, Lewis, and Hung-Wen Liu. *Comprehensive natural products II: chemistry and biology*. Vol. 1. Elsevier, **2010**.

[17] Vallee, Bert L., and Frederic L. Hoch. "Zinc, a component of yeast alcohol dehydrogenase." *Proceedings of the National Academy of Sciences* 41.6 (**1955**): 327-338.

[18] Wang, Yipeng, Ka-Yiu San, and George N. Bennett. "Cofactor engineering for advancing chemical biotechnology." *Current Opinion in Biotechnology* 24.6 (**2013**): 994-999.

[19] Sirithanakorn, Chaiyos, and John E. Cronan. "Biotin, a universal and essential cofactor: synthesis, ligation and regulation." *FEMS Microbiology Reviews* 45.4 (**2021**): fuab003.

[20] Ying, Weihai. "NAD+ and NADH in cellular functions and cell death." *Front Biosci* 11.1 (**2006**): 3129-3148.

[21] Ying, Weihai. "NAD+/NADH and NADP+/NADPH in cellular functions and cell death: regulation and biological consequences." *Antioxidants & Redox Signaling* 10.2 (**2008**): 179-206.

[22] Meijers, Rob, et al. "On the enzymatic activation of NADH." *Journal of Biological Chemistry* 276.12 (**2001**): 9316-9321.

[23] Wada, Fumio, Kazuya Hirata, and Yukiya Sakamoto. "Relation of cholesterol synthesis and NADPH oxidation by microsomal electron transport system involving P-450." *Biochimica et Biophysica Acta (BBA)-Bioenergetics* 143.1 (**1967**): 273-275.

[24] Gaskin, Felicia, and R. B. Clayton. "An interstrain difference in cholesterol synthesis in vitro in mice, dependent upon a difference in endogenous NADPH-generating capacity." *Journal of Lipid Research* 13.1 (**1972**): 106-114.

[25] Lyanagi, Takashi, Chuanwu Xia, and Jung-Ja P. Kim. "NADPH–cytochrome P450 oxidoreductase: prototypic member of the diflavin reductase family." *Archives of Biochemistry and Biophysics* 528.1 (**2012**): 72-89.

[26] Lee, Linda G., and George M. Whitesides. "Enzyme-catalyzed organic synthesis: a comparison of strategies for in situ regeneration of NAD from NADH." *Journal of the American Chemical Society* 107.24 (**1985**): 6999-7008.

[27] Josa-Culleré, Laia, et al. "Synthetic biomimetic coenzymes and alcohol dehydrogenases for asymmetric catalysis." *Catalysts* 9.3 (**2019**): 207.

[28] Zhang, Zhibo, et al. "Electrochemically driven efficient enzymatic conversion of CO2 to formic acid with artificial cofactors." *Journal of CO2 Utilization* 52 (**2021**): 101679.

[29] Jayathilake, Buddhinie S., et al. "Efficient and selective electrochemically driven enzyme-catalyzed reduction of carbon dioxide to formate using formate dehydrogenase and an artificial cofactor." *Accounts of Chemical Research* 52.3 (**2019**): 676-685.

[30] Bruice, Thomas C. "Mechanisms of flavin catalysis." *Accounts of Chemical Research* 13.8 (1980): 256-262.

[31] Walsh, Christopher. "Flavin coenzymes: at the crossroads of biological redox chemistry." *Accounts of Chemical Research* 13.5 (**1980**): 148-155.

[32] Huijbers, Mieke ME, et al. "Flavin dependent monooxygenases." *Archives of Biochemistry and Biophysics* 544 (**2014**): 2-17.

[33] Michaelis, Leonor, Maxwell P. Schubert, and C. V. Smythe. "Potentiometric study of the flavins." (**1936**): 587-607.

[34] Zhang, Ben-Li, and Sébastien Pionnier. "Cofactor recycling mechanism in asymmetric biocatalytic reduction of carbonyl compounds mediated by yeast:

which is the efficient electron donor?." *Chemistry–A European Journal* 9.15 (**2003**): 3604-3610.

[35] Rocha, Raquel A., et al. "Cofactor and process engineering for nicotinamide recycling and retention in intensified biocatalysis." *Catalysts* 12.11 (**2022**): 1454.

[36] Bachosz, Karolina, et al. "Enzymatic cofactor regeneration systems: A new perspective on efficiency assessment." *Science of The Total Environment* 868 (**2023**): 161630.

[37] Aamer, Emad, et al. "Influence of electrode potential, pH and NAD+ concentration on the electrochemical NADH regeneration." *Scientific Reports* 12.1 (**2022**): 16380.

[38] Ferrandi, Erica Elisa, Daniela Monti, and Sergio Riva. "New trends in the in situ enzymatic recycling of NAD (P)(H) cofactors." *Cascade Biocatalysis: Integrating Stereoselective and Environmentally Friendly Reactions* (**2014**): 23-42.

[39] Avigad, Gad. "Reduction of nicotinamide adenine dinucleotides by sodium cyanoborohydride." *Biochimica et Biophysica Acta (BBA)-Enzymology* 571.1 (**1979**): 171-174.

[40] Lee, Yoo Seok, Rokas Gerulskis, and Shelley D. Minteer. "Advances in electrochemical cofactor regeneration: enzymatic and non-enzymatic approaches." *Current Opinion in Biotechnology* 73 (**2022**): 14-21.

[41] Ali, Irshad, Amardeep Gill, and Sasha Omanovic. "Direct electrochemical regeneration of the enzymatic cofactor 1, 4-NADH employing nano-patterned glassy carbon/Pt and glassy carbon/Ni electrodes." *Chemical Engineering Journal* 188 (**2012**): 173-180.

[42] Ali, Irshad, et al. "Electrocatalytic CO2 fixation by regenerating reduced cofactor NADH during Calvin Cycle using glassy carbon electrode." *Plos One* 15.9 (**2020**): e0239340.

[43] Tan, Boxuan, et al. "Regeneration of the NADH cofactor by a rhodium complex immobilized on multi-walled carbon nanotubes." *Journal of the Electrochemical Society* 162.3 (**2014**): H102.

[44] Ali, Irshad, et al. "Direct electrochemical regeneration of enzymatic cofactor 1, 4-NADH on a cathode composed of multi-walled carbon nanotubes decorated with nickel nanoparticles." *The Canadian Journal of Chemical Engineering* 96.1 (**2018**): 68-73.

[45] Damian, Alexis, and Sasha Omanovic. "Electrochemical reduction of NAD+ on a polycrystalline gold electrode." *Journal of Molecular Catalysis A: Chemical* 253.1-2 (**2006**): 222-233.

[46] Kadowaki, J. T., et al. "Copper oxide-based cathode for direct NADPH regeneration." *Scientific Reports* 11.1 (**2021**): 180.

[47] Wee, Youngho, et al. "Effective multi-biocatalyst system with reusable NADH for transformation of glycerol to value-added dihydroxyacetone." *Chemical and Biological Technologies in Agriculture* 11.1 (**2024**): 156.

[48] Guisan, Jose M., ed. *Immobilization of enzymes and cells*. Vol. 22. Totowa, NJ: Humana Press, **2006**.

[49] Medipally, Hitesh, et al. "Light-Driven NADPH Cofactor Recycling by Photosystem I for Biocatalytic Reactions." *ChemCatChem* 15.18 (**2023**): e202300821.

[50] Fukuzumi, Shunichi, Yong-Min Lee, and Wonwoo Nam. "Catalytic recycling of NAD (P) H." *Journal of Inorganic Biochemistry* 199 (**2019**): 110777.

[51] Constant, Philippe, and Patrick C. Hallenbeck. "Hydrogenase." *Biohydrogen*. Elsevier, **2019**. 49-78.

[52] Adams, Michael WW, and Leonard E. Mortenson. "The purification of hydrogenase II (uptake hydrogenase) from the anaerobic N2-fixing bacterium Clostridium pasteurianum." *Biochimica et Biophysica Acta (BBA)-Bioenergetics* 766.1 (**1984**): 51-61.

[53] Volbeda, Anne, et al. "Crystal structure of the nickel–iron hydrogenase from Desulfovibrio gigas." *Nature* 373.6515 (**1995**): 580-587.

[54] Happe, Randolph P., et al. "Biological activition of hydrogen." *Nature* 385.6612 (**1997**): 126-126.

[55] Vincent, Kylie A., Alison Parkin, and Fraser A. Armstrong. "Investigating and exploiting the electrocatalytic properties of hydrogenases." *Chemical Reviews* 107.10 (**2007**): 4366-4413.

[56] Joseph Srinivasan, Shiny, et al. "E. coli Nickel-Iron Hydrogenase 1 Catalyses Non-native Reduction of Flavins: Demonstration for Alkene Hydrogenation by Old Yellow Enzyme Ene-reductases." *Angewandte Chemie* 133.25 (**2021**): 13943-13947.

[57] Németh, Brigitta, et al. "Monitoring H-cluster assembly using a semi-synthetic HydF protein." *Dalton Transactions* 48.18 (**2019**): 5978-5986.

[58] Fontecilla-Camps, Juan C., et al. "Structure/function relationships of [NiFe]-and [FeFe]-hydrogenases." *Chemical Reviews* 107.10 (**2007**): 4273-4303.

[59] Mulder, David W., et al. "Insights into [FeFe]-hydrogenase structure, mechanism, and maturation." *Structure* 19.8 (**2011**): 1038-1052.

[60] Morra, Simone. "Fantastic [FeFe]-hydrogenases and where to find them." *Frontiers in Microbiology* 13 (**2022**): 853626.

[61] Peters, John W., et al. "[FeFe]-and [NiFe]-hydrogenase diversity, mechanism, and maturation." *Biochimica et Biophysica Acta (BBA)-Molecular Cell Research* 1853.6 (**2015**): 1350-1369.

[62] Cabotaje, Princess R., et al. "Probing substrate transport effects on enzymatic hydrogen catalysis: an alternative proton transfer pathway in putatively sensory [FeFe] hydrogenase." *ACS Catalysis* 13.15 (**2023**): 10435-10446.

[63] Yadav, Shanika, et al. "Oxygen sensitivity of [FeFe]-hydrogenase: a comparative study of active site mimics inside vs. outside the enzyme." *Physical Chemistry Chemical Physics* 26.28 (**2024**): 19105-19116.

[64] Furlan, Chris, et al. "Structural insight on the mechanism of an electron-bifurcating [FeFe] hydrogenase." *Elife* 11 (**2022**): e79361.

[65] Lubner, Carolyn E., et al. "A site-differentiated [4Fe–4S] cluster controls electron transfer reactivity of Clostridium acetobutylicum [FeFe]-hydrogenase I." *Chemical Science* 13.16 (**2022**): 4581-4588.

[66] Madden, Christopher, et al. "Catalytic turnover of [FeFe]-hydrogenase based on single-molecule imaging." *Journal of the American Chemical Society* 134.3 (**2012**): 1577-1582.

[67] Smith, Phillip R., Alyssa S. Bingham, and James R. Swartz. "Generation of hydrogen from NADPH using an [FeFe] hydrogenase." *International Journal of Hydrogen Energy* 37.3 (**2012**): 2977-2983.

[68] Wittkamp, Florian, et al. "[FeFe]-Hydrogenases: recent developments and future perspectives." *Chemical Communications* 54.47 (**2018**): 5934-5942.

[69] Bingham, Alyssa S., Phillip R. Smith, and James R. Swartz. "Evolution of an [FeFe] hydrogenase with decreased oxygen sensitivity." *International Journal of Hydrogen Energy* 37.3 (**2012**): 2965-2976.

[70] Koo, Jamin, and James R. Swartz. "System analysis and improved [FeFe] hydrogenase O2 tolerance suggest feasibility for photosynthetic H2 production." *Metabolic Engineering* 49 (**2018**): 21-27.

[71] Pandey, Arti S., et al. "Dithiomethylether as a ligand in the hydrogenase H-cluster." *Journal of the American Chemical Society* 130.13 (**2008**): 4533-4540.

[72] Vogt, Sonja, et al. "The exchange activities of [Fe] hydrogenase (iron–sulfur-cluster-free hydrogenase) from methanogenic archaea in comparison with the exchange activities of [FeFe] and [NiFe] hydrogenases." *JBIC Journal of Biological Inorganic Chemistry* 13 (**2008**): 97-106.

[73] Salomone-Stagni, Marco, et al. "The iron-site structure of [Fe]-hydrogenase and model systems: an X-ray absorption near edge spectroscopy study." *Dalton Transactions* 39.12 (**2010**): 3057-3064.

[74] Shima, Seigo, et al. "Iron-Chromophore Circular Dichroism of [Fe]-Hydrogenase: The Conformational Change Required for H2 Activation." *Angewandte Chemie International Edition* 49.51 (**2010**): 9917-9921.

[75] Sargent, F. "The model [NiFe]-hydrogenases of Escherichia coli." *Advances in Microbial Physiology* 68 (**2016**): 433-507.

[76] Evans, Rhiannon M., et al. "Mechanistic exploitation of a self-repairing, blocked proton transfer pathway in an O2-tolerant [NiFe]-hydrogenase." *Journal of the American Chemical Society* 140.32 (**2018**): 10208-10220.

[77] Cracknell, James A., et al. "A kinetic and thermodynamic understanding of O2 tolerance in [NiFe]-hydrogenases." *Proceedings of the National Academy of Sciences* 106.49 (**2009**): 20681-20686.

[78] Goris, Tobias, et al. "A unique iron-sulfur cluster is crucial for oxygen tolerance of a [NiFe]-hydrogenase." *Nature chemical biology* 7.5 (**2011**): 310-318.

[79] Pandelia, Maria-Eirini, et al. "Characterization of a unique [FeS] cluster in the electron transfer chain of the oxygen tolerant [NiFe] hydrogenase from Aquifex aeolicus." *Proceedings of the National Academy of Sciences* 108.15 (**2011**): 6097-6102.

[80] Wulff, Philip, et al. "How oxygen reacts with oxygen-tolerant respiratory [NiFe]-hydrogenases." *Proceedings of the National Academy of Sciences* 111.18 (**2014**): 6606-6611.

[81] Volbeda, Anne, et al. "X-ray crystallographic and computational studies of the O2-tolerant [NiFe]-hydrogenase 1 from Escherichia coli." *Proceedings of the National Academy of Sciences* 109.14 (**2012**): 5305-5310.

[82] Pinske, Constanze, et al. "Physiology and bioenergetics of [NiFe]-hydrogenase 2-catalyzed H2-consuming and H2-producing reactions in Escherichia coli." *Journal of Bacteriology* 197.2 (**2015**): 296-306.

[83] Beaton, Stephen E., et al. "The structure of hydrogenase-2 from Escherichia coli: implications for H_2-driven proton pumping." *Biochemical Journal* 475.7 (**2018**): 1353-1370.

[84] Evans, Rhiannon M., et al. "Comprehensive structural, infrared spectroscopic and kinetic investigations of the roles of the active-site arginine in bidirectional hydrogen activation by the [NiFe]-hydrogenase 'Hyd-2'from Escherichia coli." *Chemical Science* 14.32 (**2023**): 8531-8551.

[85] Reeve, Holly A., et al. "Enzyme-modified particles for selective biocatalytic hydrogenation by hydrogen-driven NADH recycling." *ChemCatChem* 7.21 (**2015**): 3480-3487.

[86] Ramirez, Miguel A., et al. "H2-driven reduction of flavin by hydrogenase enables cleaner operation of nitroreductases for nitro-group to amine reductions." *Frontiers in Catalysis* 2 (**2022**): 906694.

[87] Dockrey, Summer A. Baker, and Alison RH Narayan. "Flavin-dependent biocatalysts in synthesis." *Tetrahedron* 75.9 (**2019**): 1115-1121.

[88] Pimviriyakul, Panu, and Pimchai Chaiyen. "Overview of flavin-dependent enzymes." *The Enzymes*. Vol. 47. Academic Press, **2020**. 1-36.

[89] Herrera-Rodriguez, Leopoldo N., et al. "Perspectives on biotechnological halogenation." *chimica oggi/Chemistry Today* 29.6 (**2011**).

[90] Latham, Jonathan, et al. "Development of halogenase enzymes for use in synthesis." *Chemical Reviews* 118.1 (**2018**): 232-269.

[91] Hernandes, Marcelo Z., et al. "Halogen atoms in the modern medicinal chemistry: hints for the drug design." *Current Drug Targets* 11.3 (**2010**): 303-314.

[92] Lu, Yunxiang, et al. "Halogen bonding for rational drug design and new drug discovery." *Expert opinion on drug discovery* 7.5 (**2012**): 375-383.

[93] Sirimulla, Suman, et al. "Halogen interactions in protein–ligand complexes: implications of halogen bonding for rational drug design." *Journal of Chemical Information and Modeling* 53.11 (**2013**): 2781-2791.

[94] Auffinger, Pascal, et al. "Halogen bonds in biological molecules." *Proceedings of the National Academy of Sciences* 101.48 (**2004**): 16789-16794.

[95] Ho, P. Shing. "Biomolecular halogen bonds." *Halogen Bonding I: Impact on Materials Chemistry and Life Sciences* (**2015**): 241-276.

[96] Rossi, Renzo, Fabio Bellina, and Marco Lessi. "Selective Palladium-Catalyzed Suzuki–Miyaura Reactions of Polyhalogenated Heteroarenes." *Advanced Synthesis & Catalysis* 354.7 (**2012**): 1181-1255.

[97] Skhiri, Aymen, et al. "Palladium-Catalysed Desulfitative Heck Reaction Tolerant to Aryl Carbon–Halogen Bonds for Access to (Poly) halo-Substituted Stilbene or Cinnamate Derivatives." *Synthesis* 48.18 (**2016**): 3097-3106.

[98] Klapars, Artis, and Stephen L. Buchwald. "Copper-catalyzed halogen exchange in aryl halides: An aromatic Finkelstein reaction." *Journal of the American Chemical Society* 124.50 (**2002**): 14844-14845.

[99] Boldon, Sophie, et al. "Supported Synthesis of Halogenated Organic Compounds." *Synthesis* 2011.24 (**2011**): 3929-3953.

[100] Chung, Won-jin, and Christopher D. Vanderwal. "Stereoselective halogenation in natural product synthesis." *Angewandte Chemie International Edition* 55.14 (**2016**): 4396-4434.

[101] Kolvari, Eskandar, et al. "Alternative methodologies for halogenation of organic compounds." *Current Organic Synthesis* 10.6 (**2013**): 837-863.

[102] Samanta, Ramesh C., and Hisashi Yamamoto. "Selective halogenation using an aniline catalyst." *Chemistry–A European Journal* 21.34 (**2015**): 11976-11979.

[103] Kosjek, Tina, and Ester Heath. "Halogenated heterocycles as pharmaceuticals." *Halogenated Heterocycles: Synthesis, Application and Environment* (**2012**): 219-246.

[104] Ludewig, Hannes, et al. "Halogenases: structures and functions." *Current Opinion in Structural Biology* 65 (**2020**): 51-60.

[105] Smith, Duncan RM, Sabine Grüschow, and Rebecca JM Goss. "Scope and potential of halogenases in biosynthetic applications." *Current Opinion in Chemical Biology* 17.2 (**2013**): 276-283.

[106] Gkotsi, Danai S., et al. "Halogenases: powerful tools for biocatalysis (mechanisms applications and scope)." *Current Opinion in Chemical Biology* 43 (**2018**): 119-126.

[107] Van Pée, Karl-Heinz, and Eugenio P. Patallo. "Flavin-dependent halogenases involved in secondary metabolism in bacteria." *Applied Microbiology and Biotechnology* 70.6 (**2006**): 631-641.

[108] Büchler, Johannes, Athena Papadopoulou, and Rebecca Buller. "Recent advances in flavin-dependent halogenase biocatalysis: sourcing, engineering, and application." *Catalysts* 9.12 (**2019**): 1030.

[109] Lewis, Jared C. "Identifying and engineering flavin dependent halogenases for selective biocatalysis." *Accounts of chemical research* 57.15 (**2024**): 2067-2079.

[110] Phintha, Aisaraphon, Kridsadakorn Prakinee, and Pimchai Chaiyen. "Structures, mechanisms and applications of flavin-dependent halogenases." *The Enzymes* 47 (**2020**): 327-364.

[111] Zeng, Jia, and Jixun Zhan. "Chlorinated natural products and related halogenases." *Israel Journal of Chemistry* 59.5 (**2019**): 387-402.

[112] Crowe, Charlotte, et al. "Halogenases: a palette of emerging opportunities for synthetic biology–synthetic chemistry and C–H functionalisation." *Chemical Society Reviews* 50.17 (**2021**): 9443-9481.

[113] Podzelinska, Kateryna, et al. "Chloramphenicol biosynthesis: the structure of CmlS, a flavin-dependent halogenase showing a covalent flavin–aspartate bond." *Journal of Molecular Biology* 397.1 (**2010**): 316-331.

[114] Fejzagić, Alexander Veljko, et al. "Halogenating enzymes for active agent synthesis: First steps are done and many have to follow." *Molecules* 24.21 (**2019**): 4008.

[115] Jităreanu, Alexandra, Ioana Cezara Caba, and Luminita Agoroaei. "Halogenation–A Versatile Tool For Drug Synthesis-The Importance Of Developing Effective And Eco-Friendly Reaction Protocols." *Curr. Anal. Biotechnol* 2030 (**2019**).

[116] Fraley, Amy E., and David H. Sherman. "Halogenase engineering and its utility in medicinal chemistry." *Bioorganic & Medicinal Chemistry Letters* 28.11 (**2018**): 1992-1999.

[117] Brown, Stephanie, and Sarah E. O'Connor. "Halogenase engineering for the generation of new natural product analogues." *ChemBioChem* 16.15 (**2015**): 2129-2135.

[118] Neubauer, Pia R., et al. "A flavin-dependent halogenase from metagenomic analysis prefers bromination over chlorination." *PLoS One* 13.5 (**2018**): e0196797.

[119] Payne, James T., Catherine B. Poor, and Jared C. Lewis. "Directed evolution of RebH for site-selective halogenation of large biologically active molecules." *Angewandte Chemie* 127.14 (**2015**): 4300-4304.

[120] Lang, Alexander, et al. "Changing the regioselectivity of the tryptophan 7-halogenase PrnA by site-directed mutagenesis." *Angewandte Chemie (International ed. in English)* 50.13 (**2011**): 2951-2953.

[121] Phintha, Aisaraphon, et al. "Dissecting the low catalytic capability of flavin-dependent halogenases." *Journal of Biological Chemistry* 296 (**2021**).

[122] Zhang, Zhengyi, and Huimin Zhao. "Tunnel engineering enables multifaceted improvements in halogenase." *Chem Catalysis* 2.10 (**2022**): 2432-2434.

[123] Minges, Hannah, et al. "Targeted enzyme engineering unveiled unexpected patterns of halogenase stabilization." *ChemCatChem* 12.3 (**2020**): 818-831.

[124] Andorfer, Mary C., et al. "Analysis of laboratory-evolved flavin-dependent halogenases affords a computational model for predicting halogenase site selectivity." *Chem Catalysis* 2.10 (**2022**): 2658-2674.

[125] Ismail, Lea, et al. "Photochemically driven biocatalysis of halogenases for the green production of chlorinated compounds." *ChemCatChem* 10.15 (**2018**): 3336-3341.

[126] Littlechild, Jennifer. "Haloperoxidases and their role in biotransformation reactions." *Current Opinion in Chemical Biology* 3.1 (**1999**): 28-34.

[127] Butler, Alison, and Moriah Sandy. "Mechanistic considerations of halogenating enzymes." *Nature* 460.7257 (**2009**): 848-854.

[128] Colpas, Gerard J., et al. "Functional models for vanadium haloperoxidase: reactivity and mechanism of halide oxidation." *Journal of the American Chemical Society* 118.14 (**1996**): 3469-3478.

[129] Colpas, Gerard J., et al. "A functional model for vanadium haloperoxidase." *Journal of the American Chemical Society* 116.8 (**1994**): 3627-3628.

[130] Hofrichter, Martin, and René Ullrich. "Heme-thiolate haloperoxidases: versatile biocatalysts with biotechnological and environmental significance." *Applied Microbiology and Biotechnology* 71.3 (**2006**): 276-288.

[131] Hillwig, Matthew L., et al. "Discovery of a promiscuous non-heme iron halogenase in ambiguine alkaloid biogenesis: implication for an evolvable enzyme family for late-stage halogenation of aliphatic carbons in small molecules." *Angewandte Chemie International Edition* 55.19 (**2016**): 5780-5784.

[132] Zhai, Guoqing, et al. "Structural insight into the catalytic mechanism of non-heme iron halogenase AdaV in 2′-chloropentostatin biosynthesis." *Acs Catalysis* 12.22 (**2022**): 13910-13920.

[133] Blasiak, Leah C., et al. "Crystal structure of the non-haem iron halogenase SyrB2 in syringomycin biosynthesis." *Nature* 440.7082 (**2006**): 368-371.

[134] Wong, Shaun D., et al. "Elucidation of the Fe (IV)= O intermediate in the catalytic cycle of the halogenase SyrB2." *Nature* 499.7458 (**2013**): 320-323.

[135] Wang, Yaya, Zixin Deng, and Xudong Qu. "Characterization of a SAM-dependent fluorinase from a latent biosynthetic pathway for fluoroacetate and 4-fluorothreonine formation in Nocardia brasiliensis." *F1000Research* 3 (**2014**): 61.

[136] Eustáquio, Alessandra S., et al. "Discovery and characterization of a marine bacterial SAM-dependent chlorinase." *Nature Chemical Biology* 4.1 (**2008**): 69-74.

[137] Ma, Long, et al. "Biological fluorination from the sea: discovery of a SAM-dependent nucleophilic fluorinating enzyme from the marine-derived bacterium Streptomyces xinghaiensis NRRL B24674." *RSC Advances* 6.32 (**2016**): 27047-27051.

[138] Eustáquio, Alessandra S., et al. "S-adenosyl-L-methionine hydrolase (adenosine-forming), a conserved bacterial and archeal protein related to SAM-dependent halogenases." *Chembiochem: a European Journal of Chemical Biology* 9.14 (**2008**): 2215.

[139] Reis, Renata AG, et al. "New frontiers in flavin-dependent monooxygenases." *Archives of Biochemistry and Biophysics* 699 (**2021**): 108765.

[140] Chenprakhon, Pirom, Thanyaporn Wongnate, and Pimchai Chaiyen. "Monooxygenation of aromatic compounds by flavin-dependent monooxygenases." *Protein Science* 28.1 (**2019**): 8-29.

[141] Palfey, Bruce A., and Claudia A. McDonald. "Control of catalysis in flavin-dependent monooxygenases." *Archives of Biochemistry and Biophysics* 493.1 (**2010**): 26-36.

[142] Deng, Yaming, et al. "Properties and mechanisms of flavin-dependent monooxygenases and their applications in natural product synthesis." *International Journal of Molecular Sciences* 23.5 (**2022**): 2622.

[143] Schroeder, Martin. "Osmium tetraoxide cis hydroxylation of unsaturated substrates." *Chemical Reviews* 80.2 (**1980**): 187-213.

[144] Enthaler, Stephan. "Palladium-catalysed hydroxylation and alkoxylation." *Chemical Society Reviews* 40.10 (**2011**): 4912-4924.

[145] Canan Koch, Stacie S., and A. Richard Chamberlin. "Modified conditions for efficient Baeyer-Villiger oxidation with m-CPBA." *Synthetic Communications* 19.5-6 (**1989**): 829-833.

[146] Peris, Gorka, and Scott J. Miller. "A nonenzymatic acid/peracid catalytic cycle for the Baeyer− Villiger oxidation." *Organic Letters* 10.14 (**2008**): 3049-3052.

[147] Katsuki, Tsutomu, and Victor Martin. "Asymmetric epoxidation of allylic alcohols: the Katsuki–Sharpless epoxidation reaction." *Organic Reactions* 48 (**2004**): 1-299.

[148] Walsh, Christopher T., and Y-C. Jack Chen. "Enzymic Baeyer–Villiger oxidations by flavin-dependent monooxygenases." *Angewandte Chemie International Edition in English* 27.3 (**1988**): 333-343.

[149] Bradford, Marion M. "A rapid and sensitive method for the quantitation of microgram quantities of protein utilizing the principle of protein-dye binding." *Analytical Biochemistry* 72.1-2 (**1976**): 248-254.

[150] Shepherd, Sarah A., et al. "Extending the biocatalytic scope of regiocomplementary flavin-dependent halogenase enzymes." *Chemical Science* 6.6 (**2015**): 3454-3460.

[151] Srinivasan, Bharath. "A guide to the Michaelis–Menten equation: steady state and beyond." *The FEBS Journal* 289.20 (**2022**): 6086-6098.

[152] Unversucht, Susanne, et al. "FADH2-dependence of tryptophan 7-halogenase." *Advanced Synthesis & Catalysis* 347.7-8 (**2005**): 1163-1167.

[153] Ernst, Simon, et al. "Photoinduced monooxygenation involving NAD (P) H-FAD sequential single-electron transfer." *Nature Communications* 11.1 (**2020**): 2600.

[154] Schroeder, Lea, et al. "Coupling and regulation mechanisms of the flavin-dependent halogenase PyrH observed by infrared difference spectroscopy." *Journal of Biological Chemistry* 300.4 (**2024**).

[155] Ismail, Mohamed, et al. "Straightforward regeneration of reduced flavin adenine dinucleotide required for enzymatic tryptophan halogenation." *ACS Catalysis* 9.2 (**2019**): 1389-1395.

[156] Van Pée, K-H., et al. "Application and modification of flavin-dependent halogenases." *Methods in enzymology*. Vol. 575. Academic Press, **2016**. 65-92.

[157] Lukey, Michael J., et al. "How Escherichia coli is equipped to oxidize hydrogen under different redox conditions 2." *Journal of Biological Chemistry* 285.6 (**2010**): 3928-3938.

[158] Adamson, Hope, et al. "Retuning the catalytic bias and overpotential of a [NiFe]-hydrogenase via a single amino acid exchange at the electron entry/exit site." *Journal of the American Chemical Society* 139.31 (**2017**): 10677-10686.

[159] Drell, Isadore L., and Frank E. Belles. *Survey of Hydrogen Combustion Properties*. No. NACA-TR-1383. **1958**.

[160] Zehner, Susanne, et al. "A regioselective tryptophan 5-halogenase is involved in pyrroindomycin biosynthesis in Streptomyces rugosporus LL-42D005." *Chemistry & Biology* 12.4 (**2005**): 445-452.

[161] Van Pée, Karl-Heinz. "Enzymatic chlorination and bromination." *Methods in enzymology*. Vol. 516. Academic Press, **2012**. 237-257.

[162] Van Pée, Karl-Heinz, and Susanne Zehner. "Enzymology and molecular genetics of biological halogenation." *Natural Production of Organohalogen Compounds* (**2003**): 171-199.

[163] Chaiyen, Pimchai, Marco W. Fraaije, and Andrea Mattevi. "The enigmatic reaction of flavins with oxygen." *Trends in Biochemical Sciences* 37.9 (**2012**): 373-380.

[164] Holtmann, Dirk, and Frank Hollmann. "The oxygen dilemma: a severe challenge for the application of monooxygenases?." *ChemBioChem* 17.15 (**2016**): 1391-1398.

[165] Frese, Marcel, and Norbert Sewald. "Enzymatic halogenation of tryptophan on a gram scale." *Angewandte Chemie International Edition* 54.1 (**2015**): 298-301.

[166] Jiang, Yuhua, et al. "The single-component flavin reductase/flavin-dependent halogenase AetF is a versatile catalyst for selective bromination and iodination of arenes and olefins." *Angewandte Chemie* 134.51 (**2022**): e202214610.

[167] Weichold, Veit, Daniela Milbredt, and Karl-Heinz van Pée. "Specific enzymatic halogenation—from the discovery of halogenated enzymes to their applications in vitro and in vivo." *Angewandte Chemie International Edition* 55.22 (**2016**): 6374-6389.

[168] Flecks, Silvana, et al. "New insights into the mechanism of enzymatic chlorination of tryptophan." *Angewandte Chemie (International ed. in English)* 47.49 (**2008**): 9533.

[169] Prakinee, Kridsadakorn, et al. "Mechanism-guided tunnel engineering to increase the efficiency of a flavin-dependent halogenase." *Nature Catalysis* 5.6 (**2022**): 534-544.

[170] Payne, J. T., M. C. Andorfer, and J. C. Lewis. "Engineering flavin-dependent halogenases." *Methods in Enzymology*. Vol. 575. Academic Press, **2016**. 93-126.

[171] Pinske, Constanze, et al. "Zymographic differentiation of [NiFe]-hydrogenases 1, 2 and 3 of Escherichia coli K-12." *BMC Microbiology* 12 (**2012**): 1-12.

[172] Besse, Caroline, Hartmut H. Niemann, and Norbert Sewald. "Increasing the Stability of Flavin-Dependent Halogenases by Disulfide Engineering." *ChemBioChem* 25.1 (**2024**): e202300700.

[173] Barker, Rhys D., et al. "Mechanism of action of flavin-dependent halogenases." *ACS Catalysis* 12.24 (**2022**): 15352-15360.

[174] Andorfer, Mary C., and Jared C. Lewis. "Understanding and improving the activity of flavin-dependent halogenases via random and targeted mutagenesis." *Annual Review of Biochemistry* 87.1 (**2018**): 159-185.

[175] Dong, Changjiang, et al. "Tryptophan 7-halogenase (PrnA) structure suggests a mechanism for regioselective chlorination." *Science* 309.5744 (**2005**): 2216-2219.

[176] Menon, Binuraj RK, et al. "Structure and biocatalytic scope of thermophilic flavin-dependent halogenase and flavin reductase enzymes." *Organic & Biomolecular Chemistry* 14.39 (**2016**): 9354-9361.

[177] Zhu, Xiaofeng, et al. "Structural insights into regioselectivity in the enzymatic chlorination of tryptophan." *Journal of Molecular Biology* 391.1 (**2009**): 74-85.

[178] Minges, Hannah, and Norbert Sewald. "Recent advances in synthetic application and engineering of halogenases." *ChemCatChem* 12.18 (**2020**): 4450-4470.

[179] Wilson, Aaron D., et al. "Hydrogen oxidation and production using nickel-based molecular catalysts with positioned proton relays." *Journal of the American Chemical Society* 128.1 (**2006**): 358-366.

[180] Yang, Jenny Y., et al. "Mechanistic insights into catalytic H2 oxidation by Ni complexes containing a diphosphine ligand with a positioned amine base." *Journal of the American Chemical Society* 131.16 (**2009**): 5935-5945.

[181] Oughli, Alaa A., et al. "Dual properties of a hydrogen oxidation Ni-catalyst entrapped within a polymer promote self-defense against oxygen." *Nature Communications* 9.1 (**2018**): 864.

[182] Tianbiao, Liu, et al. "Two Pathways for Electrocatalytic Oxidation of Hydrogen by a Nickel Bis (diphosphine) Complex with Pendant Amines in the Second Coordination Sphere." (**2013**).

[183] Ho, Ming-Hsun, et al. "Bio-inspired molecular catalysts for hydrogen oxidation and hydrogen production." *Applications of Molecular Modeling to Challenges in Clean Energy* (**2013)**. 89-111.

[184] Martínez-Montero, Lía, et al. "Asymmetric azidohydroxylation of styrene derivatives mediated by a biomimetic styrene monooxygenase enzymatic cascade." *Catalysis Science & Technology* 11.15 (**2021**): 5077-5085.

[185] Pazmiño, DE Torres, et al. "Monooxygenases as biocatalysts: classification, mechanistic aspects and biotechnological applications." *Journal of Biotechnology* 146.1-2 (**2010**): 9-24.

[186] Elder, D. P., D. Snodin, and A. Teasdale. "Analytical approaches for the detection of epoxides and hydroperoxides in active pharmaceutical ingredients, drug products and herbals." *Journal of Pharmaceutical and Biomedical Analysis* 51.5 (**2010**): 1015-1023.

[187] Botes, Adriana Leonora. *Biocatalytic resolution of epoxides: epoxide hydrolases as chiral catalysts for the synthesis of enantiomerically pure epoxides and vic diols from α-olefins*. Diss. University of the Free State, **1999**.

[188] Vandenberg, E. J. "Epoxide polymers: Synthesis, stereochemistry, structure, and mechanism." *Journal of Polymer Science Part A-1: Polymer Chemistry* 7.2 (**1969**): 525-567.

[189] Novak, K. M. "Drug Facts and Comparisons . St. Louis, Missouri." (**2002**): 619.

[190] Guan, Yuze, and Xi Chen. "Recent applications of flavin-dependent monooxygenases in biosynthesis, pharmaceutical development, and environmental science." *Catalysts* 13.12 (**2023**): 1495.

[191] Sun, Zhiyong, and Changzhu Wu. "Pickering emulsions biocatalysis: recent developments and emerging trends." *Small* 20.37 (**2024**): 2402208.

[192] Shi, Tong, et al. "Exploring the role of flavin-dependent monooxygenases in the biosynthesis of aromatic compounds." *Biotechnology for Biofuels and Bioproducts* 17.1 (**2024**): 46.

[193] Xu, Jiakun, Chunlan Wang, and Zhiqi Cong. "Strategies for substrate-regulated P450 catalysis: from substrate engineering to co-catalysis." *Chemistry–A European Journal* 25.28 (**2019**): 6853-6863.

[194] Van Schie, Morten MCH, et al. "Applied biocatalysis beyond just buffers–from aqueous to unconventional media. Options and guidelines." *Green Chemistry* 23.9 (**2021**): 3191-3206.

[195] Menon, Binuraj RK. "A rational approach to re-engineer the catalytic efficiency of flavin-dependent halogenases." *Chem Catalysis* 2.10 (**2022**): 2434-2437.

[196] Payne, James T., Mary C. Andorfer, and Jared C. Lewis. "Regioselective arene halogenation using the FAD-dependent halogenase RebH." *Angewandte Chemie International Edition* 52.20 (**2013**): 5271-5274.

[197] Liu, Han-Yu, et al. "Tri-enzyme fusion of tryptophan halogenase achieves a concise strategy for coenzyme self-sufficiency and the continuous halogenation of L-tryptophan." *Biotechnology Journal* 19.4 (**2024**): 2300557.

[198] Gkotsi, Danai S., et al. "A marine viral halogenase that iodinates diverse substrates." *Nature Chemistry* 11.12 (**2019**): 1091-1097.

[199] Hu, Yu, et al. "Functional Characterization and Molecular Basis of a Multi-Site Halogenase in Naphthacemycin Biosynthesis." *Angewandte Chemie International Edition* 64.7 (**2025**): e202418843.

[200] Liu, Li-Kai, et al. "The structure of the antibiotic deactivating, N-hydroxylating rifampicin monooxygenase." *Journal of Biological Chemistry* 291.41 (**2016**): 21553-21562.

[201] De Gonzalo, Gonzalo, Marko D. Mihovilovic, and Marco W. Fraaije. "Recent developments in the application of Baeyer–Villiger monooxygenases as biocatalysts." *ChemBioChem* 11.16 (**2010**): 2208-2231.

Appendix

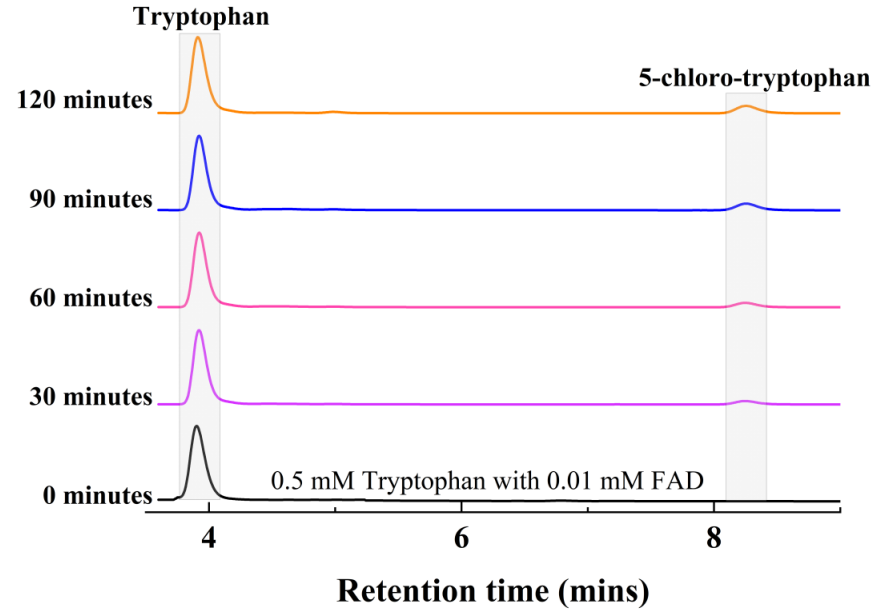


Figure A1. HPLC time point results for FAD concentrations comparison and optimisation with 0.01 mM FAD. Conditions: 30 mM NaCl, 0.5 mM L-tryptophan, 0.01 mM FAD, 5.8 μM Hyd-1, and 30 μM PyrH in 50 mM potassium phosphate buffer (pH 7.0)

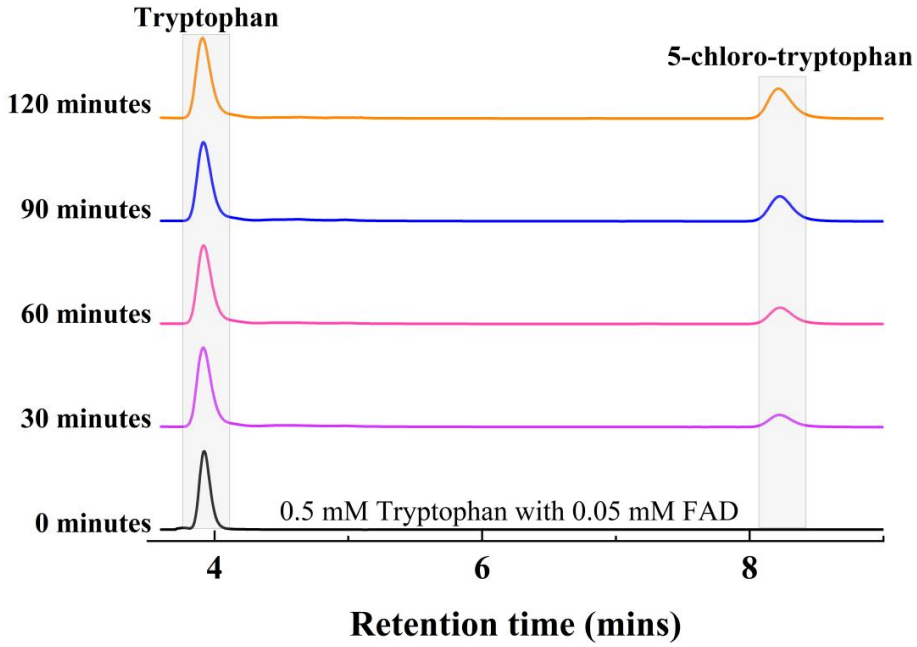


Figure A2. HPLC time point results for FAD concentrations comparison and optimisation with 0.05 mM FAD. Conditions: 30 mM NaCl, 0.5 mM L-tryptophan, 0.05 mM FAD, 5.8 μM Hyd-1, and 30 μM PyrH in 50 mM potassium phosphate buffer (pH 7.0)

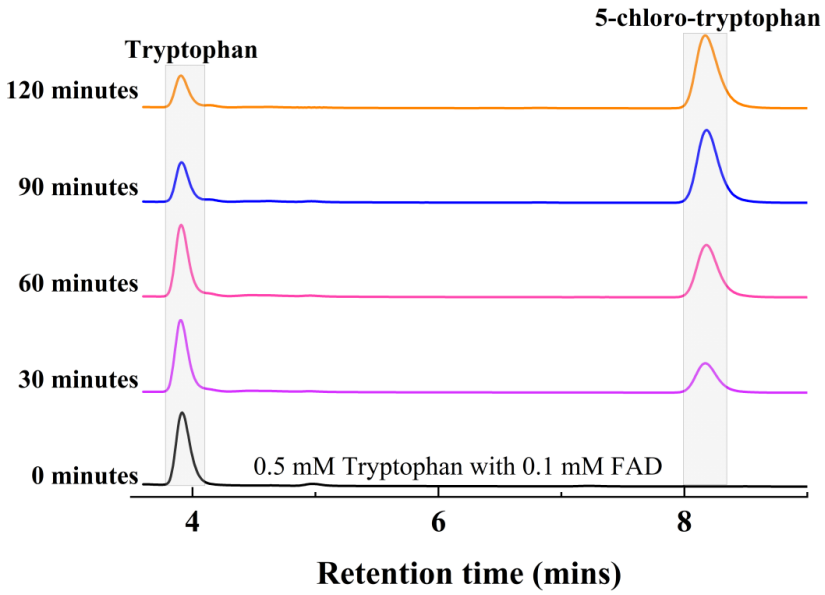


Figure A3. HPLC time point results for FAD concentrations comparison and optimisation with 0.1 mM FAD. Conditions: 30 mM NaCl, 0.5 mM L-tryptophan, 0.1 mM FAD, 5.8 μM Hyd-1, and 30 μM PyrH in 50 mM potassium phosphate buffer (pH 7.0)

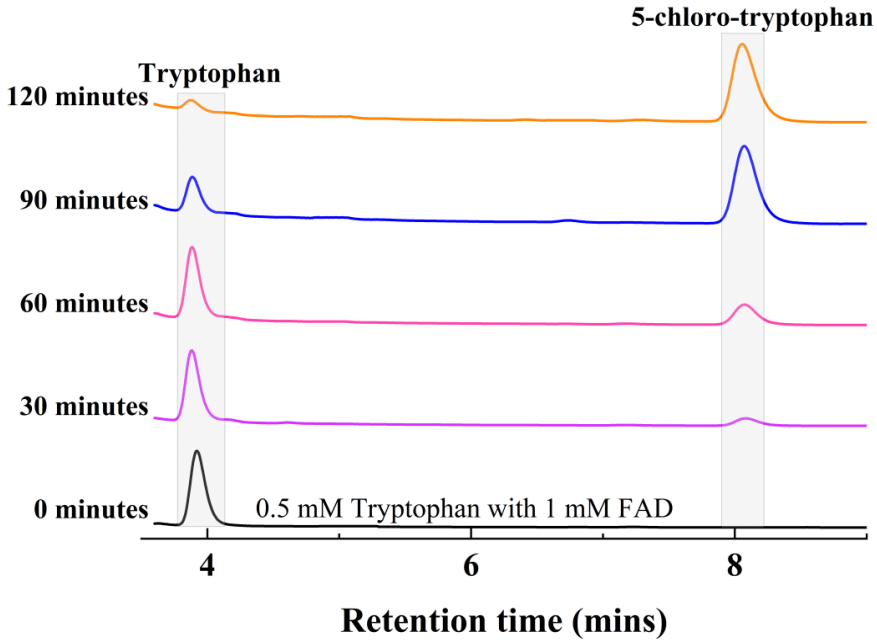


Figure A4. HPLC time point results for FAD concentrations comparison and optimization with 1 mM FAD. Conditions: 30 mM NaCl, 0.5 mM L-tryptophan, 1 mM FAD, 5.8 μM Hyd-1, and 30 μM PyrH in 50 mM potassium phosphate buffer (pH 7.0)

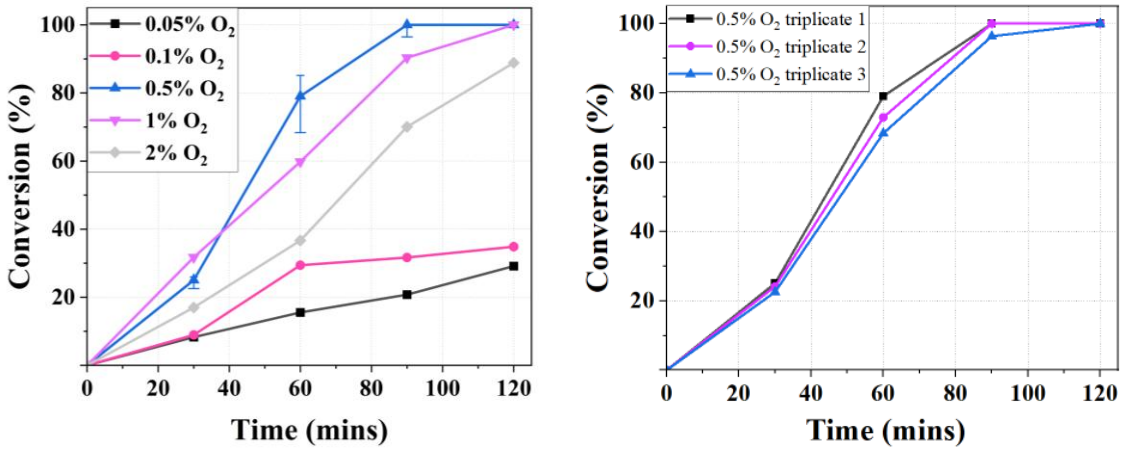


Figure A5. Time course conversion measurements for chlorination by PyrH and Hyd-1/H_2, used to determine optimal O_2 concentration with optimal FAD concentration of 0.5 mM (left); Conversion over time for triplicate 0.5% of O_2 concentrations comparison (right).

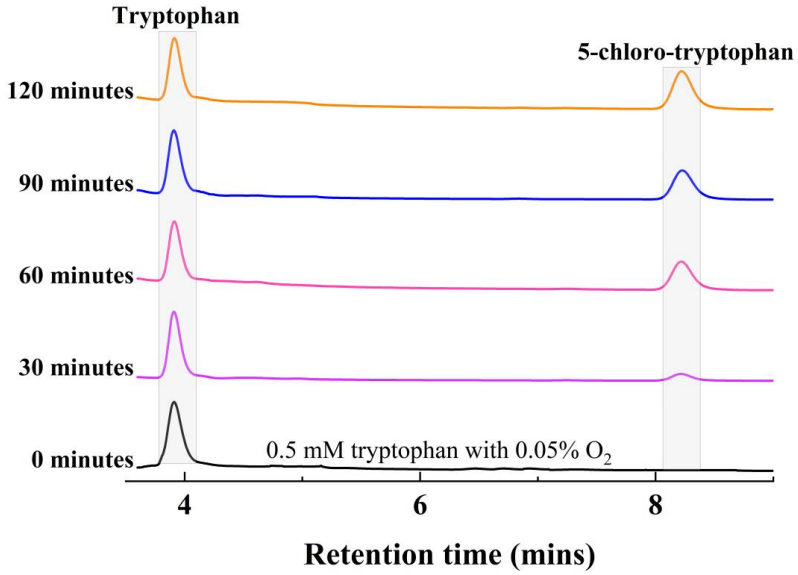


Figure A6. HPLC time point results for O_2 concentrations comparison and optimisation with 0.05% O_2. Conditions: 30 mM NaCl, 0.5 mM L-tryptophan, 0.5 mM FAD, 5.8 μM Hyd-1, and 30 μM PyrH with 0.05% O_2 in 50 mM potassium phosphate buffer (pH 7.0)

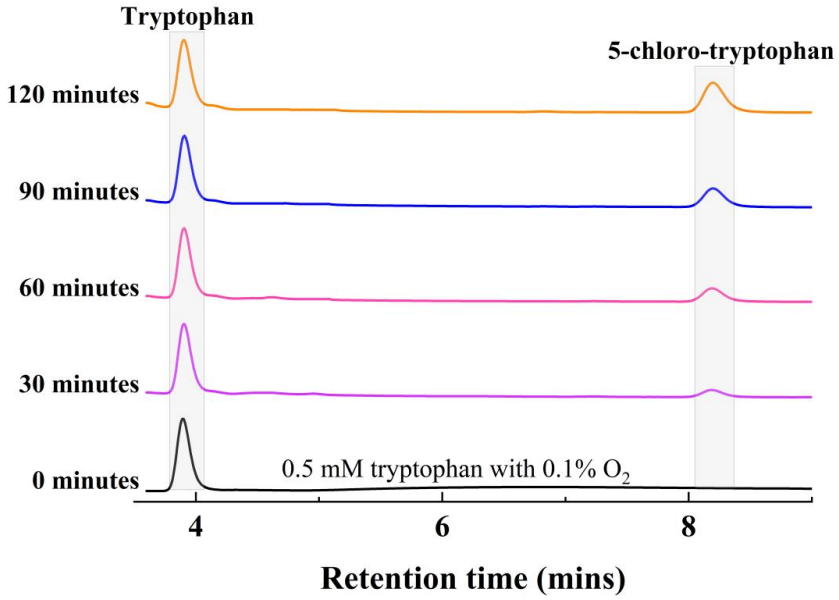


Figure A7. HPLC time point results for O_2 concentrations comparison and optimisation with 0.1% O_2. Conditions: 30 mM NaCl, 0.5 mM L-tryptophan, 0.5 mM FAD, 5.8 μM Hyd-1, and 30 μM PyrH with 0.1% O_2 in 50 mM potassium phosphate buffer (pH 7.0)

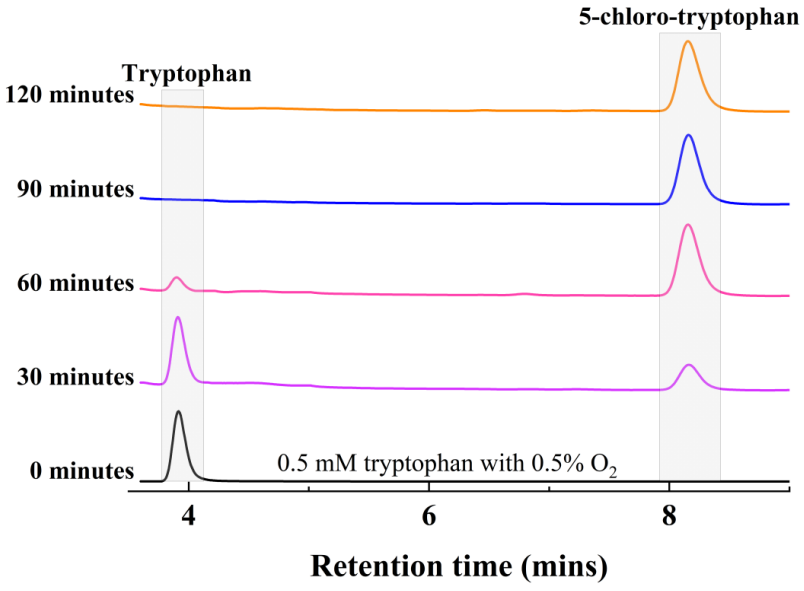


Figure A8. HPLC time point results for O_2 concentrations comparison and optimisation with 0.5% O_2 triplicate 1. Conditions: 30 mM NaCl, 0.5 mM L-tryptophan, 0.5 mM FAD, 5.8 μM Hyd-1, and 30 μM PyrH with 0.5% O_2 in 50 mM potassium phosphate buffer (pH 7.0)

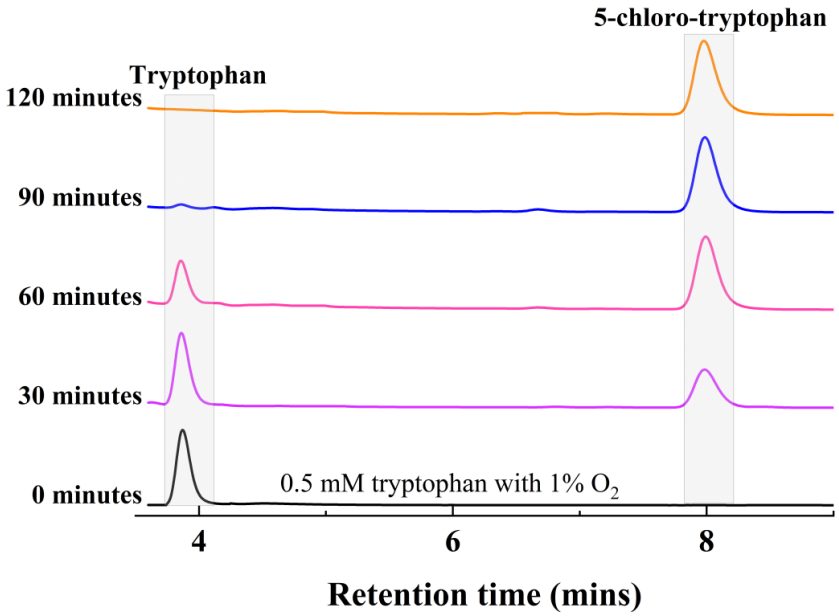


Figure A9. HPLC time point results for O_2 concentrations comparison and optimisation with 1% O_2. Conditions: 30 mM NaCl, 0.5 mM L-tryptophan, 0.5 mM FAD, 5.8 μM Hyd-1, and 30 μM PyrH with 1% O_2 in 50 mM potassium phosphate buffer (pH 7.0)

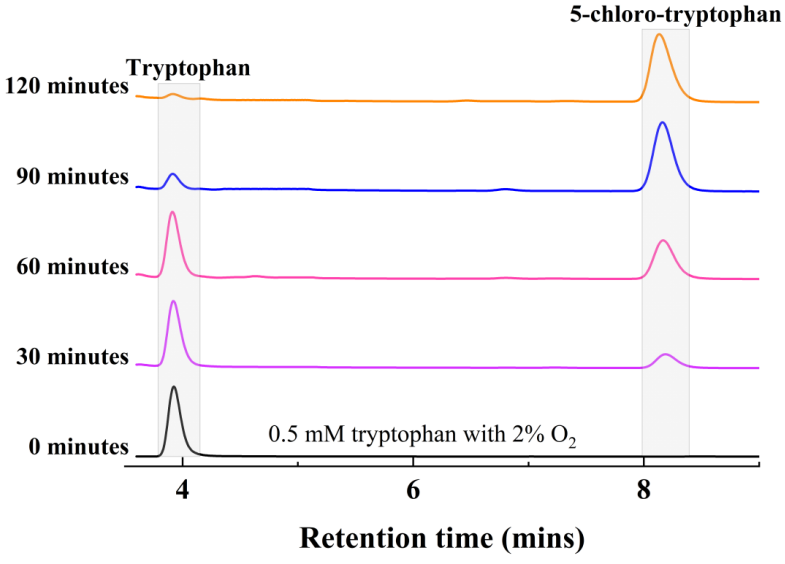


Figure A10. HPLC time point results for O_2 concentrations comparison and optimisation with 2% O_2. Conditions: 30 mM NaCl, 0.5 mM L-tryptophan, 0.5 mM FAD, 5.8 μM Hyd-1, and 30 μM PyrH with 2% O_2 in 50 mM potassium phosphate buffer (pH 7.0)

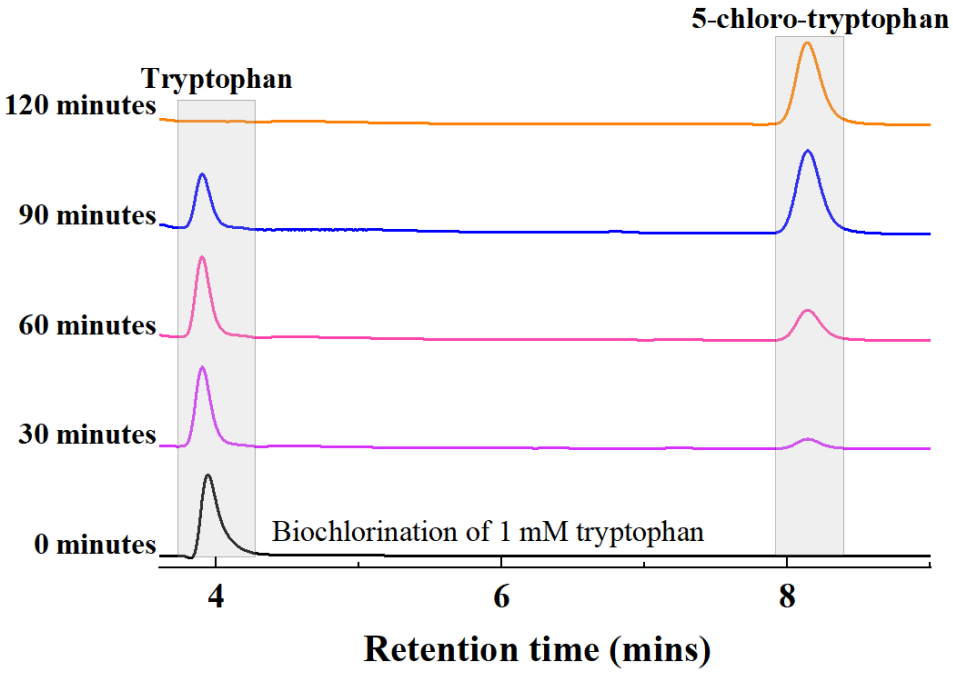


Figure A11. HPLC time point results for biochlorination with the substrate concentration of 1 mM. Reaction conditions: 30 mM NaCl, 5.8 μM Hyd-1 and 30 μM PyrH, 1 mM L-tryptophan, in potassium phosphate buffer (50 mM, pH 7.0) at 0.5 mM FAD and 0.5 % O_2 in H_2.

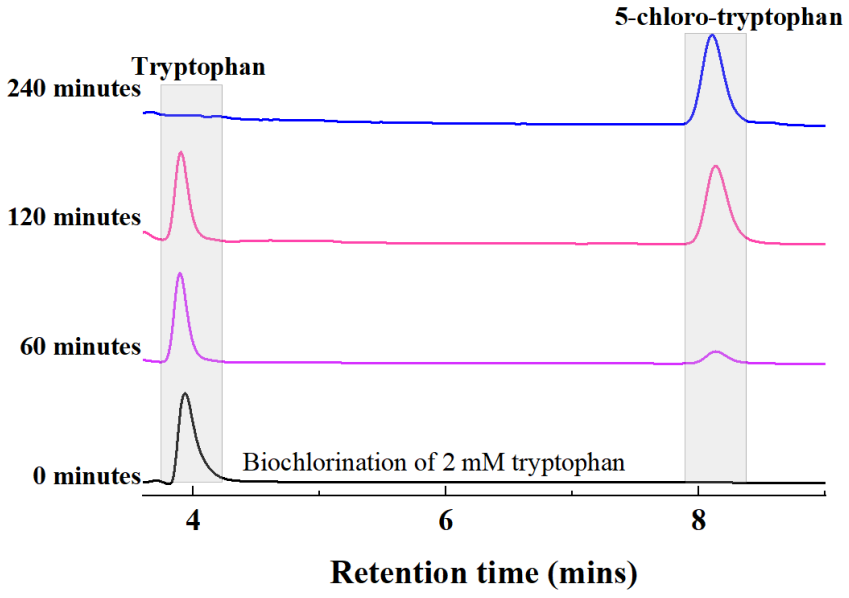


Figure A12. HPLC time point results for biochlorination with the substrate concentration of 2 mM. Reaction conditions: 30 mM NaCl, 5.8 μM Hyd-1 and 30 μM PyrH, 2 mM L-tryptophan, in potassium phosphate buffer (50 mM, pH 7.0) at 0.5 mM FAD and 0.5 % O_2 in H_2.

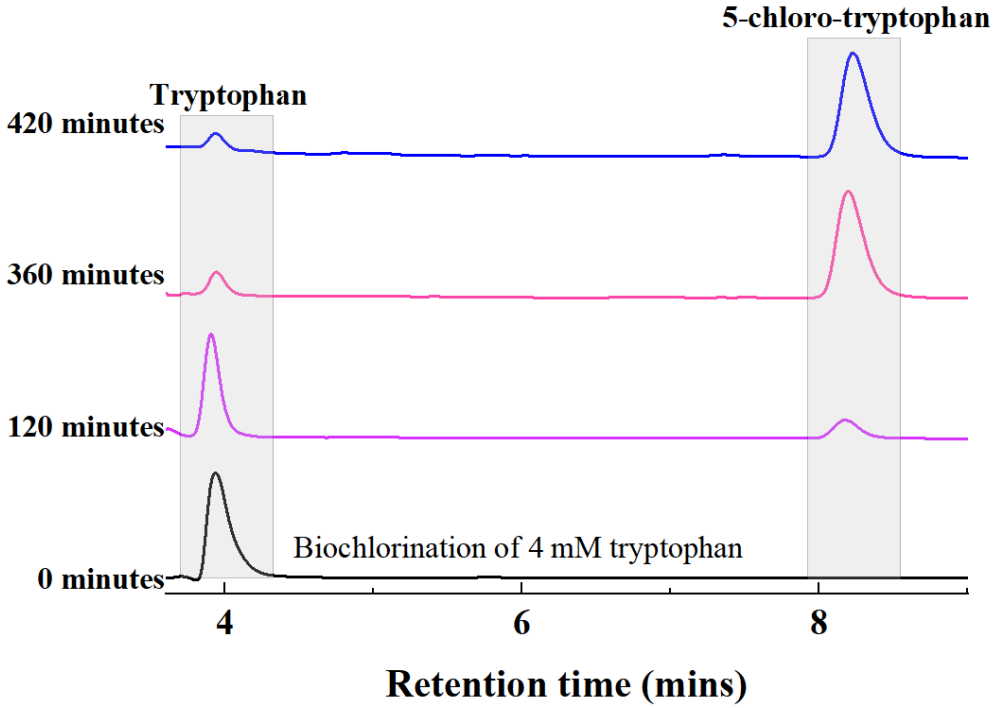


Figure A13. HPLC time point results for biochlorination with 4 mM substrate and 3.5 µM Hyd-1. Reaction conditions: 30 mM NaCl, 5.8 µM Hyd-1 and 30 µM PyrH, 4 mM L-tryptophan, in potassium phosphate buffer (50 mM, pH 7.0) at 0.5 mM FAD and 0.5 % O_2 in H_2.

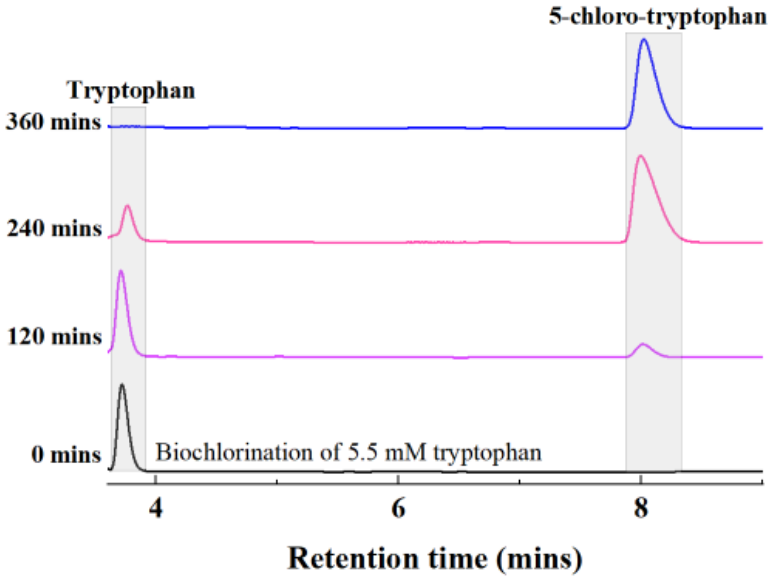


Figure A14. HPLC time point results for biochlorination triplicate 1 with the substrate tryptophan concentration of 5.5 mM. Reaction conditions: 30 mM NaCl, 5.8 µM Hyd-1 and 30 µM PyrH, in potassium phosphate buffer (50 mM, pH 7.0) at 0.5 mM FAD and 0.5 % O_2 in H_2

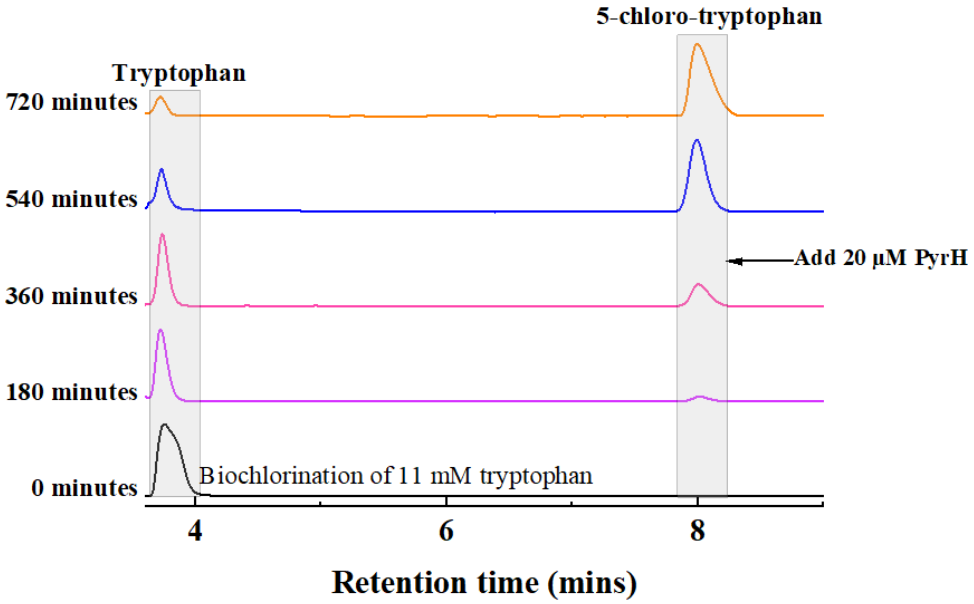


Figure A15. HPLC time point results for biochlorination triplicate 1 with the substrate tryptophan of 11 mM. Reaction conditions: 30 mM NaCl, 5.8 µM Hyd-1 and 30 µM PyrH, 20 µM PyrH was added at 360 minutes. Potassium phosphate buffer (50 mM, pH 7.0) at 0.5 mM FAD and 0.5 % O_2 in H_2

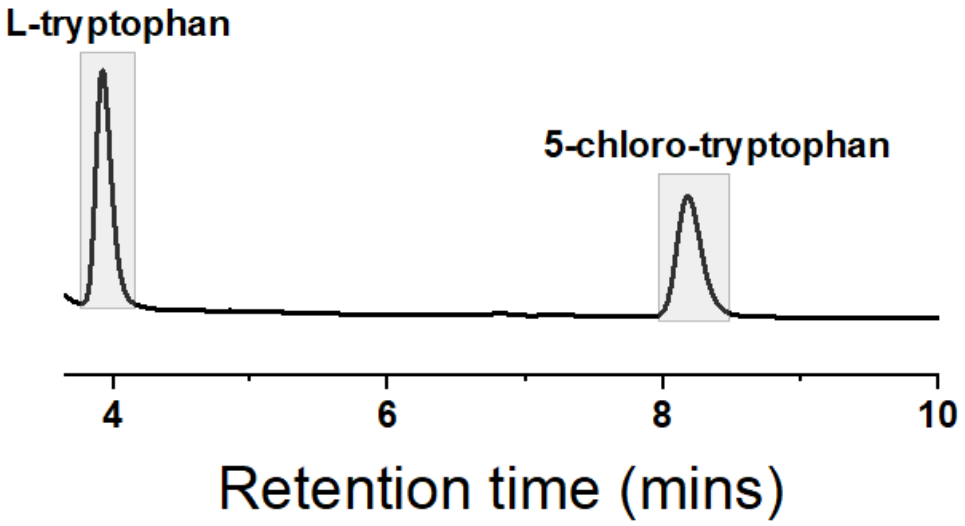


Figure A16. H_2-driven halogenation under constant flow with 6.5 µM Hyd-1. Reaction conditions: 0.5 mM L-tryptophan, 0.5 mM FAD, 30 µM PyrH, 6.5 µM Hyd-1, 20 mM NaCl and constant gas environment at 0.5% O_2 / 99.5% H_2.

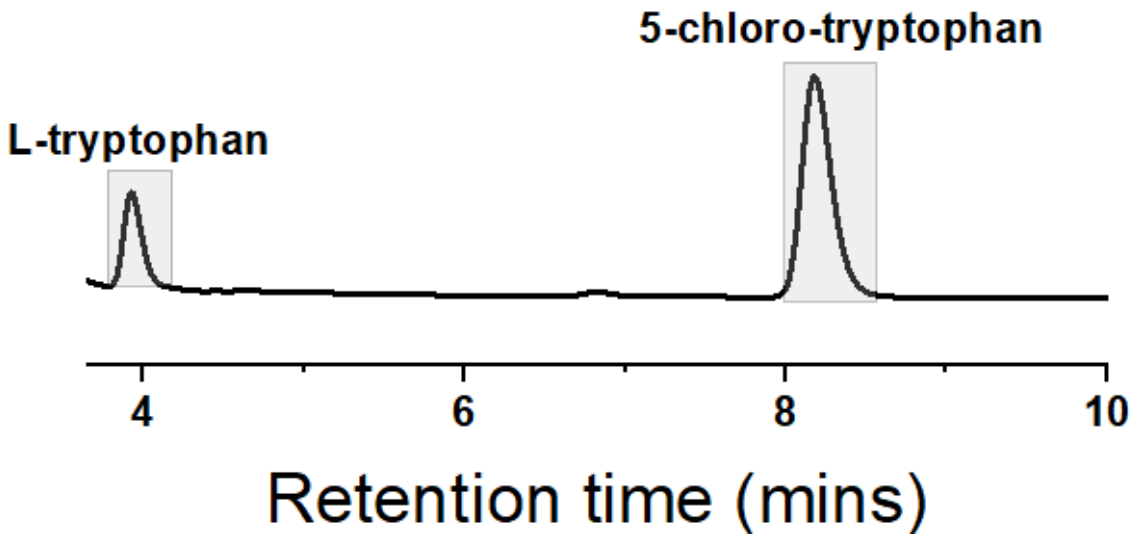


Figure A17. H_2-driven halogenation under constant flow with 8 µM Hyd-1. Reaction conditions: 0.5 mM L-tryptophan, 0.5 mM FAD, 30 µM PyrH, 8 µM Hyd-1, 20 mM NaCl and constant gas environment at 0.5% O_2 / 99.5% H_2.

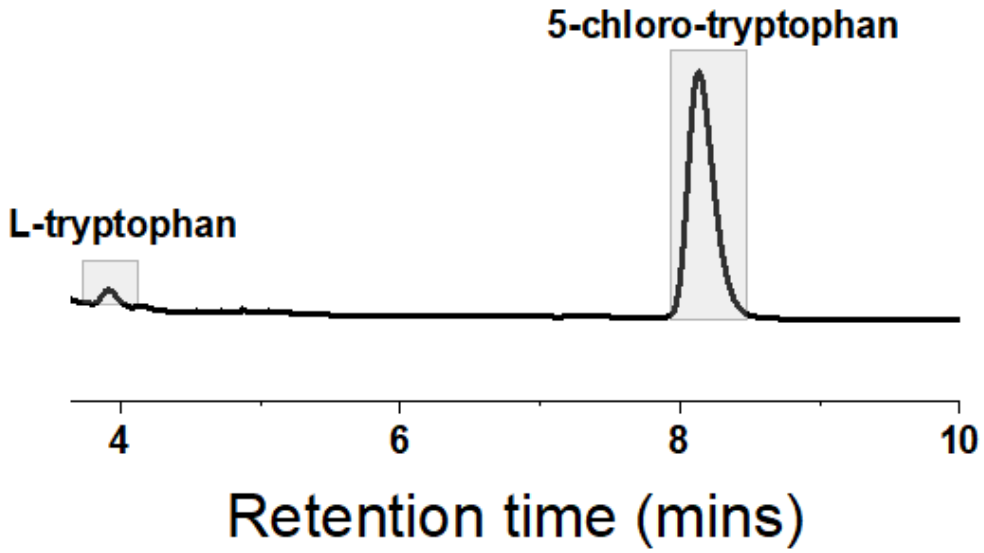


Figure A18. H_2-driven halogenation under constant flow with 10 µM Hyd-1. Reaction conditions: 0.5 mM L-tryptophan, 0.5 mM FAD, 30 µM PyrH, 10 µM Hyd-1, 20 mM NaCl and constant gas environment at 0.5% O_2 / 99.5% H_2.

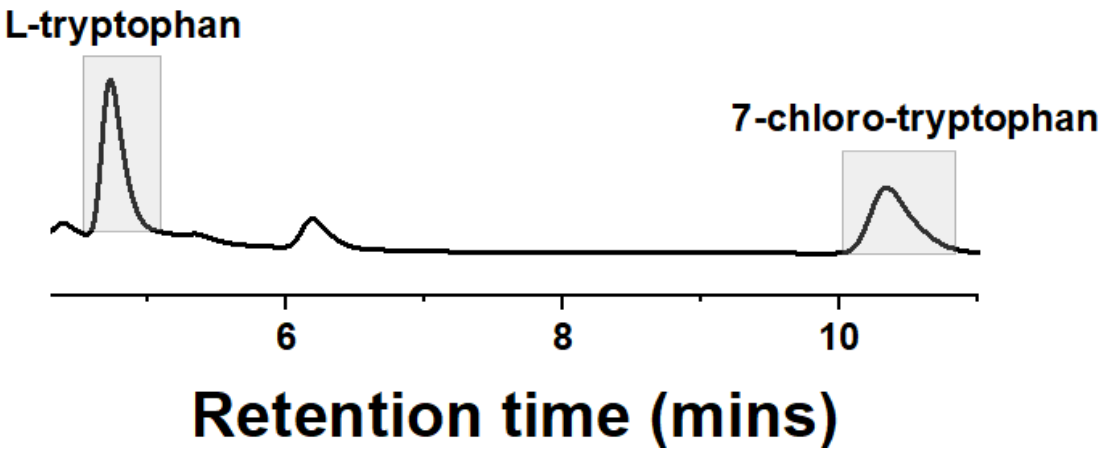


Figure A19. HPLC trace of Hyd-2-driven chlorination of L-tryptophan catalysed by PrnA under 30℃, achieving around 20% conversion after 2 hours. Reaction conditions: 0.5 mM FAD, 0.5 mM L-tryptophan, 30 μM PrnA and 10 μM Hyd-2 with a balloon of gas mixture of 0.5% O_2 / 99.5% H_2

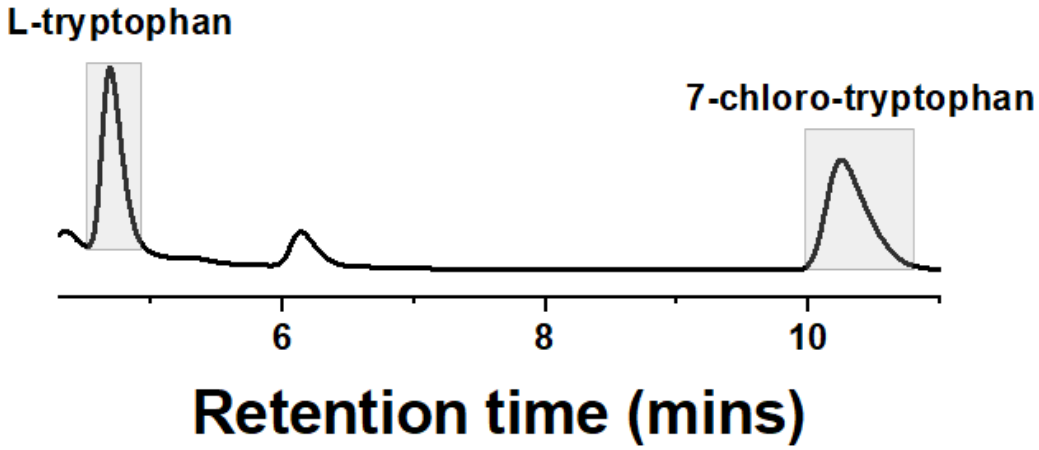


Figure A20. HPLC trace of Hyd-2-driven chlorination of L-tryptophan catalysed by PrnA under 35℃, achieving around 39% conversion after 2 hours. Reaction conditions: 0.5 mM FAD, 0.5 mM L-tryptophan, 30 μM PrnA and 10 μM Hyd-2 with a balloon of gas mixture of 0.5% O_2 / 99.5% H_2

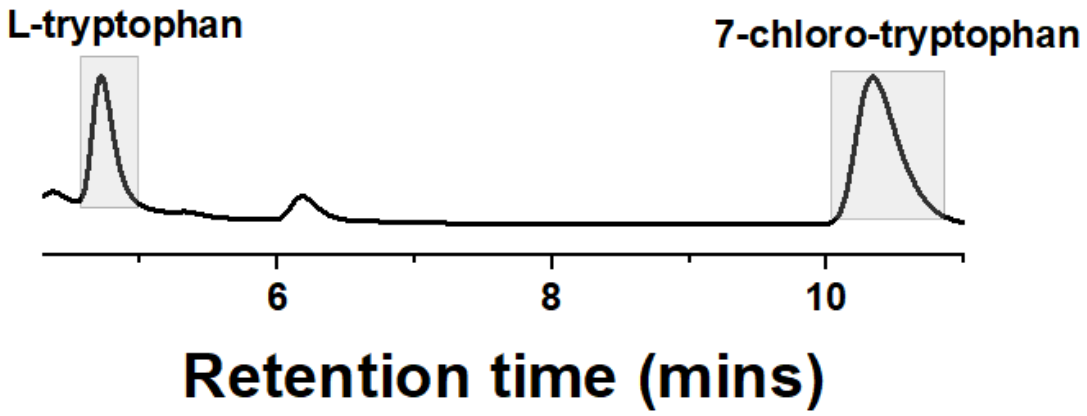


Figure A21. HPLC trace of Hyd-2-driven chlorination of L-tryptophan catalysed by PrnA under 40℃, achieving around 51% conversion after 2 hours. Reaction conditions: 0.5 mM FAD, 0.5 mM L-tryptophan, 30 μM PrnA and 10 μM Hyd-2 with a balloon of gas mixture of 0.5% O_2 / 99.5% H_2

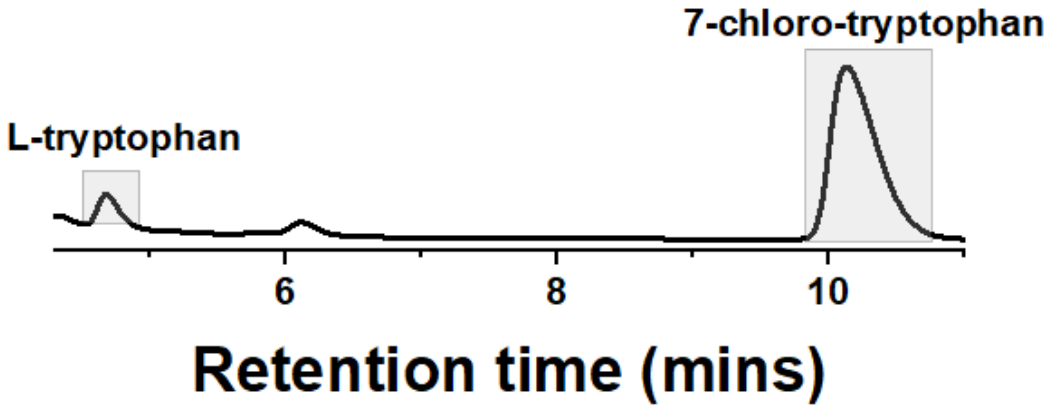


Figure A22. HPLC trace of Hyd-2-driven chlorination of L-tryptophan catalysed by PrnA under 45℃, achieving around 86% conversion after 2 hours. Reaction conditions: 0.5 mM FAD, 0.5 mM L-tryptophan, 30 μM PrnA and 10 μM Hyd-2 with a balloon of gas mixture of 0.5% O_2 / 99.5% H_2

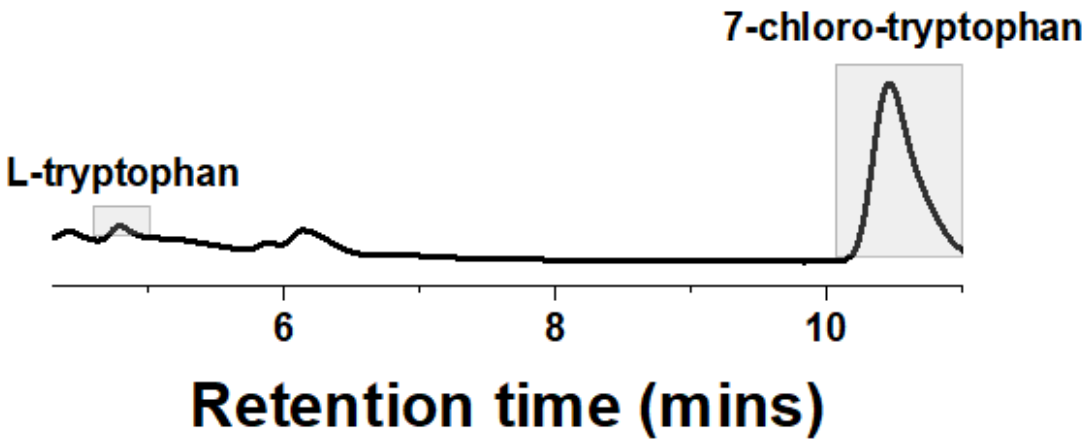


Figure A23. HPLC trace of Hyd-2-driven chlorination of L-tryptophan catalysed by PrnA under 50℃, achieving around 96% conversion after 2 hours. Reaction conditions: 0.5 mM FAD, 0.5 mM L-tryptophan, 30 μM PrnA and 10 μM Hyd-2 with a balloon of gas mixture of 0.5% O_2 / 99.5% H_2